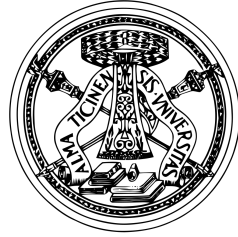


UNIVERSITÀ DEGLI STUDI DI PAVIA



LAUREA MAGISTRALE IN MATEMATICA

(MASTER'S THESIS IN MATHEMATICS)

**Stability of space-time isogeometric
methods for wave propagation problems**

Author:

Sara FRASCHINI

Supervisors:

Andrea MOIOLA
Giancarlo SANGALLI

Dipartimento di Matematica "Felice Casorati"

July 20, 2021

Alla mia famiglia

UNIVERSITÀ DEGLI STUDI DI PAVIA

Abstract

Dipartimento di Matematica “Felice Casorati”

Stability of space-time isogeometric methods for wave propagation problems

by Sara FRASCHINI

The goal of this thesis is to investigate the first steps towards an unconditionally stable space-time isogeometric method (IGA method) with maximal regularity, using a tensor-product approach, for the homogeneous Dirichlet problem for the second-order wave equation.

The unconditional stability of space-time discretization for wave propagation problems is a topic of significant and recent interest, by virtue of the advantages of space-time methods when compared with more standard space discretization plus time-stepping. These methods gained an increasing interest only recently, due to the improvement in computer technology, which is now capable of handling algorithms with significantly high computational costs. However, it is important to find efficient solvers for such problems: this is another interesting challenge together with the establishment of unconditional stability.

In the case of classic Galerkin continuous finite element methods (FEM), several stabilizations have been proposed, most of them relying only on *heuristics*, without actually proving their effectiveness. Inspired by one of these works, we address the stability problem by studying the IGA method for an ordinary differential equation (ODE) closely related to the wave equation.

We study the conditioned stability of the IGA discretization for the following problem

$$\partial_{tt}u(t) + \mu u(t) = f(t), \quad \text{for } t \in (0, T), \quad u(0) = \partial_t u(t)|_{t=0} = 0,$$

where $T > 0$ is the final instant of time and $\mu > 0$ is the square of the wave-number. Eventually, we propose a stabilization, whose good behaviour is supported by numerical tests, and a possible extension to the wave-equation is suggested.

Contents

Abstract	v
1 Introduction	1
Outline	3
2 Preliminaries	5
2.1 Sobolev spaces in $(0, T)$	5
2.2 Spline spaces over a real interval	6
Univariate B-splines	7
Spline spaces	8
2.3 Variational methods	10
2.3.1 Well-posedness of abstract problems	10
2.3.2 Galerkin method	14
2.4 Preliminaries on compact perturbations	17
Galerkin method applied to Gårding-type problems	20
3 Second-order ordinary differential equation	23
3.1 Variational formulation for $\partial_{tt}u + \mu u = f$	23
3.2 Isogeometric discretization	25
3.2.1 Approximation properties of spline spaces with an initial boundary condition	27
3.2.2 Bound on the mesh-size, stability and quasi-optimality constants	31
Extension to quadratic IGA with maximal regularity of conditioned stability for piecewise continuous linear FEM	32
Application of Theorem 2.4.12 to quadratic IGA with maximal regularity	37
4 Numerical methods for $\partial_{tt}u + \mu u = f$	41
4.1 Conditioned stability	41
4.1.1 Errors committed by piecewise continuous linear finite element method	41
4.1.2 Inf-sup tests for piecewise continuous linear finite element method	45
4.1.3 Errors committed by quadratic isogeometric discretization with maximal regularity	49
4.1.4 Inf-sup tests for quadratic isogeometric discretization with maximal regularity	51
4.2 Unconditional stability	54

4.2.1	Stabilization of piecewise continuous linear finite element method	54
	Empirical reason for the unconditional stability of the perturbed FEM discretization	58
4.2.2	Stabilization for quadratic isogeometric discretization with maximal regularity	60
5	Conclusions	67
	Bibliography	73

Chapter 1

Introduction

The most widely used approaches for the numerical solution of time-dependent linear partial differential equations are based on semi-discretization in space and time, using a time-stepping approach: at each fixed discrete time instant, a corresponding discretization in space is considered. The proposed methodology is applied to parabolic differential equations and to hyperbolic problems in Chapter 6 and Chapter 8 of (Quarteroni, 2009). A possible alternative is the simultaneous discretization in space and time, i.e., a space-time discretization. Space-time methods for time-dependent linear partial differential equations present some advantages when compared with more standard space discretization plus time-stepping. For example, the approximate solutions are available at all times in the interval of interest and it could also be possible to use techniques that are already been used for elliptical problems, such as multigrid methods (Hackbusch, 2013) and domain decomposition (Chapter 14 of Quarteroni, 2009), which may allow parallelisation in time (Gander, 2015). A possible drawback is that a global linear system must be solved at once. Therefore, fast solvers and preconditioning become essential. For instance, in the case of space-time isogeometric discretization for parabolic problems see (Loli et al., 2020).

Let us now consider the homogeneous Dirichlet problem for the second-order wave equation:

$$\begin{cases} \partial_{tt}u(x, t) - \Delta_x u(x, t) = g(x, t) & (x, t) \in \Omega \times (0, T) \\ u(x, t) = 0 & (x, t) \in \partial\Omega \times [0, T] \\ u(x, 0) = \partial_t u(x, t)|_{t=0} = 0 & x \in \Omega, \end{cases} \quad (1.1)$$

where $\Omega \subset \mathbb{R}^d$, with $d = 1, 2, 3$, is an open bounded Lipschitz domain and, for a real value $T > 0$, $(0, T)$ is a time interval. In (Steinbach and Zank, 2020) the authors introduce a space-time variational formulation of (1.1), where integration by parts is also applied with respect to the time variable, and the classic anisotropic Sobolev spaces with homogeneous initial and boundary conditions are employed. Stability of a conforming tensor-product space-time discretization of this variational formulation with piecewise polynomial, continuous solution and test functions, requires a Courant – Friedrichs – Lewy (CFL) condition, i.e.,

$$h_t \leq Ch_x, \quad (1.2)$$

with a constant $C > 0$, depending on the constant of a spatial inverse inequality, where h_t and h_x are the (uniform) mesh-sizes in time and space, e.g. see (Steinbach and Zank, 2019; Zank, 2020, for the piecewise linear case). The CFL condition is necessary for convergence while solving certain partial differential equations (usually hyperbolic PDEs) numerically. It arises in the numerical analysis of explicit time integration schemes. According to that, the time step must be less than a certain value, otherwise the simulation produces incorrect results. The condition is named after Richard Courant, Kurt Friedrichs, and Hans Lewy who described it in (Courant, Friedrichs, and Lewy, 1928).

Several approaches have been proposed in order to overcome restriction (1.2). In (Steinbach and Zank, 2019) the authors, following the work of (Zlotnik, 2017), introduce a perturbation of the tensor-product space-time piecewise linear discretization of (1.1). As a result, they can prove unconditional stability and optimal convergence rates in space-time norms. In particular, they start by considering the ordinary differential equation

$$\partial_{tt}u(t) + \mu u(t) = f(t), \quad \text{for } t \in (0, T), \quad u(0) = \partial_t u(t)|_{t=0} = 0, \quad (1.3)$$

where $\mu > 0$, and its piecewise linear finite element discretization, since its stability is linked to the stability of the space-time standard FEM discretization of (1.1). They perturb the conforming discrete bilinear form, by considering the L^2 orthogonal projection on the piecewise constant finite element space. As a consequence, the new discrete system is unconditionally stable and convergence results hold without restrictions on the mesh-size. Finally, they extend this stabilization to the discretization for the wave-equation (1.1). In (Zank, 2021b), M. Zank generalises this stabilization idea to an arbitrary polynomial degree with global continuity. In particular, he provides numerical examples for a one-dimensional spatial domain, where the unconditional stability and optimal convergence rates in space-time norms are shown. On the other hand, theoretical considerations showing that such stabilization works are left to future papers.

In (Löscher, Steinbach, and Zank, 2021) the authors consider a suitable linear transformation that defines an isomorphism between the anisotropic solution and test spaces. In this way they are able to define a Galerkin-Bubnov formulation that is unconditionally stable without further perturbations. In particular, the operator they use is the modified Hilbert transformation introduced in (Steinbach and Zank, 2020; Steinbach and Zank, 2021b; Zank, 2021a). However, in (Löscher, Steinbach, and Zank, 2021), they only give numerical examples for a one- and a two-dimensional spatial domain, where the unconditional stability and optimal convergence rates in space-time norms are illustrated, and theoretical results are left to a future work.

As it is proven in (Zank, 2020), although the variational formulation to find the weak solution of (1.1) in a suitable anisotropic Sobolev subspace W of $H^1(\Omega \times (0, T))$ is well-defined for the right-hand-side g being in the dual of the anisotropic Sobolev test space V , it is not possible to establish unique solvability. Indeed, the *solution-to-data* operator between W and V' is not bijective. This is due to the fact that a stability condition, with respect to

the dual norm of the right-hand-side, is not satisfied, see Theorem 4.2.24 of (Zank, 2020). As a consequence, by the *bounded inverse Theorem* (or *inverse mapping Theorem*), the *solution-to-data* linear map cannot be bijective. To ensure existence and uniqueness of a weak solution, we need to assume that $g \in L^2(\Omega \times (0, T))$. This is a standard assumption to ensure sufficient regularity for the weak solution, and therefore, to obtain linear convergence for piecewise linear finite element approximations, but, as observed before, stability of common finite element discretizations require some CFL condition. In (Steinbach and Zank, 2021a) the authors introduce a new variational setting by enlarging the solution space. In this new framework they can prove that the *solution-to-data* linear map is an isomorphism. Based on these results, they aim to derive a space–time finite element method for the numerical solution of the wave equation that is unconditionally stable.

The goal of this thesis is to investigate the first steps towards an unconditionally stable space-time isogeometric method with maximal regularity, using a tensor-product approach, for the wave problem (1.1). In particular, following (Steinbach and Zank, 2019), the starting point is the analysis and the stabilization of the conforming discretization of (1.3).

The choice of isogeometric methods can be advantageous due to the high degree of approximation of B-spline technology (Hughes, Reali, and Sangalli, 2008; Sande, Manni, and Speleers, 2019) and due to the exact representation of the geometry with non uniform rational B-splines (NURBS), which simplifies mesh refinement, as further communications with CAD are not necessary (Hughes, Cottrell, and Bazilevs, 2005). In particular, the choice of isogeometric methods with maximal regularity can be advantageous in the case of wave propagation problems to tackle the so-called *pollution-effect*, which occurs in high-frequency wave problems (Babuška and Sauter, 2000). Indeed, a typical solution is to raise the order of the method: for the same number of degrees of freedom, methods that use piecewise polynomials of higher degree and regularity should perform better (Hughes, Reali, and Sangalli, 2008). Therefore, the choice of the IGA method with maximal regularity seems to be particularly suitable for this type of problems.

Outline

The rest of this thesis is organised as follows: in Chapter 2 Sobolev spaces, spline spaces and variational methods are fixed and their most important properties are repeated. In Chapter 3 the quadratic isogeometric method with maximal regularity for the ODE (1.3) is investigated. In Chapter 4 some numerical results are shown. In Chapter 5 a short summary of the thesis and some suggestions for future work are given.

Chapter 2

Preliminaries

In this Chapter we present notations for spaces with their properties and a general variational setting, recalling the Banach-Nečas-Babuška Theorem and the Lax-Milgram Lemma.

All the normed spaces that we will consider in the thesis will be real vector spaces. Hence, we are not going to specify this, except for the cases where it is preferable to underline.

In the whole work, for a real value $T > 0$, $(0, T)$ is a time interval.

2.1 Sobolev spaces in $(0, T)$

In this section we recall some useful Sobolev spaces that we will consider from now on.

With the usual notations, for $p \in \mathbb{N}$, the Hilbert space $H^p(0, T)$ is the Sobolev space of (classes of) real-valued functions endowed with the inner product $\langle \cdot, \cdot \rangle_{H^p(0, T)}$ and the induced norm $\|\cdot\|_{H^p(0, T)}$, i.e.

$$H^p(0, T) := \{u \in L^2(0, T) : \partial_t^m u \in L^2(0, T) \forall 0 \leq m \leq p\},$$

$$\langle u, v \rangle_{H^p(0, T)} := \int_0^T u(t)v(t) dt + \sum_{m=1}^p \int_0^T \partial_t^m u(t) \partial_t^m v(t) dt, \quad u, v \in H^p(0, T).$$

Also, we will consider the seminorm

$$|u|_{H^p(0, T)} := \sqrt{\int_0^T (\partial_t^p u(t))^2 dt}, \quad u \in H^p(0, T).$$

Since $H^1(0, T) \subset AC([0, T])$, the space of absolutely continuous functions, see (Brezis, 2011), we can define the following subspaces of $H^1(0, T)$

$$H_{0,*}^1(0, T) = \{u \in H^1(0, T) : u(0) = 0\},$$

$$H_{*,0}^1(0, T) = \{u \in H^1(0, T) : u(T) = 0\},$$

endowed with the Hilbertian norm

$$\|u\|_{H_{0,*}^1(0, T)} := |u|_{H^1(0, T)} = \|\partial_t u\|_{L^2(0, T)},$$

$$\|v\|_{H_{*,0}^1(0, T)} := |v|_{H^1(0, T)} = \|\partial_t v\|_{L^2(0, T)},$$

for $u \in H_{0,*}^1(0, T)$ and for $v \in H_{*,0}^1(0, T)$.

Clearly, for $1 \leq p \leq q$, $H^q(0, T) \subset H^p(0, T)$ with a continuous embedding, thus we can also define the following spaces

$$\begin{aligned} H_{0,*}^p(0, T) &= \{u \in H^p(0, T) : u(0) = 0\}, \\ H_{*,0}^p(0, T) &= \{u \in H^p(0, T) : u(T) = 0\}. \end{aligned}$$

Let $\delta \in \mathbb{R}$, with $\delta > T$. Recalling that the space $C_c^\infty(0, \delta)$ is dense in $H_0^1(0, \delta)$, the set

$$C_c^\infty(0, T] := \{\phi|_{(0,T]} : \phi \in C_c^\infty(0, \delta)\}$$

is dense in $H_{0,*}^1(0, T)$. Let $\eta \in \mathbb{R}$, with $\eta < 0$. Analogously, the set

$$C_c^\infty[0, T) := \{\phi|_{[0,T)} : \phi \in C_c^\infty(-\eta, T)\}$$

is dense in $H_{*,0}^1(0, T)$.

In $H_{0,*}^1(0, T)$ and $H_{*,0}^1(0, T)$ there hold inequalities of Poincaré type with sharp constants, see Lemma 3.4.5 of (Zank, 2020), i.e., for all $u \in H_{0,*}^1(0, T)$ and $v \in H_{*,0}^1(0, T)$, there hold

$$\|u\|_{L^2(0,T)} \leq \frac{2T}{\pi} \|\partial_t u\|_{L^2(0,T)} \quad \text{and} \quad \|v\|_{L^2(0,T)} \leq \frac{2T}{\pi} \|\partial_t v\|_{L^2(0,T)}, \quad (2.1)$$

and the constants in these inequalities are sharp. Thus, $\|\cdot\|_{H^1(0,T)}$ and $|\cdot|_{H^1(0,T)}$ are equivalent Hilbertian norm in $H_{0,*}^1(0, T)$ and in $H_{*,0}^1(0, T)$.

Remark 2.1.1. *The estimates (2.1) are more accurate (by a factor of about 0.1) than those proposed in (Steinbach and Zank, 2019). Therefore, the estimate proven by using (2.1) are slightly different from those in (Steinbach and Zank, 2019).*

The dual spaces $[H_{0,*}^1(0, T)]'$ and $[H_{*,0}^1(0, T)]'$ are Hilbert spaces, and they can be characterised as completions of $L^2(0, T)$ with respect to their dual Hilbertian norm, see (Wloka, Thomas, and Thomas, 1987).

2.2 Spline spaces over a real interval

In this Chapter we will give a brief overview of B-splines and of the most common spline spaces, all seen in the simple case of one-dimensional domains, which are the subjects of interest of Chapter 3. Our main references are (De Boor, 1978; Schumaker, 2007; Höllig and Hörner, 2013) and Chapter 1 of (Lyche, Manni, and Speleers, 2018). Note that there is a lot of literature on splines, given to the fact that they have application in several branches of the sciences.

First of all, let us remark that splines, in one- or plus- dimensional cases, in the broad sense of the term, are functions consisting of pieces of smooth functions glued together in a certain smooth way. The most popular species

is the one where the pieces are algebraic polynomials and inter-smoothness is imposed by means of equality of derivatives up to a given order. This species is the one of interest for isogeometric analysis, and is therefore the one we will consider in this Chapter in the one-dimensional case.

Univariate B-splines

The concept of knot vector is essential to define univariate B-splines.

Definition 2.2.1. A knot vector (or knot sequence) Ξ is a nondecreasing sequence of real numbers,

$$\Xi := \{\xi_i\}_{i=1}^m = \{\xi_1 \leq \dots \leq \xi_m\}, \quad m \in \mathbb{N}_{>0}.$$

The elements ξ_i are called knots and, if $\xi_1 \neq \xi_m$, the nondecreasing distinct knots are called break points.

Provided that $m \geq p + 2$, we can define univariate B-splines of degree p over the knot vector Ξ .

Definition 2.2.2. Suppose for a nonnegative integer p and some integer j that $\xi_j \leq \dots \leq \xi_{j+p+1}$ are $p + 2$ real numbers taken from a knot vector Ξ . The j -th B-spline of degree p is defined recursively by

$$b_{j,p,\Xi}(x) := \begin{cases} \frac{x-\xi_j}{\xi_{j+p}-\xi_j} b_{j,p-1,\Xi}(x) + \frac{\xi_{j+p+1}-x}{\xi_{j+p+1}-\xi_{j+1}} b_{j+1,p-1,\Xi}(x) & x \in [\xi_j, \xi_{j+p+1}) \\ 0 & \text{otherwise} \end{cases} \quad (2.2)$$

starting with

$$b_{i,0,\Xi}(x) := \begin{cases} 1 & x \in [\xi_i, \xi_{i+1}), \\ 0 & \text{otherwise,} \end{cases}$$

where we adopt the convention $0/0 = 0$.

Formula (2.2) is known as Cox-de Boor recursion formula.

Let us underline the following properties. For a proof and for more details on B-splines properties we refer to Chapter 1 of (Lyche, Manni, and Speleers, 2018)

- For degree 0 the B-spline $B_{i,0,\Xi}$ is simply the characteristic function of the half open interval $[\xi_i; \xi_{i+1})$, if $\xi_i \neq \xi_{i+1}$.
- A B-spline is right-continuous.
- A B-spline is locally supported on the interval given by the extreme knots used in its definition, i.e., $\text{supp}(b_{j,p,\Xi}) \subseteq [\xi_j, \xi_{j+p+1}]$ is a compact subinterval of $[\xi_j, \xi_{j+p+1}]$.

- A B-spline is nonnegative everywhere, and positive in the interior part of its support (if $\xi_{j+p+1} \neq \xi_j$), i.e.,

$$\begin{aligned} b_{j,p,\Xi}(x) &\geq 0 \quad \forall x \in \mathbb{R}, \\ b_{j,p,\Xi}(x) &> 0 \quad \forall x \in (\xi_j, \xi_{j+p+1}). \end{aligned}$$

- A B-spline $b_{j,p,\Xi}$ has a piecewise polynomial structure of degree less than or equal to p over the subintervals defined by the knots.
- We say that a knot has multiplicity m if it occurs exactly m times in the knot sequence. If ξ is a knot of $b_{j,p,\Xi}$ of multiplicity $m \leq p + 1$, then

$$b_{j,p,\Xi} \in C^{p-m}(\xi),$$

i.e., its derivatives of order $0, \dots, p - m$ are continuous at ξ , and $C^{-1}(\xi)$ denotes discontinuity at ξ . In particular, the maximal regularity at knots is C^{p-1} .

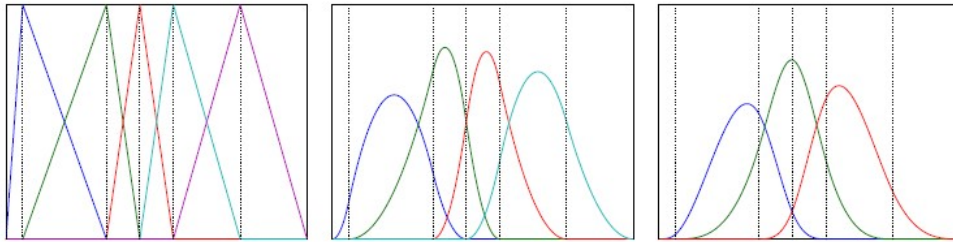


FIGURE 2.1: Several examples of B-splines of degree $p = 1, 2, 3$ respectively. The knot positions are visualized by vertical dotted lines. The same knot vector is chosen for the different degrees, with only simple knots, i.e., with knots with multiplicity equal to 1.

Spline spaces

Let $n > p \geq 0$ be two integers and let

$$\Xi := \{\xi_i\}_{i=1}^{n+p+1} = \{\xi_1 \leq \dots \leq \xi_{n+p+1}\}, \quad (2.3)$$

be a given knot vector. This knot sequence allows us to define a set of n B-splines of degree p , i.e.,

$$\{b_{1,p,\Xi}, \dots, b_{n,p,\Xi}\}.$$

We are now interested in considering a family of B-splines which is a basis of the space of piecewise polynomials of degree p on the intervals defined by the break points of the knot vector Ξ . Since the B-splines we are going to consider are restricted to the interval $[\xi_{p+1}, \xi_{n+1}]$, we define the B-splines to be left continuous at the right endpoint, in order to avoid an asymmetry.

Namely, we require that its value at ξ_{n+1} is obtained by taking limits from the left:

$$b_{j,p,\Xi}(\xi_{n+1}) := \lim_{x \rightarrow \xi_{n+1}^-} b_{j,p,\Xi}(x), \quad j = 1, \dots, n.$$

Definition 2.2.3. The knot vector (2.3) is said to be open on an interval $[a, b]$ if it satisfies

$$a = \xi_1 = \dots = \xi_{p+1} < \xi_{p+2} \leq \dots \leq \xi_n < \xi_{n+1} = \dots = \xi_{n+p+1} = b.$$

From now on we will simply say *open knot vector* without specifying the defining range $[a, b]$, except in cases where we are interested in underlying the defining domain.

Remark 2.2.4. The B-splines $\{b_{1,p,\Xi}, \dots, b_{n,p,\Xi}\}$ defined by an open knot vector Ξ satisfy the following properties:

- **Partition of unity:**

$$\sum_{i=1}^n b_{i,p,\Xi}(x) = 1, \quad \forall x \in [\xi_{p+1}, \xi_{n+1}].$$

- **Interpolation property:** $b_{1,p,\Xi}$ and $b_{n,p,\Xi}$ are interpolatory at ξ_{p+1} and ξ_{n+1} respectively, i.e.,

$$\begin{aligned} b_{1,p,\Xi}(\xi_{p+1}) &= 1, \\ b_{n,p,\Xi}(\xi_{n+1}) &= 1. \end{aligned}$$

- **Linear independence:** they are linearly independent on $[\xi_{p+1}, \xi_{n+1}]$.

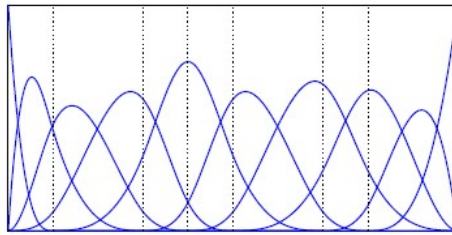


FIGURE 2.2: The B-spline basis of degree $p = 3$ on an open knot sequence. The knot positions are visualized by vertical dotted lines. The interior knots are simple, i.e., their multiplicity is equal to 1.

Let Δ be a sequence of real numbers:

$$\Delta := \{\eta_0 < \eta_1 < \dots < \eta_{l+1}\}. \quad (2.4)$$

Furthermore, let $\mathbf{r} := (r_1, \dots, r_l)$ be a vector of integers such that $-1 \leq r_i \leq p - 1$ for $i = 1, \dots, l$. The space $S_p^{\mathbf{r}}(\Delta)$ of piecewise polynomials of degree p

with smoothness \mathbf{r} over the partition (2.4) is defined by

$$S_p^{\mathbf{r}}(\Delta) := \{s : [\eta_0, \eta_{l+1}] \rightarrow \mathbb{R} \mid s \in \mathbb{P}_p([\eta_i, \eta_{i+1}]) \ i = 0, \dots, l-1, \\ s \in \mathbb{P}_p([\eta_l, \eta_{l+1}]), s \in C^{r_i}(\eta_i) \ i = 1, \dots, l\}. \quad (2.5)$$

Theorem 2.2.5 (Lyche, Manni, and Speleers, 2018). *The piecewise polynomial space (2.5) is characterized in terms of B-splines by*

$$S_p^{\mathbf{r}}(\Delta) = \text{span}\{b_{i,p,\Xi}\}_{i=1}^n, \quad (2.6)$$

where $\Xi := \{\xi_1 \leq \dots \leq \xi_{n+p+1}\}$ is an open knot sequence with $n := \dim(S_p^{\mathbf{r}}(\Delta))$ such that

$$\xi_1 = \dots = \xi_{p+1} := \eta_0, \quad \xi_{n+1} = \dots = \xi_{n+p+1} := \eta_{l+1},$$

and

$$\xi_{p+2}, \dots, \xi_n := \overbrace{\eta_1, \dots, \eta_1}^{p-r_1}, \dots, \overbrace{\eta_l, \dots, \eta_l}^{p-r_l}.$$

The space (2.6) is called *spline space*. We will denote it by $S_{\Xi}^p([\xi_{p+1}, \xi_{n+1}])$ in the case of C^{p-1} global regularity, or with $S_h^p([\xi_{p+1}, \xi_{n+1}])$, where h is defined as $h := \max\{|\xi_{i+1} - \xi_i| : i = 1, \dots, n+p+1\}$. Our choice will depend on which notation is most convenient for the case we consider.

Definition 2.2.6. *The coefficients of the B-splines generating the spline space are called control points or degrees of freedom. The elements in (2.6) are also called B-spline curves.*

Let us note that an affine transformation of a B-spline curve is obtained by applying the transformation to control points (Hughes, Cottrell, and Bazilevs, 2005). This is one of the many reasons why these curves are widely used in Computer-Aided Design (CAD).

Remark 2.2.7. *In general, control points do not interpolate B-spline curves in knots. Instead, extremal control points interpolate B-spline curves at the extremal knots ξ_{p+1} and ξ_{n+1} .*

Remark 2.2.8. *In this section on spline spaces we could have followed a more general treatment, instead of considering only open knot vectors. This was not of interest to us, since open knot vectors are the ones used in CAD and isogeometric analysis. See (Lyche, Manni, and Speleers, 2018) if you are interested in a more general discussion.*

2.3 Variational methods

2.3.1 Well-posedness of abstract problems

In this Section we introduce an abstract variational problem and determine the conditions under which this problem is well-posed. The main references of this Section are Chapter 2 of (Ern and Guermond, 2004) and (Norikazu, 2018).

Let V and W be two vector spaces endowed with norms $\|\cdot\|_V$ and $\|\cdot\|_W$. Let $a : W \times V \rightarrow \mathbb{R}$ be a given bounded bilinear form and let $\mathcal{F} \in V'$. Let us consider the following abstract variational problem

$$\begin{cases} \text{Find } u \in W \text{ such that} \\ a(u, v) = \langle \mathcal{F}, v \rangle_{V', V} \quad \forall v \in V. \end{cases} \quad (2.7)$$

W is called the *solution space* and V is called the *test space*.

Remark 2.3.1. A significant question is: what do we mean by **solution** of a partial differential equation (PDE)? One could ask for the PDE of order k to be solved pointwise by one (or more) functions of class C^k , or even by one (or more) of class C^∞ : in this case the solution(s) is (are) called *classical* or *strong solution(s)*. However, in general, solutions to relevant problems are not so regular. Therefore, the concept of a *weak solution* is introduced for a given PDE and, if necessary, its regularity is studied. Typically, the variational formulation (2.7) results from the weak formulation of PDEs. Consider, for example, the Poisson problem:

$$\begin{cases} -\Delta u(x) = f(x) & x \in \Omega \\ u(x) = 0 & x \in \partial\Omega, \end{cases}$$

where $\Omega \subset \mathbb{R}^n$ is an open bounded Lipschitz domain. By integration by part, its weak formulation reads as follows

$$\begin{cases} \text{Find } u \in H_0^1(\Omega) \text{ such that} \\ \langle \nabla u, \nabla v \rangle_{L^2(\Omega)} = \langle f, v \rangle_\Omega \quad \forall v \in H_0^1(\Omega), \end{cases} \quad (2.8)$$

where $f \in H^{-1}(\Omega)$ is given. In particular, in (2.8), the bilinear form is defined as

$$\begin{aligned} a : H_0^1(\Omega) \times H_0^1(\Omega) &\longrightarrow \mathbb{R} \quad \text{s.t.} \\ a(u, v) &= \langle \nabla u, \nabla v \rangle_{L^2(\Omega)} \quad \forall (u, v) \in H_0^1(\Omega) \times H_0^1(\Omega). \end{aligned}$$

Definition 2.3.2 (Hadamard). Problem (2.7) is said to be *well-posed* if it admits one and only one solution and if the following a priori estimate holds:

$$\exists C > 0 : \forall \mathcal{F} \in V', \quad \|u\|_W \leq C \|\mathcal{F}\|_{V'}. \quad (2.9)$$

Remark 2.3.3. The notion of well-posedness of a problem captures many of the desirable characteristics for a solution of a PDE. In particular, condition (2.9) is very important for problems arising from physical applications. Indeed, it is clearly preferable that the solution has a “little” change when the specific conditions of the problem have “little” changes.

Remark 2.3.4. A bounded, linear operator $\mathcal{A} : W \rightarrow V'$ is associated with the bounded bilinear form $a(\cdot, \cdot)$ by setting

$$\langle \mathcal{A}u, v \rangle_{V', V} := a(u, v), \quad u \in W, v \in V.$$

Therefore, problem (2.7) amounts to seeking $u \in W$ such that $\mathcal{A}u = \mathcal{F}$ in V' .

The two following statements are equivalent:

- The variational problem (2.7) is well-posed.
- The bounded linear operator $\mathcal{A} : W \rightarrow V'$ associated with the continuous bilinear form $a(\cdot, \cdot)$ is an isomorphism.

Also, every bounded, linear operator $\mathcal{A} : W \rightarrow V'$ defines a bounded bilinear form $a : W \times V \rightarrow \mathbb{R}$ by setting

$$a(u, v) := \langle \mathcal{A}u, v \rangle_{V', V}, \quad u \in W, v \in V.$$

The Banach-Nečas-Babuška Theorem. This Theorem gives necessary and sufficient conditions for the well-posedness of (2.7).

Theorem 2.3.5 (Banach-Nečas-Babuška, (Norikazu, 2018)). *Let $(W, \|\cdot\|_W)$ be a real Banach space, let $(V, \|\cdot\|_V)$ be a real reflexive, Banach space. Then the following statements are equivalent:*

1. The variational problem (2.7) is well-posed.
2. For the bounded bilinear form $a : W \times V \rightarrow \mathbb{R}$ there hold:
 - There exists a constant $\beta > 0$ such that

$$\inf_{u \in W} \sup_{v \in V} \frac{a(u, v)}{\|u\|_W \|v\|_V} \geq \beta. \quad (2.10)$$

- For each $v \in V$,

$$(\forall u \in W, a(u, v) = 0) \implies (v = 0) \quad (2.11)$$

3. There exist two constants $\beta, \gamma > 0$ such that

$$\begin{aligned} \inf_{u \in W} \sup_{v \in V} \frac{a(u, v)}{\|u\|_W \|v\|_V} &\geq \beta, \\ \inf_{v \in V} \sup_{u \in W} \frac{a(u, v)}{\|u\|_W \|v\|_V} &\geq \gamma. \end{aligned}$$

Condition (2.10) is usually called the *inf-sup* condition or the *Babuška-Brezzi* condition.

Remark 2.3.6. *The following statements hold:*

- Given V and W two real normed spaces, condition (2.10) is expressed equivalently as

$$\exists \beta > 0 : \beta \|u\|_W \leq \sup_{v \in V} \frac{a(u, v)}{\|v\|_V} \quad \forall u \in W.$$

Under the assumptions of Theorem 2.3.5:

- The well-posedness of (2.7) is satisfied with

$$\|u\|_W \leq \frac{1}{\beta} \|\mathcal{F}\|_{V'}.$$

In general, given V and W two normed spaces, if (2.7) admits unique solution for every $\mathcal{F} \in V'$, then condition (2.9) is equivalent to (2.10) with $\beta = \frac{1}{C}$.

- We can translate conditions (2.10), (2.11) into conditions for the linear operator $\mathcal{A}(\cdot)$, see (Ern and Guermond, 2004).

$$(2.10) \iff (\ker(\mathcal{A}) = \{0\} \text{ and } \text{Im}(\mathcal{A}) \text{ is closed}) \iff (\mathcal{A}^* \text{ is surjective}),$$

$$(2.11) \iff (\ker(\mathcal{A}^*) = \{0\}) \iff (\mathcal{A}^* \text{ is injective}),$$

where \mathcal{A}^* is the adjoint operator of \mathcal{A} .

In general, given X and Y two real normed vector spaces and a linear operator $\mathcal{A} : X \rightarrow Y$, if \mathcal{A} is invertible, then the adjoint operator of \mathcal{A} is invertible and satisfies $(\mathcal{A}^*)^{-1} = (\mathcal{A}^{-1})^*$, see (Fessler, 2004) for the case of Hilbert spaces (the generalisation of the results to the case of any normed space is straightforward). In particular, as a consequence of $(\mathcal{A}^*)^{-1} = (\mathcal{A}^{-1})^*$ and of the equality in norm between an operator and its adjoint, if \mathcal{A} is isomorphism, then \mathcal{A}^* is an isomorphism with the same continuity constants (also for the inverse maps). The BNB Theorem 2.3.5 guarantees that, if $X = W$ is a real Banach space, and $Y = V'$, with V that is a real reflexive Banach space, the reverse is also true, i.e., if \mathcal{A}^* is an isomorphism, then \mathcal{A} is an isomorphism.

- The well-posedness of the adjoint problem

$$\begin{cases} \text{Find } v \in V \text{ such that} \\ a(u, v) = \langle \mathcal{G}, u \rangle_{W', W} \quad \forall u \in W, \end{cases}$$

where $\mathcal{G} \in W'$, is equivalent to \mathcal{A}^* being an isomorphism.

The Lax-Milgram Lemma. Consider the case where the solution space and the test space are identical Hilbert spaces. Thus, the abstract variational problem has the following formulation:

$$\begin{cases} \text{Find } u \in V \text{ such that} \\ a(u, v) = \langle \mathcal{F}, v \rangle_{V', V} \quad \forall v \in V \end{cases} \quad (2.12)$$

The Lax-Milgram Lemma gives *sufficient* conditions under which problem (2.12) is well-posed.

Lemma 2.3.7 (Lax-Milgram). Let V be a Hilbert space, let $a : V \times V \rightarrow \mathbb{R}$ be a bounded bilinear form. Assume that $a(\cdot, \cdot)$ is coercive, i.e,

$$\exists \alpha > 0 : \forall u \in V, a(u, u) \geq \alpha \|u\|_V^2. \quad (2.13)$$

Let $\mathcal{F} \in V'$. Then problem (2.7) is well-posed with the following a priori estimate

$$\|u\|_V \leq \frac{1}{\alpha} \|\mathcal{F}\|_{V'}.$$

The Lax-Milgram Lemma can be viewed as a Corollary of the Banach-Nečas-Babuška Theorem, since the coercivity of $a(\cdot, \cdot)$ implies statement 2 of Theorem 2.3.5.

Lemma 2.3.8. *The coercivity condition (2.13) implies conditions (2.10), (2.11) of the BNB Theorem.*

Proof. Let $u \in V$. Condition (2.10) is immediately deduced from

$$\alpha \|u\|_V \stackrel{(2.13)}{\leq} \frac{a(u, u)}{\|u\|_V} \leq \sup_{v \in V} \frac{a(u, v)}{\|v\|_V}.$$

Let now $v \in V$. As a consequence of coercivity there hold

$$\sup_{u \in V} a(u, v) \geq a(v, v) \stackrel{(2.13)}{\geq} \alpha \|v\|_V^2.$$

Therefore, $\sup_{u \in V} a(u, v) = 0$ implies $v = 0$, i.e., (2.11). \square

Remark 2.3.9. *The reversal of Lemma 2.3.8 is wrong, i.e., (2.13) is not equivalent to the well-posedness of (2.12). However, when the bilinear form $a(\cdot, \cdot)$ is symmetric and positive, coercivity is equivalent to well-posedness, see (Ern and Guermond, 2004).*

2.3.2 Galerkin method

Let W_h be a finite-dimensional subspace of W and V_h be a finite-dimensional subspace of V . The Galerkin method constructs an approximation of the solution u of the abstract variational problem (2.7) by solving the following problem

$$\begin{cases} \text{Find } u_h \in W_h \text{ such that} \\ a(u_h, v_h) = \langle \mathcal{F}|_{V_h}, v_h \rangle_{V_h', V_h} \quad \forall v_h \in V_h. \end{cases} \quad (2.14)$$

W_h is called the *solution space* or the *trial space*, whereas V_h is called the *test space*. If the trial space and the test space are the same, the Galerkin method is the following problem:

$$\begin{cases} \text{Find } u_h \in V_h \text{ such that} \\ a(u_h, v_h) = \langle \mathcal{F}|_{V_h}, v_h \rangle_{V_h', V_h} \quad \forall v_h \in V_h. \end{cases} \quad (2.15)$$

Typically, the former is called *Galerkin-Petrov method*, whereas the latter is called *Galerkin-Bubnov method*.

Remark 2.3.10. *We can also consider W_h and V_h as closed subspaces of W and V respectively, but, for the numerical approximation of u , we are interested in finite-dimensional subspaces of the trial and test spaces.*

We are interested in investigating the well-posedness of the approximate problems (2.14), (2.15), in proving a stability condition, i.e., a uniform (w.r.t a numerical parameter h indexing the discrete spaces) a priori estimate (2.9) for the discrete problem, and convergence results (w.r.t h) of the discrete solution to the abstract one. Let us begin by considering the first and second questions. The following Proposition is straightforward.

Proposition 2.3.11. *If the variational problem (2.12) satisfies Lax-Milgram hypothesis, then the variational problem (2.15) is well-posed. In particular, for all $\mathcal{F} \in V'$ the stability estimate $\|u_h\|_V \leq \frac{1}{\alpha} \|\mathcal{F}\|_{V'}$ holds.*

Proof. We can apply Lax-Milgram Lemma 2.3.7 since the bilinear form $a(\cdot, \cdot)$ is coercive in V_h . \square

In general, instead, there is no guarantee that conditions (2.10), (2.11) of the BNB Theorem are automatically transferred from the abstract problem to the approximate problem. Thanks to the BNB Theorem, the well-posedness of (2.14) is equivalent to the following discrete conditions:

- There exists a constant $\beta_h > 0$ such that

$$\inf_{u_h \in W_h} \sup_{v_h \in V_h} \frac{a(u_h, v_h)}{\|u_h\|_{W_h} \|v_h\|_{V_h}} \geq \beta_h. \quad (2.16)$$

- For each $v_h \in V_h$,

$$(\forall u_h \in W_h, a(u_h, v_h) = 0) \implies (v_h = 0) \quad (2.17)$$

Condition (2.16) is usually called *discrete inf-sup condition*.

Remark 2.3.12. *In many cases, the subscript h denotes the mesh-size of the discretization and, in general, we are interested in proving an a priori estimate (2.9) for the discrete problem that is independent of h . Hence, the discrete inf-sup condition (2.16) is not sufficient for the desired stability, if no information on the value of β_h is available.*

Remark 2.3.13. *Evaluating the bilinear form $a(\cdot, \cdot)$ and the linear operator $\mathcal{F}(\cdot)$ on the basis functions of the spaces W_h and V_h , we obtain a linear system that is equivalent to the general approximate problem (2.14), see (Ern and Guermond, 2004). We use the notation \mathbf{A} for the system matrix, which will be referred to as the stiffness matrix.*

There hold the following statements.

1. *The well-posedness of the approximate problem is equivalent to non-singularity of \mathbf{A} .*
2. *If the abstract bilinear form $a(\cdot, \cdot)$ of problem (2.12) is coercive, \mathbf{A} is positive definite, i.e., defined $M := \dim(V_h)$, there holds*

$$(\exists \alpha > 0 : \forall u \in V, a(u, u) \geq \alpha \|u\|_V^2) \implies \\ (\forall X \in \mathbb{R}^M, (\mathbf{A}X, X) \geq 0 \text{ and } ((\mathbf{A}X, X) = 0 \iff X = 0)).$$

3. If $a(\cdot, \cdot)$ is symmetric, \mathbf{A} is symmetric.
4. Condition (2.16) is equivalent to $\ker(A) = \{0\}$, i.e., to the injectivity of \mathbf{A} .
5. Condition (2.17) is equivalent to $\text{rank}(\mathbf{A}) = \dim(V_h)$, i.e., to the surjectivity of \mathbf{A} .
6. If $\dim(V_h) = \dim(W_h)$, (2.16) is equivalent to (2.17).

For a proof we refer to (Ern and Guermond, 2004).

Let us now consider the convergence of the discrete solution to the abstract solution. In this connection, we recall some classic results.

Lemma 2.3.14 (Galerkin orthogonality). *Let u be the solution of the general abstract problem (2.7) and u_h be the solution of the general approximate problem (2.14), then there holds*

$$a(u - u_h, v_h) = 0 \quad \forall v_h \in V_h. \quad (2.18)$$

Proof. This is immediate using the bilinearity of $a(\cdot, \cdot)$. \square

Lemma 2.3.15 (Céa). *Let the hypothesis of Lax-Milgram Lemma 2.3.7 be satisfied. Assuming u is the solution of (2.12) and u_h is the solution of (2.15), then the following estimate holds*

$$\|u - u_h\|_V \leq \frac{C_a}{\alpha} \inf_{v_h \in V_h} \|u - v_h\|_V, \quad (2.19)$$

where C_a is the continuity constant of $a(\cdot, \cdot)$.

Proof. Let $v_h \in V_h$. As a consequence of coercivity, bilinearity, continuity and Galerkin orthogonality there hold

$$\begin{aligned} \alpha \|u - u_h\|^2 &\stackrel{(2.13)}{\leq} a(u - u_h, u - u_h) \\ &= a(u - u_h, u - v_h + v_h - u_h) \\ &= a(u - u_h, u - v_h) + a(u - u_h, v_h - u_h) \quad (\text{bilinearity of } a(\cdot, \cdot)) \\ &\stackrel{(2.18)}{=} a(u - u_h, u - v_h) \\ &\leq C_a \|u - u_h\|_V \|u - v_h\| \quad (\text{continuity of } a(\cdot, \cdot)). \end{aligned}$$

\square

Remark 2.3.16. *Note that (2.19) is a quasi-optimality estimate. Typically, a quasi-optimality bound is an important result, since, according to that, the error committed by the Galerkin method depends on two terms. The first one, which is $\frac{C_a}{\alpha}$ in this case, is a stability term: it is only related to the continuous problem. The second one, i.e., the best approximation error $\inf_{v_h \in V_h} \|u - v_h\|_V$, measures how well the discrete space is able to approximate the solution u . In particular, if $(V_h)_h$ are dense in V , i.e., if*

$$\inf_{v_h \in V_h} \|u - v_h\|_V \xrightarrow{h \rightarrow 0} 0 \quad \forall u \in V,$$

estimate (2.19) tells us that we eventually reach convergence.

In the Banach-Nečas-Babuška setting, quasi-optimality estimates are also obtained.

Let us assume that the general abstract problem (2.7) is well-posed. We denote by C_a the continuity constant of the bilinear form $a(\cdot, \cdot)$. Let us suppose that the discrete problem (2.14) satisfies the two BNB conditions (2.16), (2.17), and that the discrete inf-sup condition is independent of the index h (this is the case of greatest interest), and we denote it by β_{dis} . The following result holds.

Proposition 2.3.17. *Assuming u is the solution of (2.12) and u_h is the solution of (2.14), then the following quasi-optimality estimate holds*

$$\|u - u_h\|_W \leq \left[1 + \frac{C_a}{\beta_{dis}} \right] \inf_{w_h \in W_h} \|u - w_h\|_W,$$

where C_a is the continuity constant of $a(\cdot, \cdot)$ and β_{dis} is the inf-sup uniform constant of the discrete problem (2.14).

Proof. For any $w \in W$ we define $w_h := G_h w \in W_h$ as the Galerkin projection satisfying

$$a(G_h w, v_h) = a(w, v_h) \quad \forall v_h \in V_h,$$

which is well defined thanks to the well-posedness of the discrete problem. Hence, by using the stability estimate (2.16) with β_{dis} and the continuity of $a(\cdot, \cdot)$ with C_a , there hold

$$\begin{aligned} \beta_{dis} \|G_h w\|_W &\leq \sup_{0 \neq v_h \in V_h} \frac{a(G_h w, v_h)}{\|v_h\|_V} \quad (\text{discrete infsup}) \\ &= \sup_{0 \neq v_h \in V_h} \frac{a(w, v_h)}{\|v_h\|_V} \\ &\leq C_a \|w\|_W \quad (\text{boundness of } a(\cdot, \cdot)). \end{aligned}$$

Since $u_h = G_h u$ and $w_h = G_h w$ for all $w_h \in W_h$, we conclude

$$\begin{aligned} \|u - u_h\|_W &\leq \|u - w_h\|_W + \|G_h(w_h - u)\|_W \\ &\leq \left[1 + \frac{C_a}{\beta_{dis}} \right] \|u - w_h\|_W. \end{aligned}$$

□

2.4 Preliminaries on compact perturbations

In this Section we recall the definitions of two important classes of bounded linear operators between Hilbert spaces, emphasizing the most important properties that will be useful in Chapter 3. The main references of this Section are (Sayas, 2006; Brezis, 2011; Sayas, Brown, and Hassell, 2019; Moiola, 2021).

Definition 2.4.1 (Compact operator). *Let H_1 and H_2 be two Hilbert (or Banach) spaces. A bounded linear operator $K : H_1 \rightarrow H_2$ is compact if the image of a bounded sequence admits a converging subsequence, i.e., the image of a bounded set in H_1 is pre-compact in H_2 .*

Definition 2.4.2 (Fredholm operator). *Let H_1 and H_2 be two Hilbert spaces. A bounded linear operator $T : H_1 \rightarrow H_2$ is a Fredholm operator of index 0 if it is the sum of an invertible one and a compact one.*

Remark 2.4.3. *Actually, definition 2.4.2 is a possible characterization of Fredholm operators of index 0. E.g. (Brezis, 2011) defines $T : H_1 \rightarrow H_2$ (bounded linear operator between Hilbert spaces) as Fredholm operator of $\text{Ind}(T) := \dim(\text{Ker}T) - \dim(\text{Im}T)^\perp$ if $\dim(\text{Ker}T), \dim(\text{Im}T)^\perp < \infty$. For a proof of the equivalence with this classic definition we refer to (Moiola, 2021).*

Henceforth, Fredholm operators of index 0 will be refer to as Fredholm operators.

An important result is the *Fredholm alternative*, which, in its simplest form, reads as follows; see (Brezis, 2011).

Theorem 2.4.4 (Fredholm alternative). *Let $T : H_1 \rightarrow H_2$ be a Fredholm operator. Then T is injective if and only if it is surjective. In this case its inverse is bounded.*

Remark 2.4.5. *Note that the boundedness of the inverse of an invertible Fredholm operator is due to the “bounded inverse Theorem”.*

Remark 2.4.6. *In a finite dimensional setting Fredholm operators are precisely those associated to square matrices. Indeed, an invertible linear operator between finite-dimensional spaces corresponds to an invertible square matrix, and all finite-range operators are compact, since all bounded sequences of \mathbb{R}^n admits converging subsequences. Thus, Theorem 2.4.2 is an extension of the finite-dimensional case.*

Abstract problem and Galerkin method. Let H be an Hilbert space and $\mathcal{F} \in H'$. Let now consider the following variational problem

$$\begin{cases} \text{Find } u \in H \text{ such that} \\ a(u, v) := b(u, v) + d(u, v) = \langle \mathcal{F}, v \rangle_{H', H} \quad \forall v \in H, \end{cases} \quad (2.20)$$

where:

1. The bilinear form $b(\cdot, \cdot)$ is bounded and coercive.
2. The bilinear form $d(\cdot, \cdot)$ defines a compact operator $\mathcal{D} : H \rightarrow H'$ by setting

$$\langle \mathcal{D}u, v \rangle_{H', H} := d(u, v), \quad u, v \in H.$$
3. The linear operator $\mathcal{A} := \mathcal{B} + \mathcal{D} : H \rightarrow H'$ associated to the bilinear form $a(\cdot, \cdot)$ is injective, where

$$\langle \mathcal{B}u, v \rangle_{H', H} := b(u, v) \quad u, v \in H.$$

Assumptions 1 and 2, and Lax-Milgram Lemma 2.3.7, ensure that the operator \mathcal{A} is Fredholm. As a consequence of assumption 3 and Theorem 2.4.2, problem (2.20) is well-posed.

Let now consider a family of finite-dimensional subspaces $V_h \subset H$ directed in a real non-negative parameter $h \rightarrow 0$ and let $\pi_h : H \rightarrow V_h$ be the orthogonal projection. Let us also assume that

$$\pi_h u \xrightarrow{h \rightarrow 0} u, \quad \forall u \in H, \quad (2.21)$$

i.e., $(V_h)_h$ is a dense discrete family of subspaces in H . As in Section 2.3.2, we refer to the following problem as the Galerkin approximation of (2.20):

$$\begin{cases} \text{Find } u_h \in V_h \text{ such that} \\ a(u_h, v_h) = \langle \mathcal{F}|_{V_h}, v_h \rangle \quad \forall v_h \in V_h. \end{cases} \quad (2.22)$$

In our work the subscript h corresponds to the sequence of mesh-sizes of our discretization.

The results that we are going to recall establish the uniform (w.r.t. h) well posedness of problem (2.22), provided the mesh-size is *small enough* (Proposition 8.8 of Sayas, Brown, and Hassell, 2019). Moreover, a quasi-optimality estimate will follow.

Proposition 2.4.7. *In the hypothesis (1)-(3) for the bilinear forms, there exist two constants $C, \bar{h} > 0$ such that the following inf-sup estimate holds*

$$\beta \|u_h\|_H \leq \sup_{0 \neq v_h \in V_h} \frac{b(u_h, v_h) + d(u_h, v_h)}{\|v_h\|_H} \quad \forall u_h \in V_h, \quad \forall h \leq \bar{h}.$$

Remark 2.4.8. *The bound on the mesh-size and the inf-sup constant are not explicit because the proof of this result is made by contradiction.*

Corollary 2.4.9. *Let the hypothesis of Proposition 2.4.7 be satisfied. Let $h \leq \bar{h}$. Then problem (2.22) is well-posed, with the following stability estimate*

$$\|u_h\|_H \leq \frac{1}{\beta} \|\mathcal{F}\|_{H'}, \quad \mathcal{F} \in H'.$$

Note that Corollary 2.4.9 is a consequence of Remark 2.3.13 and of BNB Theorem 2.3.5.

Corollary 2.4.10. *Under the hypothesis of Proposition 2.4.7, let $h \leq \bar{h}$. Then a quasi-optimality estimate holds*

$$\|u - u_h\|_H \leq \left(1 + \frac{\|\mathcal{B} + \mathcal{D}\|}{\beta}\right) \inf_{v_h \in V_h} \|u - v_h\|_H, \quad (2.23)$$

where u, u_h are the solutions of (2.20), (2.22) respectively and with $\|\cdot\|$ we denote the operator norm of linear bounded maps from H to H' .

Remark 2.4.11. Note that Corollary 2.4.10 is a consequence of Proposition 2.3.17 and tells that we eventually reach convergence for $h \rightarrow 0$, since the succession of discrete spaces is dense in H .

Galerkin method applied to Gårding-type problems

In this Section we consider a special case of Fredholm operators. Roughly speaking, we consider Fredholm operators whose compact perturbation we can "quantify". For these operators it is possible to have stability and error estimates with explicit constants. The theory we are interested in is that of *Galerkin method applied to Gårding-type problems*. Our main reference are (Spence, 2014; Moiola, 2021).

Let H be a real Hilbert space, $V_h \subset H$ a finite-dimensional subspace, $a(\cdot, \cdot)$ and $\mathcal{F}(\cdot)$ a bounded bilinear form and a bounded linear operator on H , respectively. Let us now consider the following abstract variational problem

$$\begin{cases} \text{Find } u \in H \text{ such that} \\ a(u, v) = \langle \mathcal{F}, v \rangle_{H', H} \quad \forall v \in H, \end{cases} \quad (2.24)$$

and its Galerkin discretization

$$\begin{cases} \text{Find } u_h \in V_h \text{ such that} \\ a(u_h, v_h) = \langle \mathcal{F}|_{V_h}, v_h \rangle_{V_h', V_h} \quad \forall v_h \in V_h. \end{cases} \quad (2.25)$$

Theorem 2.4.12 (Galerkin method with Gårding inequality). *Let $H \subset V$ be real Hilbert spaces and the inclusion be compact. Let $a(\cdot, \cdot)$ be a bounded bilinear form on H with respect to a continuity constant $C_a > 0$:*

$$|a(v, w)| \leq C_a \|v\|_H \|w\|_H \quad \forall v, w \in H,$$

that satisfies the Gårding inequality with respect to $\alpha, C_v > 0$

$$a(v, v) \geq \alpha \|v\|_H^2 - C_v \|v\|_V^2 \quad \forall v \in H. \quad (2.26)$$

Assume that the only $u_0 \in H$ such that $a(u_0, v) = 0$ for all $v \in H$ is $u_0 = 0$ (so that the variational problem (2.24) is well-posed for any right-hand side). Let $\mathcal{F}(\cdot)$ be a bounded linear operator on H and u be the solution of the variational problem (2.24).

Given $g \in V$, let $z_g \in H$ be the solution of the adjoint problem

$$a(v, z_g) = (g, v)_V \quad \forall v \in H, \quad (2.27)$$

where $(\cdot, \cdot)_V$ is the scalar product in V . Let $V_h \subset H$ be a finite-dimensional subspace of H and define

$$\eta(V_h) := \sup_{0 \neq g \in V} \inf_{v_h \in V_h} \frac{\|z_g - v_h\|_H}{\|g\|_V}. \quad (2.28)$$

If $\eta(V_h)$ satisfies the threshold condition

$$\eta(V_h) \leq \frac{1}{C_a} \sqrt{\frac{\alpha}{2C_V}}, \quad (2.29)$$

then the Galerkin method (2.25) is well-posed with the following stability estimate

$$\|u_h\|_H \leq C_{stab} \left(1 + \frac{2C_a}{\alpha} \right) \|\mathcal{F}\|_{H'},$$

where C_{stab} is the stability constant of the abstract problem (2.24), and its solution u_h satisfies the quasi-optimality bound

$$\|u - u_h\|_H \leq \frac{2C_a}{\alpha} \inf_{v_h \in V_h} \|u - v_h\|_H.$$

Remark 2.4.13. Note the following facts.

1. The Gårding inequality (2.26) and the compact inclusion $H \subset V$ imply that the solution-to-data operator $\mathcal{A} : H \rightarrow H', u \mapsto a(u, \cdot)$ is Fredholm (of index 0). For a proof we refer to (Spence, 2014). Therefore, the assumption

“the only $u_0 \in H$ such that $a(u_0, v) = 0$ for all $v \in H$ is $u_0 = 0$ ”

implies the well-posedness of the variational problem (2.24), since the above assumption is equivalent to the injectivity of \mathcal{A} . In particular we can apply Theorem 2.4.4.

2. The well-posedness of the adjoint problem (2.27) (w.r.t. the dual norm $\|g\|_{H'}$, and hence w.r.t. $\|g\|_V$) is a consequence of the well-posedness of the primal problem (2.24). Indeed, if $\mathcal{A} : H \rightarrow H'$ is an isomorphism, its adjoint operator $\mathcal{A}^* : H \rightarrow H'$ is an isomorphism, with $(\mathcal{A}^*)^{-1} = (\mathcal{A}^{-1})^*$, see (Fessler, 2004). Also, as a consequence of $(\mathcal{A}^*)^{-1} = (\mathcal{A}^{-1})^*$, there holds $\|(\mathcal{A}^*)^{-1}\| = \|\mathcal{A}^{-1}\|$. Hence, the stability constant of the adjoint problem (w.r.t. the dual norm $\|g\|_{H'}$) is equal to the stability constant of the primal problem.
3. The parameter $\eta(V_h)$ precisely quantify how well V_h approximates the solution of the adjoint problem, whose data g is an element of the larger space V . Thus, roughly speaking, Theorem 2.4.12 states that if the discrete space is sufficiently fine, the Galerkin method applied to a Gårding-type (well-posed) problem is well-posed, stable and quasi-optimal.

Chapter 3

Second-order ordinary differential equation

3.1 Variational formulation for $\partial_{tt}u + \mu u = f$

As a model problem we consider the following second-order linear equation:

$$\partial_{tt}u(t) + \mu u(t) = f(t), \quad \text{for } t \in (0, T), \quad u(0) = \partial_t u(t)|_{t=0} = 0, \quad (3.1)$$

where $\mu > 0$.

The variational formulation of (3.1) reads as follows:

$$\begin{cases} \text{Find } u \in H_{0,*}^1(0, T) & \text{such that} \\ a(u, v) = \langle f, v \rangle_{(0, T)} & \forall v \in H_{*,0}^1(0, T), \end{cases} \quad (3.2)$$

where $T > 0$ and $f \in [H_{*,0}^1(0, T)]'$ are given, and where the bilinear form $a(\cdot, \cdot) : H_{0,*}^1(0, T) \times H_{*,0}^1(0, T) \rightarrow \mathbb{R}$ is

$$a(u, v) := -\langle \partial_t u, \partial_t v \rangle_{L^2(0, T)} + \mu \langle u, v \rangle_{L^2(0, T)}, \quad (3.3)$$

for all $u \in H_{0,*}^1(0, T)$, $v \in H_{*,0}^1(0, T)$. The notation $\langle \cdot, \cdot \rangle_{(0, T)}$ denotes the duality pairing as extension of the inner product in $L^2(0, T)$, and the Sobolev spaces $H_{0,*}^1(0, T)$, $H_{*,0}^1(0, T)$ are introduced in Section 2.1. Note that the first initial condition $u(0) = 0$ is incorporated in the solution space $H_{0,*}^1(0, T)$, whereas the second initial condition $\partial_t u(t)|_{t=0} = 0$ is considered as a natural condition in the variational formulation.

Thanks to the Cauchy-Schwarz inequality and the Poincaré inequality (2.1), the bilinear form $a(\cdot, \cdot)$ is bounded with

$$|a(u, v)| \leq \left(1 + \frac{4T^2\mu}{\pi^2}\right) |u|_{H^1(0, T)} |v|_{H^1(0, T)}, \quad (3.4)$$

for all $(u, v) \in H_{0,*}^1(0, T) \times H_{*,0}^1(0, T)$.

In order to prove the well-posedness of (3.2) we consider an equivalent variational problem. Thus, we introduce the isomorphism

$$\overline{\mathcal{H}}_T : H_{0,*}^1(0, T) \longrightarrow H_{*,0}^1(0, T) \quad (3.5)$$

$$u \mapsto u(T) - u(\cdot), \quad (3.6)$$

where its inverse is given by

$$\overline{\mathcal{H}}_T^{-1} : H_{*,0}^1(0, T) \longrightarrow H_{0,*}^1(0, T)$$

$$v \mapsto v(0) - v(\cdot).$$

Since the above mappings are actually isometries with respect to $|\cdot|_{H^1(0,T)}$, then the well-posedness of (3.2) is equivalent to the well-posedness (with the same stability constant) of the following problem

$$\begin{cases} \text{Find } u \in H_{0,*}^1(0, T) \text{ such that} \\ a(u, \overline{\mathcal{H}}_T v) = \langle f, \overline{\mathcal{H}}_T v \rangle_{(0,T)} \quad \forall v \in H_{0,*}^1(0, T), \end{cases} \quad (3.7)$$

where the solution and test space coincide. Note that the continuity of the bilinear form in (3.7) is an immediate consequence of estimate (3.4). Unfortunately, at least for μ sufficiently large, the bilinear form of (3.7) is not coercive, hence, we cannot rely on the classical Lax-Milgram Lemma 2.3.7, but we need more specific tools. The branch of functional analysis that we exploit is called *Fredholm theory* and studies compact perturbations of linear bounded operators. In particular, there holds the following Theorem.

Theorem 3.1.1 (Zank, 2020). *For a given $f \in [H_{*,0}^1(0, T)]'$, there exists a unique solution $u \in H_{0,*}^1(0, T)$ of the variational formulation (3.7), and the following a priori estimate holds*

$$|u|_{H^1(0,T)} \leq \left(\frac{2 + \sqrt{\mu T}}{2} \right) \|f\|_{[H_{*,0}^1(0,T)]'}. \quad (3.8)$$

In addition, (3.8) is optimal with respect to the order of μ and T .

The well-posedness of (3.7) is an immediate consequence of the results presented in Section 2.4. Indeed, defining two bounded linear operators $\mathcal{B}, \mathcal{D} : H_{0,*}^1(0, T) \rightarrow [H_{0,*}^1(0, T)]'$ by

$$\begin{aligned} \langle \mathcal{B}u, v \rangle_{(0,T)} &:= \langle \partial_t u, \partial_t v \rangle_{L^2(0,T)}, \quad u, v \in H_{0,*}^1(0, T) \\ \langle \mathcal{D}u, v \rangle_{(0,T)} &:= \langle u, v(T) - v \rangle_{L^2(0,T)}, \quad u, v \in H_{0,*}^1(0, T), \end{aligned}$$

the map $\mathcal{B} + \mu \mathcal{D} : H_{0,*}^1(0, T) \rightarrow [H_{0,*}^1(0, T)]'$ is an injective Fredholm operator of index 0, where the compactness of \mathcal{D} follows from the properties of trace operators. However, estimate (3.8) gives an explicit dependency relation of its stability constant on T, μ . In order to prove (3.8), we use the notation \mathcal{A}

for the bounded linear operator related to the bilinear form (3.3), i.e.,

$$\begin{aligned} \mathcal{A} : H_{0,*}^1(0, T) &\rightarrow [H_{*,0}^1(0, T)]' \quad \text{s.t.} \\ \langle \mathcal{A}u, v \rangle_{(0,T)} &:= a(u, v), \quad u \in H_{0,*}^1(0, T), v \in H_{*,0}^1(0, T). \end{aligned}$$

Since \mathcal{A} is an isomorphism, its adjoint operator $\mathcal{A}^* : H_{*,0}^1(0, T) \rightarrow [H_{0,*}^1(0, T)]'$ is an isomorphism with $(\mathcal{A}^*)^{-1} = (\mathcal{A}^{-1})^*$, see (Fessler, 2004). As a consequence, given $g \in [H_{0,*}^1(0, T)]'$, the adjoint problem

$$\begin{cases} \text{Find } z \in H_{*,0}^1(0, T) & \text{such that} \\ a(w, z) = \langle g, w \rangle_{(0,T)} & \forall w \in H_{0,*}^1(0, T) \end{cases} \quad (3.9)$$

is well-posed. In particular, it is possible to compute the exact solution of problem (3.9) using a Green's function, if the right-hand side $g \in [H_{0,*}^1(0, T)]'$ depends on a fixed $u \in H_{0,*}^1(0, T)$; for more details we refer to (Zank, 2020). For the optimality of the estimate we refer to Theorem 4.2.6 of (Zank, 2020).

3.2 Isogeometric discretization

As discrete spaces for the Galerkin discretization of (3.2) we choose to consider spline spaces of degree two with maximal regularity, i.e., piecewise polynomials of degree two with global C^1 regularity.

Given a positive integer N , let $\Xi := \{t_1, \dots, t_{N+3}\}$ be an open knot vector in $[0, T]$ with the interior knots that appear just once, i.e., $0 = t_1 = t_2 = t_3 < \dots < t_{N+1} = t_{N+2} = t_{N+3} = T$. By means of Cox-de Boor recursion formulas (2.2) we define the quadratic univariate B-spline basis functions $b_{i,2} : [0, T] \rightarrow \mathbb{R}$ for $i = 1, \dots, N$ (we omit the subscript Ξ to lighten the notation). Thus, the univariate spline space is defined as

$$S_h^2 := \text{span}\{b_{i,2}\}_{i=1}^N,$$

where h is the mesh-size, i.e., $h := \max\{|t_{i+1} - t_i| : i = 1, \dots, N+2\}$.

We introduce the spline space with initial conditions as

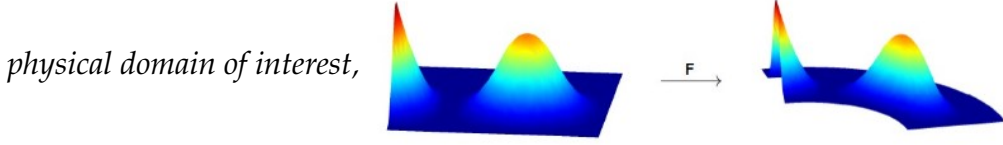
$$\begin{aligned} V_{0,*}^h &:= S_h^2 \cap H_{0,*}^1(0, 1) = \{v_h \in S_h^2 : v_h(0) = 0\} \\ &= \text{span}\{b_{i,2}\}_{i=2}^N, \end{aligned} \quad (3.10)$$

which is our isogeometric solution space, and the spline space

$$\begin{aligned} V_{*,0}^h &:= S_h^2 \cap H_{*,0}^1(0, 1) = \{v_h \in S_h^2 : v_h(T) = 0\} \\ &= \text{span}\{b_{i,2}\}_{i=1}^{N-1}, \end{aligned} \quad (3.11)$$

which is our isogeometric test space. Note that $V_{0,*}^h = \text{span}\{b_{i,2}\}_{i=2}^N$ and $V_{*,0}^h = \text{span}\{b_{i,2}\}_{i=1}^{N-1}$ since the first and last B-spline basis functions of an open knot vector are interpolating functions.

Remark 3.2.1. Typically, in isogeometric discretizations, and in the GeoPDEs library that we are going to use for the numerical experiments, one considers the parametric domain $[0, 1]^n$ and the splines/NURBS on this domain. Once these spaces are constructed, one maps, via a NURBS function F , the parametric domain to the



and the discrete solution and test spaces are the pushforward by F of splines/NURBS spaces on $[0, 1]^n$.

In our case, the map F would be $F : [0, 1] \rightarrow [0, T]$ s.t. $\tau \mapsto T\tau$. Therefore, doing the pushforward of the spline spaces on the parametric interval, we would obtain spline spaces on $[0, T]$ with B-spline basis functions that are the pushforward of the B-spline basis functions on $[0, 1]$. It is then sufficient for us to construct the discrete spaces directly on $[0, T]$.

A conforming Galerkin-Petrov isogeometric discretization of (3.2) is the following problem

$$\begin{cases} \text{Find } u_h \in V_{0,*}^h & \text{such that} \\ a(u_h, v_h) = \langle f, v_h \rangle_{(0,T)} & \forall v_h \in V_{*,0}^h. \end{cases} \quad (3.12)$$

As in the continuous framework, the restricted operator

$$\begin{aligned} \overline{\mathcal{H}}_{T|V_{0,*}^h} : V_{0,*}^h &\longrightarrow V_{*,0}^h \\ u_h &\mapsto u_h(T) - u_h(\cdot) \end{aligned}$$

is actually an isometric isomorphism with respect to $|\cdot|_{H^1(0,T)}$. Therefore, the well-posedness of (3.12) is equivalent to the well-posedness (with the same stability constant) of the conforming Galerkin-Bubnov isogeometric discretization of (3.7):

$$\begin{cases} \text{Find } u_h \in V_{0,*}^h & \text{such that} \\ a(u_h, \overline{\mathcal{H}}_T v_h) = \langle f, \overline{\mathcal{H}}_T v_h \rangle_{(0,T)} & \forall v_h \in V_{0,*}^h. \end{cases} \quad (3.13)$$

The isogeometric spaces $V_{0,*}^h$ define a dense discrete sequence in $H_{0,*}^1(0, T)$ (as we will see in Section 3.2.1), directed in the real parameter h . Hence, we can conclude the following Theorem.

Theorem 3.2.2. There exists two constants $C(T, \mu), \bar{h} > 0$ such that, if $h \leq \bar{h}$, problem (3.13) is well-posed, with the stability estimate

$$|u_h|_{H^1(0,T)} \leq C(T, \mu) \|f\|_{[H_{*,0}^1(0,T)]'} \quad f \in [H_{*,0}^1(0, T)]',$$

where u_h is the unique solution of (3.13). Moreover, if $h \leq \bar{h}$, a quasi-optimality estimate holds

$$|u - u_h|_{H^1(0,T)} \leq \left(1 + C(T, \mu) \|\mathcal{A}\|\right) \inf_{v_h \in V_{0,*}^h} |u - v_h|_{H^1(0,T)},$$

where $u \in H_{0,*}^1(0, T)$ is the unique solution of (3.7), and where $\|\cdot\|$ is the norm of the solution-to-data operator $\mathcal{A} : H_{0,*}^1(0, T) \rightarrow [H_{0,*}^1(0, T)]'$, related to the bilinear form of the variational formulation (3.7).

Proof. Theorem 3.2.2 is a straightforward consequence of the results presented in Section 2.4, i.e., Proposition 2.4.7, Corollary 2.4.9 and Corollary 2.4.10. \square

3.2.1 Approximation properties of spline spaces with an initial boundary condition

So far we have shown that, if the IGA discretization is *sufficiently fine*, problem (3.13) is well posed, stability holds and we eventually reach convergence. However, we would like to make explicit the threshold on the mesh-size and (possibly) the stability and quasi-optimality constants. In order to get these results we need a priori error estimate in the Sobolev semi-norm $|\cdot|_{H^1(0,T)}$ for approximation in spline spaces of maximal smoothness on grids defined by arbitrary break points. As pointed out in the paper (Sande, Manni, and Speleers, 2019), classical error estimates for spline approximation are expressed in terms of:

1. A power of the mesh-size.
2. An appropriate semi-norm of the function to be approximated.
3. A constant which is independent of the previous quantities.

However, we are interested in estimates with the constant of point 3 made explicit. In this respect, article (Sande, Manni, and Speleers, 2019) is relevant to us, since we slightly modify the construction of this work in order to obtain the estimates we need for test and trial spaces of our interest. In particular, the authors study the approximation properties of spline spaces, without boundary conditions, and of periodic spline spaces. We partially extend their work by including an initial boundary condition.

Let $S_{\Xi}^p(0, T)$ be the spline space of degree $p \geq 0$ and maximal regularity, where Ξ is the open knot vector that defines the B-spline basis functions of $S_{\Xi}^p(0, T)$. We firstly observe that we use the terms *knot vector* and *break points* as introduced in Section 2.2, unlike (Sande, Manni, and Speleers, 2019) in which the sequence of break points is called knot vector. Let $Q_p^q : H^q(0, T) \rightarrow$

$S_{\Xi}^p(0, T)$, $q = 0, \dots, p$, be a sequence of bounded linear operators such that

$$Q_p^0 := P_p \quad \text{is the } L^2(0, T) \text{ orthogonal projection on } S_{\Xi}^p(0, T), \quad (3.14)$$

$$(Q_p^q u)(t) := u(0) + \int_0^t (Q_{p-1}^{q-1} \partial_t u)(s) ds, \quad (3.15)$$

$$1 \leq q \leq p, \quad \forall u \in H^q(0, T),$$

Firstly, let now observe the reason why the operators Q_q^p maps $H^q(0, T)$ into $S_{\Xi}^p(0, T)$. Let K be the integral operator such that, for $f \in L^2(0, T)$,

$$Kf(t) := \int_0^t f(s) ds. \quad (3.16)$$

Recall from Theorem 17 of (Lyche, Manni, and Speleers, 2018) that the spline space $S_{\Xi}^p(0, T)$ satisfies

$$\partial_t^q S_{\Xi}^p(0, T) = S_{\Xi}^{p-q}(0, T), \quad \text{for any } q = 0, \dots, p, \quad (3.17)$$

where, by abuse of notation, we denote by the letter Ξ both the open knot vector $\{t_1, \dots, t_{N+p+1}\}$ (with $0 = t_1 = \dots = t_{p+1} < \dots < t_{N+1} = \dots = t_{N+p+1} = T$) and the one obtained from $\{t_1, \dots, t_{N+p+1}\}$ by reducing the external nodes from $p+1$ to $p-q+1$. Thus, as a consequence of (3.17) and of the Fundamental Theorem of Calculus, there holds

$$S_{\Xi}^p(0, T) = \mathbb{P}_0 + K(S_{\Xi}^{p-1}(0, T)), \quad \forall p \geq 1 \quad (3.18)$$

where \mathbb{P}_0 is the space of constant functions. Hence, by an inductive argument, the range of Q_p^q is a subspace of $S_{\Xi}^p(0, T)$. The linearity and continuity of Q_p^q are straightforward.

Proposition 3.2.3. *The maps Q_p^q defined in (3.14) and (3.15) are projection operators with range $S_{\Xi}^p(0, T)$. They also satisfies*

$$\partial_t Q_p^q = Q_{p-1}^{q-1} \partial_t, \quad \text{for all } p \geq 1, q = 1, \dots, p. \quad (3.19)$$

Proof. Equality (3.19) is satisfied by definition.

If $q = 0$, Q_p^q is a projection operator by definition. We use an inductive argument in order to prove that $Q_p^q(Q_p^q u) = Q_p^q u$ for all $u \in H^q(0, T)$ if $p \geq 1$

and $q = 1, \dots, p$. Let $p = q = 1$, then

$$\begin{aligned}
Q_1^1(Q_1^1 u)(t) &= Q_1^1\left(u(0) + \int_0^{(\cdot)} (Q_0^0 \partial_t u)(s) ds\right)(t) \\
&= Q_1^1(u(0)) + Q_1^1\left(\int_0^{(\cdot)} (Q_0^0 \partial_t u)(s) ds\right)(t) \quad (\text{linearity of } Q_q^p) \\
&= u(0) + \int_0^t Q_0^0\left(\partial_t \int_0^{(\cdot)} (Q_0^0 \partial_t u)(s) ds\right)(\tau) d\tau \quad (\text{definition of } Q_q^p) \\
&\stackrel{(3.19)}{=} u(0) + \int_0^t Q_0^0\left(\partial_t \int_0^{(\cdot)} (\partial_t Q_1^1 u)(s) ds\right)(\tau) d\tau \\
&= u(0) + \int_0^t Q_0^0(\partial_t Q_1^1 u(\tau) - \partial_t(Q_1^1 u(0))) d\tau \quad (\text{Fundamental Th. of Calculus}) \\
&\stackrel{(3.19)}{=} u(0) + \int_0^t Q_0^0(Q_0^0 \partial_t u(\tau)) d\tau \\
&= u(0) + \int_0^t (Q_0^0 \partial_t u)(\tau) d\tau \quad (Q_0^0 \text{ is } L^2(0, T)\text{-projection}).
\end{aligned}$$

Let now assume that the statement is true for $p \geq 1$, $q = 1, \dots, p$, and let now consider $p + 1$, $q = 1, \dots, p + 1$. Hence, as before, there hold the following identities

$$\begin{aligned}
Q_{p+1}^q(Q_{p+1}^q u)(t) &= Q_{p+1}^q\left(u(0) + \int_0^{(\cdot)} (Q_p^{q-1} \partial_t u)(s) ds\right)(t) \\
&= u(0) + \int_0^t Q_p^{q-1}\left(\partial_t \int_0^{(\cdot)} (Q_p^{q-1} \partial_t u)(s) ds\right)(\tau) d\tau \\
&= u(0) + \int_0^t (Q_p^{q-1} \partial_t u)(\tau) d\tau.
\end{aligned}$$

If $q = 0$, the range of Q_p^q is clearly $S_{\Xi}^p(0, T)$. Indeed Q_p^0 is the $L^2(0, T)$ -projection on $S_{\Xi}^p(0, T)$, hence, in particular, $Q_p^0|_{S_{\Xi}^p(0, T)} \equiv Id$. If $p \geq 1$ and $q = 1, \dots, p$, the fact that the range of Q_p^q is $S_{\Xi}^p(0, T)$ is straightforward. Indeed, by using an inductive argument and (3.17), one can prove that $Q_p^q|_{S_{\Xi}^p(0, T)} \equiv Id$ also for $p \geq 1$ and $q = 1, \dots, p$. \square

Let now recall Theorem 1 of (Sande, Manni, and Speleers, 2019).

Theorem 3.2.4 (E. Sande, C. Manni, H. Speleers). *For any sequence of break points that defines the open knot vector Ξ with maximal regularity, let h denote its maximal knot distance, and let P_p denote the $L^2(0, T)$ orthogonal projection onto the spline space $S_{\Xi}^p(0, T)$. Then, for any function $u \in H^r(0, T)$ with $r \geq 1$,*

$$\|u - P_p u\|_{L^2(0, T)} \leq \left(\frac{h}{\pi}\right)^r |u|_{H^r(0, T)}, \quad (3.20)$$

for all $p \geq r - 1$.

Remark 3.2.5. Let P be the $L^2(0, T)$ orthogonal projection onto a finite dimensional subspace \mathcal{X} of $L^2(0, T)$. For $A \subseteq L^2(0, T)$ we define

$$E(A, \mathcal{X}) = \sup_{u \in A} \|u - Pu\|_{L^2(0, T)},$$

i.e., $E(A, \mathcal{X})$ is the “maximal of the minimal distances” between A and the projection space \mathcal{X} . The Kolmogorov L^2 n -width of A is defined as

$$d_n(A) = \inf_{\mathcal{X} \subseteq L^2(0, T), \dim \mathcal{X} = n} E(A, \mathcal{X}).$$

The projection space \mathcal{X} is called an optimal subspace for $d_n(A)$ if $d_n(A) = E(A, \mathcal{X})$.

Let $r \geq 1$ and let $A = \{u \in H^r(0, T) : \|\partial_t^r u\|_{L^2(0, T)} \leq 1\}$. Clearly, for any finite subspace \mathcal{X} of $L^2(0, T)$ the following estimate holds

$$\|u - Pu\|_{L^2(0, T)} \leq E(A, \mathcal{X}) \|\partial_t^r u\|_{L^2(0, T)} \quad \forall u \in H^r(0, T),$$

and, in (Sande, Manni, and Speleers, 2019), an error estimate of the form

$$\|u - Pu\|_{L^2(0, T)} \leq C \|\partial_t^r u\|_{L^2(0, T)} \quad \forall u \in H^r(0, T) \quad (3.21)$$

is said to be sharp if

$$C = E(A, \mathcal{X}).$$

Also, in (Sande, Manni, and Speleers, 2019), a projection error estimate of the form (3.21) is said to be optimal if the subspace we project onto is optimal for the Kolmogorov L^2 n -width of A and the projection error estimate is sharp.

In (Sande, Manni, and Speleers, 2019) the following results are proven.

- If $r = 1$ and $p = 0$ and the sequence of break points that defines Ξ is uniform, then the estimate (3.20) is optimal.
- If $r = 1$ and $p > 0$ and the sequence of break points that defines Ξ is uniform, then the estimate (3.20) is asymptotically (with respect to the dimension of the spline space $S_{\Xi}^p(0, T)$) optimal.

In general, the authors conjecture that:

for all degree $p \geq 0$ there exists a sequence of break points such that for at least an $r = 1, \dots, p + 1$, the estimate (3.20) is optimal.

As a consequence of Theorem 3.2.4 there holds the following result, partially extending Theorem 3 of (Sande, Manni, and Speleers, 2019).

Theorem 3.2.6. Let $u \in H^r(0, T)$ for $r \geq 2$. For any $q = 1, \dots, r - 1$ and any sequence of break points that defines the open knot vector Ξ with maximal regularity, let h denote its maximal knot distance, and let Q_p^q be the projection onto $S_{\Xi}^p(0, T)$ defined in (3.15). Then,

$$|u - Q_p^q u|_{H^q(0, T)} \leq \left(\frac{h}{\pi}\right)^{r-q} |u|_{H^r(0, T)}, \quad (3.22)$$

for all $p \geq r - 1$.

Proof. Firstly, as a consequence of the Fundamental Theorem of Calculus for absolutely continuous functions, observe that the space $H^r(0, T)$, with $r \geq 1$, satisfies

$$H^r(0, T) = \mathbb{P}_0 + K(H^{r-1}(0, T)) = \dots = \mathbb{P}_{r-1} + K^r(H^0(0, T)), \quad (3.23)$$

where \mathbb{P}_{r-1} is the space of polynomials of degree at most $r - 1$ and K is the integral operator defined in (3.16).

From (3.23) we know that $u \in H^r(0, T)$ can be written as $u = g + K^q v$, for $g \in \mathbb{P}_{q-1} \subset S_{\Xi}^p$, with $q \geq 1$, and $v \in H^{r-q}(0, T)$. Since the projection operator $Q_p^q : H^q(0, T) \rightarrow S_{\Xi}^p(0, T)$ is surjective and $\partial^q Q_p^q = Q_{p-q}^{q-q} \partial^q = P_{p-q} \partial^q$, as a consequence of Theorem 3.2.4 there hold the following relations

$$\begin{aligned} \|\partial^q(u - Q_p^q u)\|_{L^2(0, T)} &= \|v - P_{p-q} v\|_{L^2(0, T)} \\ &\stackrel{(\text{if } p-q \geq r-q-1 \geq 0)}{\leq} \left(\frac{h}{\pi}\right)^{r-q} \|\partial^{r-q} v\|_{L^2(0, T)} = \|\partial^r u\|_{L^2(0, T)}, \end{aligned}$$

$q \leq r - 1$ and $p \geq r - 1$. Since $q = 1, \dots, r - 1$, the last inequality holds for $r \geq 2$. \square

Remark 3.2.7. The density of the family of spline spaces $(V_{0,*}^h)_h$ in $H_{0,*}^1(0, T)$ is a consequence of the result (3.22) with $p = r = 2$, $q = 1$, and of the density of $C_c^\infty(0, T]$ in $H_{0,*}^1(0, T)$ observed in Section 2.1.

Proof. Let $u \in H_{0,*}^1(0, T)$ and let $\epsilon > 0$ be fixed. As a consequence of the density of $C_c^\infty(0, T]$ in $H_{0,*}^1(0, T)$, there exists $\phi \in C_c^\infty(0, T]$ such that

$|u - \phi|_{H^1(0, T)} \leq \frac{\epsilon}{2}$. As a consequence of (3.22), there exists $\bar{h} > 0$ such that $|\phi - Q_2^1 \phi|_{H^1(0, T)} \leq \frac{\epsilon}{2}$ for all $h \leq \bar{h}$. We then obtain:

$$\begin{aligned} \inf_{v_h \in V_{0,*}^h} |u - v_h|_{H^1(0, T)} &\leq |u - Q_2^1 \phi|_{H^1(0, T)} \\ &\leq |u - \phi|_{H^1(0, T)} + |\phi - Q_2^1 \phi|_{H^1(0, T)} \leq \epsilon \quad \forall h \leq \bar{h}. \end{aligned}$$

\square

Let us recall that we have modified the projection operator of (Sande, Manni, and Speleers, 2019) in order to get a projection operator whose restriction to $H_{0,*}^1(0, T) \cap H^q(0, T)$ ($q \geq 1$) assumes values in $V_{0,*}^h$ defined in (3.10).

3.2.2 Bound on the mesh-size, stability and quasi-optimality constants

In this Section we give two results of conditioned stability *with an explicit bound on the mesh-size* and we also make explicit the stability and quasi-optimality constants.

Extension to quadratic IGA with maximal regularity of conditioned stability for piecewise continuous linear FEM

A first result is an extension to the IGA discretization of Theorem 4.7 of (Steinbach and Zank, 2020).

Theorem 3.2.8. *Let*

$$h \leq \frac{\pi^2}{\sqrt{2}(2 + \sqrt{\mu T})\mu T} \quad (3.24)$$

be satisfied. Then, the bilinear form $a(\cdot, \cdot)$ as defined in (3.3) satisfies the inf-sup condition

$$\frac{2\pi^2}{(2 + \sqrt{\mu T})^2(\pi^2 + 4\mu T^2)} |u_h|_{H^1(0,T)} \leq \sup_{0 \neq v_h \in V_{0,*}^h} \frac{a(u_h, \overline{\mathcal{H}}_T v_h)}{|v_h|_{H^1(0,T)}}, \quad (3.25)$$

for all $u_h \in V_{0,*}^h$.

Proof. Let $u_h \in V_{0,*}^h$. As a consequence of Lax-Milgram Lemma 2.3.7, let $w \in H_{0,*}^1(0, T)$ be the unique solution of the variational problem

$$-\int_0^T \partial_t w(t) \partial_t (\overline{\mathcal{H}}_T v)(t) dt = -\mu \int_0^T u_h(t) (\overline{\mathcal{H}}_T v)(t) dt \quad \forall v \in H_{0,*}^1(0, T). \quad (3.26)$$

Hence, recalling that $(\overline{\mathcal{H}}_T v)(t) = v(T) - v(t)$,

$$\begin{aligned} a(u_h, \overline{\mathcal{H}}_T(u_h - w)) &= -\int_0^T \partial_t u_h(t) \partial_t [(\overline{\mathcal{H}}_T u_h)(t) - (\overline{\mathcal{H}}_T w)(t)] dt \\ &\quad + \mu \int_0^T u_h(t) [(\overline{\mathcal{H}}_T u_h)(t) - (\overline{\mathcal{H}}_T w)(t)] dt \\ &\stackrel{(3.26)}{=} \int_0^T \partial_t u_h(t) \partial_t [u_h(t) - w(t)] dt - \int_0^T \partial_t w(t) [\partial_t u_h(t) - \partial_t w(t)] dt \\ &= \int_0^T [\partial_t u_h(t) - \partial_t w(t)]^2 dt = |u_h - w|_{H^1(0,T)}^2. \end{aligned} \quad (3.27)$$

Also, thanks to Lax-Milgram Lemma 2.3.7, let $z \in H_{0,*}^1(0, T)$ be the unique solution of the following variational problem

$$\begin{aligned} -\int_0^T \partial_t z(t) \partial_t (\overline{\mathcal{H}}_T v)(t) dt &= -\int_0^T \partial_t u_h(t) \partial_t (\overline{\mathcal{H}}_T v)(t) dt \\ &\quad + \mu \int_0^T u_h(t) (\overline{\mathcal{H}}_T v)(t) dt \quad \forall v \in H_{0,*}^1(0, T) \end{aligned} \quad (3.28)$$

Since $w \in H_{0,*}^1(0, T)$ is the solution of (3.26), problem (3.28) is equivalent to

$$-\int_0^T \partial_t [z(t) - (u_h(t) - w(t))] \partial_t (\overline{\mathcal{H}}_T v)(t) dt = 0 \quad \forall v \in H_{0,*}^1(0, T),$$

from which we conclude, by choosing $v = z - (u_h - w) \in H_{0,*}^1(0, T)$, that $z(t) = u_h(t) - w(t)$ for all $t \in [0, T]$, since $u_h(0) = w(0) = z(0) = 0$. Therefore, from (3.27), we conclude that

$$a(u_h, \overline{\mathcal{H}}_T(u_h - w)) = |z|_{H^1(0,T)}^2. \quad (3.29)$$

On the other hand, the variational formulation (3.28) gives

$$\begin{aligned} |z|_{H^1(0,T)} &\stackrel{(3.28)}{=} \frac{a(u_h, \overline{\mathcal{H}}_T z)}{|z|_{H^1(0,T)}} \leq \sup_{0 \neq v \in H_{0,*}^1(0,T)} \frac{a(u_h, \overline{\mathcal{H}}_T v)}{|v|_{H^1(0,T)}} \\ &\stackrel{(3.28)}{=} \sup_{0 \neq v \in H_{0,*}^1(0,T)} \frac{\langle \partial_t z, \partial_t v \rangle_{L^2(0,T)}}{|v|_{H^1(0,T)}} \stackrel{(C-S)}{\leq} |z|_{H^1(0,T)}. \end{aligned}$$

Hence, by using (3.8), there hold the following

$$|z|_{H^1(0,T)} = \sup_{0 \neq v \in H_{0,*}^1(0,T)} \frac{a(u_h, \overline{\mathcal{H}}_T v)}{|v|_{H^1(0,T)}} \stackrel{(3.8)}{\geq} \frac{2}{2 + \sqrt{\mu T}} |u_h|_{H^1(0,T)},$$

from which, recalling (3.29), we conclude

$$a(u_h, \overline{\mathcal{H}}_T(u_h - w)) \stackrel{(3.29)}{=} |z|_{H^1(0,T)}^2 \geq \frac{4}{(2 + \sqrt{\mu T})^2} |u_h|_{H^1(0,T)}^2. \quad (3.30)$$

We now discretize the first variational formulation (3.26). Let $w_h \in V_{0,*}^h$ be the unique solution of the following variational problem

$$\int_0^T \partial_t w_h(t) \partial_t v_h(t) dt = -\mu \int_0^T u_h(t) (\overline{\mathcal{H}}_T v_h)(t) dt \quad \forall v_h \in V_{0,*}^h. \quad (3.31)$$

By using Céa's Lemma 2.3.15 and the error estimate (3.22) with $r = 2$, $p = 2$, $q = 1$, there hold the following relations

$$\begin{aligned} |w - w_h|_{H^1(0,T)} &\leq \inf_{0 \neq v_h \in V_{0,*}^h} |w - v_h|_{H^1(0,T)} \quad (\text{Céa}) \\ &\leq |w - Q_2^1 w|_{H^1(0,T)} \stackrel{(3.22)}{\leq} \frac{h}{\pi} \|\partial_{tt} w\|_{L^2(0,T)} \stackrel{(3.31)}{=} \mu \frac{h}{\pi} \|u_h\|_{L^2(0,T)}. \end{aligned} \quad (3.32)$$

Furthermore, Galerkin orthogonality (2.18) is satisfied

$$\int_0^T [\partial_t w(t) - \partial_t w_h(t)] \partial_t v_h(t) dt = 0 \quad \forall v_h \in V_{0,*}^h. \quad (3.33)$$

As a consequence of (3.33), we have

$$\begin{aligned}
a(u_h, \overline{\mathcal{H}}_T(w - w_h)) &= \int_0^T \partial_t u_h(t) \partial_t [w(t) - w_h(t)] dt + \mu \int_0^T u_h(t) [\overline{\mathcal{H}}_T(w - w_h)](t) dt \\
&\stackrel{(3.33)}{=} \mu \int_0^T u_h(t) [\overline{\mathcal{H}}_T(w - w_h)](t) dt \\
&\leq \mu \|u_h\|_{L^2(0,T)} \|\overline{\mathcal{H}}_T(w - w_h)\|_{L^2(0,T)}.
\end{aligned} \tag{3.34}$$

As a consequence of Lax-Milgram Lemma 2.3.7, let now $\psi \in H_{0,*}^1(0, T)$ be the unique solution of the following variational problem

$$-\int_0^T \partial_t \psi(t) \partial_t [\overline{\mathcal{H}}_T v](t) dt = \int_0^T (\overline{\mathcal{H}}_T(w - w_h))(t) (\overline{\mathcal{H}}_T v)(t) dt \quad \forall v \in H_{0,*}^1(0, T). \tag{3.35}$$

In particular, by choosing $v = w - w_h \in H_{0,*}^1(0, T)$ and recalling (3.33), we obtain

$$\begin{aligned}
\|\overline{\mathcal{H}}_T(w - w_h)\|_{L^2(0,T)}^2 &= \int_0^T [\overline{\mathcal{H}}_T(w - w_h)](t) [\overline{\mathcal{H}}_T(w - w_h)](t) dt \\
&\stackrel{(3.35)}{=} - \int_0^T \partial_t \psi(t) \partial_t [\overline{\mathcal{H}}_T(w - w_h)](t) dt \\
&= \int_0^T \partial_t \psi(t) [\partial_t w(t) - \partial_t w_h(t)] dt \\
&\stackrel{(3.33)}{=} \int_0^T \partial_t [\psi(t) - Q_2^1 \psi(t)] [\partial_t w(t) - \partial_t w_h(t)] dt \\
&\leq |\psi - Q_2^1 \psi|_{H^1(0,T)} |w - w_h|_{H^1(0,T)} \\
&\stackrel{(3.22),(3.32)}{\leq} \left(\frac{h}{\pi}\right)^2 \mu \|\partial_t \psi\|_{L^2(0,T)} \|u_h\|_{L^2(0,T)} \\
&\stackrel{(3.35)}{=} \left(\frac{h}{\pi}\right)^2 \mu \|\overline{\mathcal{H}}_T(w - w_h)\|_{L^2(0,T)} \|u_h\|_{L^2(0,T)},
\end{aligned}$$

i.e.,

$$\|\overline{\mathcal{H}}_T(w - w_h)\|_{L^2(0,T)} \leq \frac{h^2}{\pi^2} \mu \|u_h\|_{L^2(0,T)}.$$

Therefore, by using (3.34) and Poincaré inequality (2.1),

$$a(u_h, \overline{\mathcal{H}}_T(w - w_h)) \stackrel{(3.34)}{\leq} \left(\frac{h}{\pi} \mu\right)^2 \|u_h\|_{L^2(0,T)}^2 \stackrel{(2.1)}{\leq} \left(\frac{2T}{\pi^2} \mu h\right)^2 |u_h|_{H^1(0,T)}^2 \tag{3.36}$$

follows. Hence, as a consequence of (3.30) and (3.36) we conclude

$$\begin{aligned} a(u_h, \overline{\mathcal{H}}_T(u_h - w_h)) &= a(u_h, \overline{\mathcal{H}}_T(u_h - w)) + a(u_h, \overline{\mathcal{H}}_T(w - w_h)) \\ &\stackrel{(3.30), (3.36)}{\geq} \left[\frac{4}{(2 + \sqrt{\mu}T)^2} - \left(\frac{2T}{\pi^2} \mu h \right)^2 \right] |u_h|_{H^1(0,T)}^2 \\ &\geq \frac{2}{(2 + \sqrt{\mu}T)^2} |u_h|_{H^1(0,T)}^2, \end{aligned}$$

if

$$\left(\frac{2T}{\pi^2} \mu h \right)^2 \leq \frac{2}{(2 + \sqrt{\mu}T)^2}$$

is satisfied, i.e.,

$$h \leq \frac{\pi^2}{\sqrt{2}(2 + \sqrt{\mu}T)\mu T}.$$

We now consider a lower bound for $|u_h|_{H^1(0,T)}$ dependent of $|u_h - w_h|_{H^1(0,T)}$. Indeed, we have

$$\|\partial_t(u_h - w_h)\|_{L^2(0,T)} \leq \|\partial_t u_h\|_{L^2(0,T)} + \|\partial_t w_h\|_{L^2(0,T)},$$

and, thanks to (3.31) and Poincaré inequality (2.1),

$$\begin{aligned} \|\partial_t w_h\|_{L^2(0,T)}^2 &= - \int_0^T \partial_t w_h(t) \partial_t (\overline{\mathcal{H}}_T w_h)(t) dt \stackrel{(3.31)}{=} -\mu \int_0^T u_h(t) (\overline{\mathcal{H}}_T w_h)(t) dt \\ &\leq \mu \|u_h\|_{L^2(0,T)} \|\overline{\mathcal{H}}_T w_h\|_{L^2(0,T)} \stackrel{(2.1)}{\leq} \frac{4T^2}{\pi^2} \mu |u_h|_{H^1(0,T)} |w_h|_{H^1(0,T)}, \end{aligned}$$

i.e.,

$$|u_h - w_h|_{H^1(0,T)} \leq \left(1 + \frac{4T^2}{\pi^2} \mu \right) |u_h|_{H^1(0,T)}.$$

Therefore, we obtain the following inequality

$$\frac{2\pi^2}{(2 + \sqrt{\mu}T)^2(\pi^2 + 4\mu T^2)} |u_h|_{H^1(0,T)} \leq \frac{a(u_h, \overline{\mathcal{H}}_T(u_h - w_h))}{|u_h - w_h|_{H^1(0,T)}}.$$

□

Hence, we obtain the following result.

Theorem 3.2.9. *Let (3.24) be satisfied. Then, problem (3.13) is well-posed with the stability estimate*

$$|u_h|_{H^1(0,T)} \leq \frac{(2 + \sqrt{\mu}T)^2(\pi^2 + 4\mu T^2)}{2\pi^2} \|f\|_{[H_{*,0}^1(0,T)]'}, \quad (3.37)$$

where $f \in [H_{*,0}^1(0, T)]'$ and u_h is the unique solution of (3.13). Moreover, a quasi-optimality estimate holds

$$|u - u_h|_{H^1(0, T)} \leq \left[1 + \frac{(2 + \sqrt{\mu}T)^2(\pi^2 + 4\mu T^2)^2}{2\pi^4} \right] \inf_{v_h \in V_{0,*}^h} |u - v_h|_{H^1(0, T)}, \quad (3.38)$$

where u is the unique solution of (3.7).

Proof. The well-posedness with stability estimate (3.37) is an immediate consequence of BNB Theorem 2.3.5.

In order to prove (3.38), we repeat, with explicit constants, the proof of Proposition 2.3.17. For any $w \in H_{0,*}^1(0, T)$ we define $w_h := G_h w$ as the Galerkin projection satisfying

$$a(G_h w, \overline{\mathcal{H}}_T v_h) = a(w, \overline{\mathcal{H}}_T v_h) \quad \forall v_h \in V_{0,*}^h,$$

which is well defined thanks to the well-posedness of the discrete problem. Hence, by using the stability estimate (3.25) and the continuity of $a(\cdot, \cdot)$ (3.4), there hold

$$|G_h w|_{H^1(0, T)} \leq \frac{(2 + \sqrt{\mu}T)^2(\pi^2 + 4\mu T^2)^2}{2\pi^4} |w|_{H^1(0, T)}.$$

Indeed,

$$\begin{aligned} \frac{2\pi^2}{(2 + \sqrt{\mu}T)^2(\pi^2 + 4\mu T^2)} |G_h w|_{H^1(0, T)} &\stackrel{(3.25)}{\leq} \sup_{0 \neq v_h \in V_{0,*}^h} \frac{a(G_h w, \overline{\mathcal{H}}_T v_h)}{|v_h|_{H^1(0, T)}} \\ &= \sup_{0 \neq v_h \in V_{0,*}^h} \frac{a(w, \overline{\mathcal{H}}_T v_h)}{|v_h|_{H^1(0, T)}} \\ &\stackrel{(3.4)}{\leq} \left(1 + \frac{4T^2\mu}{\pi^2} \right) |w|_{H^1(0, T)}. \end{aligned}$$

Since $u_h = G_h u$ and $v_h = G_h v_h$ for all $v_h \in V_{0,*}^h$, we conclude

$$\begin{aligned} |u - u_h|_{H^1(0, T)} &\leq |u - v_h|_{H^1(0, T)} + |G_h(v_h - u)|_{H^1(0, T)} \\ &\leq \left[1 + \frac{(2 + \sqrt{\mu}T)^2(\pi^2 + 4\mu T^2)^2}{2\pi^4} \right] |u - v_h|_{H^1(0, T)}. \end{aligned}$$

□

Thus, we are in a position to state a convergence result for the isogeometric solution u_h of the variational formulation (3.7).

Corollary 3.2.10. *Let $u \in H_{0,*}^1(0, T)$ and $u_h \in V_{0,*}^h$ be the unique solutions of the variational formulations (3.7) and (3.13), respectively. Let $u \in H^3(0, T)$ and (3.24)*

be satisfied. Then, there holds true the error estimate

$$|u - u_h|_{H^1(0,T)} \leq \frac{1}{\pi^2} \left[1 + \frac{(2 + \sqrt{\mu T})^2 (\pi^2 + 4\mu T^2)^2}{2\pi^4} \right] h^2 |u|_{H^3(0,T)}. \quad (3.39)$$

Proof. Estimate (3.39) is a straightforward consequence of quasi-optimality (3.38) and of (3.22) with $r = 3, p = 2, q = 1$. \square

Remark 3.2.11. Note that the bound on the mesh-size (3.24) is about 2.015 times the bound

$$h \leq \frac{2\sqrt{3}}{(2 + \sqrt{\mu T})\mu T}$$

of (Steinbach and Zank, 2019). It's also about 1.81 times the more accurate bound

$$h \leq \frac{\sqrt{3}\pi}{\sqrt{2}(2 + \mu T)\mu T}$$

of (Zank, 2020). Therefore, in order to get stability and convergence, our mesh-size can be approximately twice the mesh-size of piece-wise linear FEM.

Application of Theorem 2.4.12 to quadratic IGA with maximal regularity

Another way to get a bound on the mesh-size, so that, if it is respected, the well-posedness of IGA, stability and convergence (with explicit constants) are guaranteed, is the theory of Galerkin method applied to Gårding-type problems discussed in Section 2.4.

Let now consider problem (3.7) and its isogeometric discretization (3.13). Actually, these problems lie within the framework of Theorem 2.4.12. Indeed, as a consequence of Rellich-Kondrachov Theorem, the inclusion $H_{0,*}^1(0, T) \subset L^2(0, T)$ is compact. Furthermore, the following result holds.

Lemma 3.2.12. Let $b > \frac{\mu T^2}{2}$. The bilinear form defined in (3.3) satisfies the Gårding inequality:

$$a(v, \overline{\mathcal{H}}_T v) \geq \left(1 - \frac{\mu T^2}{2b}\right) |v|_{H^1(0,T)}^2 - \frac{2+b}{2} \mu \|v\|_{L^2(0,T)}^2 \quad \forall v \in H_{0,*}^1(0, T). \quad (3.40)$$

Proof. The bilinear form defined in (3.3) satisfies the following inequalities

$$\begin{aligned} a(v, \overline{\mathcal{H}}_T v) &= \langle \partial_t v, \partial_t v \rangle_{L^2(0,T)} - \mu \langle v, v \rangle_{L^2(0,T)} + \mu \langle v, v(T) \rangle_{L^2(0,T)} \\ &\geq |v|_{H^1(0,T)}^2 - \mu \|v\|_{L^2(0,T)}^2 - \mu \int_0^T |v(t)v(T)| dt \\ &\stackrel{(C-S)}{\geq} |v|_{H^1(0,T)}^2 - \mu \|v\|_{L^2(0,T)}^2 - \mu \|v\|_{L^2(0,T)} \sqrt{T} |v(T)| \\ &\stackrel{(F.T.C), (Young)}{\geq} |v|_{H^1(0,T)}^2 - \mu \|v\|_{L^2(0,T)}^2 - \frac{\mu b}{2} \|v\|_{L^2(0,T)}^2 - \frac{\mu T^2}{2b} |v|_{H^1(0,T)}^2 \\ &= \left(1 - \frac{\mu T^2}{2b}\right) |v|_{H^1(0,T)}^2 - \frac{2+b}{2} \mu \|v\|_{L^2(0,T)}^2, \end{aligned}$$

for all $b > 0$, where we used Cauchy Schwarz inequality, Young inequality and the Fundamental Theorem of Calculus. In order to obtain positive coefficients in (3.40) we add the constraint $b > \frac{\mu T^2}{2}$. \square

Also, Theorem 3.1.1 guarantees that problem (3.7) is well-posed, then, the only $u_0 \in H_{0,*}^1(0, T)$ such that $a(u_0, \overline{\mathcal{H}}_T v) = 0$ for all $v \in H_{0,*}^1(0, T)$ is $u_0 = 0$. Therefore, we conclude the following result.

Theorem 3.2.13. *Let*

$$h \leq \frac{\pi^5}{(\pi^2 + 4\mu T^2)[\pi^2 + 2\mu T^2(2 + \sqrt{\mu}T)]} \sqrt{\frac{2b - \mu T^2}{2b(2 + b)\mu}} \quad (3.41)$$

be satisfied, with $b > \frac{\mu T^2}{2}$. Then, problem (3.13) is well-posed with the stability estimate

$$\|u_h\|_{H^1(0,T)} \leq (2 + \sqrt{\mu}T) \left[\frac{3b + \mu T^2 \left(\frac{8b}{\pi^2} - \frac{1}{2} \right)}{2b - \mu T^2} \right] \|f\|_{[H_{*,0}^1(0,T)]'}, \quad (3.42)$$

where $f \in [H_{*,0}^1(0, T)]'$ and u_h is the unique solution of (3.13). Moreover, a quasi-optimality estimate holds

$$|u - u_h|_{H^1(0,T)} \leq \frac{4b}{\pi^2} \frac{\pi^2 + 4\mu T^2}{2b - \mu T^2} \inf_{v_h \in V_{0,*}^h} |u - v_h|_{H^1(0,T)}, \quad (3.43)$$

where $u \in H_{0,*}^1(0, T)$ is the unique solution of (3.7).

Proof. Let $b > \frac{\mu T^2}{2}$ and let $\eta(V_{0,*}^h)$ be the parameter defined in (2.28) and related to the sequence of isogeometric spaces in (3.10). By using the projection operator (3.15) with $p = 2$, $q = 1$, the error estimate (3.22) with $r = 2$, the Poincaré inequality (2.1) and the a priori estimate of the abstract problem (3.8), we obtain

$$\eta(V_{0,*}^h) \leq \frac{h}{\pi} \left[1 + \frac{2\mu T^2}{\pi^2} (2 + \sqrt{\mu}T) \right]. \quad (3.44)$$

Let see why (3.44) holds. Let $z_g \in H_{0,*}^1(0, T)$ be the solution of the adjoint problem (2.27) with respect to our context, i.e., given $g \in L^2(0, T)$, z_g is the unique element of $H_{0,*}^1(0, T)$ that satisfies

$$a(v, \overline{\mathcal{H}}_T z_g) = (g, v)_{L^2(0,T)} \quad \forall v \in H_{0,*}^1(0, T).$$

Therefore, $z := \overline{\mathcal{H}}_T z_g \in H_{*,0}^1(0, T)$ is the unique solution of

$$a(v, z) = (g, v)_{L^2(0,T)} \quad \forall v \in H_{0,*}^1(0, T),$$

i.e.,

$$-\langle \partial_t v, \partial_t z \rangle_{L^2(0,T)} + \mu \langle v, z \rangle_{L^2(0,T)} = (g, v)_{L^2(0,T)} \quad \forall v \in H_{0,*}^1(0, T).$$

As a consequence, the distributional derivative $\partial_{tt}z$ is represented by $g - \mu z \in L^2(0, T)$. Hence, $z \in H^2(0, T)$ and $z_g = \overline{\mathcal{H}}_T^{-1} z = z(0) - z \in H^2(0, T)$ with

$$\partial_{tt}z_g = \mu \overline{\mathcal{H}}_T z_g - g.$$

Note that the adjoint problem has the same stability estimate (w.r.t. the dual norm $\|\mathcal{G}\|_{[H_{0,*}^1(0,T)]'}$) of the primal problem, as noted in the second point of Remark 2.4.13. Then, the following relations hold

$$\begin{aligned} \inf_{v_h \in V_{0,*}^h} |z_g - v_h|_{H^1(0,T)} &\leq |z_g - Q_2^1 z_g|_{H^1(0,T)} \stackrel{(3.22)}{\leq} \frac{h}{\pi} \|\partial_{tt}z_g\|_{L^2(0,T)} \\ &= \frac{h}{\pi} \|\mu \overline{\mathcal{H}}_T z_g - g\|_{L^2(0,T)} \\ &\leq \frac{h}{\pi} \left(\|g\|_{L^2(0,T)} + \mu \|\overline{\mathcal{H}}_T z_g\|_{L^2(0,T)} \right) \\ &\stackrel{(2.1)}{\leq} \frac{h}{\pi} \left(\|g\|_{L^2(0,T)} + \frac{2T}{\pi} \mu |z_g|_{H^1(0,T)} \right) \\ &\stackrel{(3.8)}{\leq} \frac{h}{\pi} \left(\|g\|_{L^2(0,T)} + \frac{4T^2}{\pi^2} \mu \frac{2 + \sqrt{\mu}T}{2} \|g\|_{L^2(0,T)} \right) \\ &= \frac{h}{\pi} \left[1 + \frac{2\mu T^2}{\pi^2} (2 + \sqrt{\mu}T) \right] \|g\|_{L^2(0,T)}, \end{aligned}$$

which implies estimate (3.44). Therefore, from condition (2.29) where (3.40) is the Gårding inequality of our problem (3.13), we deduce that, if

$$\frac{h}{\pi} \left[1 + \frac{2\mu T^2}{\pi^2} (2 + \sqrt{\mu}T) \right] \leq \frac{\pi^2}{\pi^2 + 4\mu T^2} \sqrt{\frac{2b - \mu T^2}{2b(2+b)\mu}},$$

i.e.,

$$h \leq \frac{\pi^5}{(\pi^2 + 4\mu T^2)[\pi^2 + 2\mu T^2(2 + \sqrt{\mu}T)]} \sqrt{\frac{2b - \mu T^2}{2b(2+b)\mu}},$$

then problem (3.13) is well-posed, and conditions (3.42), (3.43) are satisfied. \square

Remark 3.2.14. *The choice*

$$b = \frac{\mu T^2 + \sqrt{\mu^2 T^4 + 4\mu T^2}}{2} \tag{3.45}$$

maximises $\sqrt{\frac{2b - \mu T^2}{2b(2+b)\mu}}$ in the upper bound of (3.41).

As a consequence of Theorem 3.2.13, we can state a convergence result for the isogeometric solution u_h of the variational formulation (3.7).

Corollary 3.2.15. *Let $u \in H_{0,*}^1(0, T)$ and $u_h \in V_{0,*}^h$ be the unique solutions of the variational formulations (3.7) and (3.13), respectively. Let $u \in H^3(0, T)$ and (3.41)*

be satisfied. Then, there holds true the error estimate

$$|u - u_h|_{H^1(0,T)} \leq \frac{4b \pi^2 + 4\mu T^2}{\pi^4 2b - \mu T^2} h^2 |u|_{H^3(0,T)}. \quad (3.46)$$

Proof. Estimate (3.46) is a straightforward consequence of quasi-optimality (3.43) and of (3.22) with $r = 3, p = 2, q = 1$. \square

Remark 3.2.16. *The analysis proposed in this Section, which is based on techniques that exploit the Gårding inequality and are alternative to those proposed by O. Steinbach and M. Zank (extended to the IGA case in the previous Section) is useful to understand how the IGA behaves in the case of generic polynomial degree and maximal regularity. Indeed, from the proof of Theorem 3.2.13 it emerges that the threshold on h (3.41) does not change when the polynomial degree and the regularity of the spline test and trial functions are raised. Only the order of convergence of Corollary 3.41 changes: for a generic polynomial degree $p \geq 1$ and an exact solution $u \in H^{p+1}(0, T)$, the order of convergence is p . On the other hand, how the upper bound (3.24) behaves in h is not immediately clear from the proof of Theorem 3.2.8. This is a consequence of the various auxiliary problems considered, in which the regularity of the corresponding solutions is a key point.*

Remark 3.2.17. *Asymptotically for $\mu \rightarrow \infty$ the optimal value (3.45) satisfies $b \simeq \mu T^2$. We then obtain*

$$h \leq \bar{h}_2 := \frac{\pi^5}{(\pi^2 + 4\mu T^2)[\pi^2 + 2\mu T^2(2 + \sqrt{\mu}T)]} \sqrt{\frac{1}{2\mu(2 + \mu T^2)'}}$$

in place of (3.41) with a general value $b > \frac{\mu T^2}{2}$.

Let us now recall estimate (3.24) obtained by extending Theorem 4.7 of (Steinbach and Zank, 2020) to quadratic IGA with maximal regularity, i.e.,

$$h \leq \bar{h}_1 := \frac{\pi^2}{\sqrt{2}(2 + \sqrt{\mu}T)\mu T}.$$

Therefore, the techniques of O. Steinbach and M. Zank and those ones using the Gårding inequality (2.26) give constraints on h of order

$$\begin{aligned} \bar{h}_1 &\simeq \mathcal{O}(\mu^{-3/2}), \\ \bar{h}_2 &\simeq \mathcal{O}(\mu^{-7/2}), \end{aligned}$$

respectively. Thus, we conclude that, asymptotically, threshold (3.41) is a stronger constraint than (3.24). However, asymptotically, stability estimate (3.42) behaves as $\mathcal{O}(\mu^{3/2})$, whereas, stability estimate (3.37) behaves as $\mathcal{O}(\mu^2)$. Therefore, we conclude that stability estimate (3.42) has a slower growth than (3.37) for $\mu \rightarrow \infty$.

Chapter 4

Numerical methods for

$$\partial_{tt}u + \mu u = f$$

In this Chapter we numerically study our model problem (3.1).

All the simulations are performed in MATLAB on a Intel(R) Core(TM) i3-4005U CPU @ 1.70GHz 1.70 GHz laptop, with 4,00 GB RAM.

All the isogeometric discretizations are performed using GeoPDEs, which is an open source and free package for the research and teaching of Isogeometric Analysis, written in Octave and fully compatible with MATLAB. See (Vázquez, 2016) for a complete explanation of its design and its main features.

4.1 Conditioned stability

4.1.1 Errors committed by piecewise continuous linear finite element method

In (Steinbach and Zank, 2019; Zank, 2020; Steinbach and Zank, 2020) the authors study the conditioned stability of the piecewise continuous linear finite element discretization of (3.1) and introduce a stabilized method (Steinbach and Zank, 2019; Zank, 2020), which they then extend to the wave equation (1.1) (Steinbach and Zank, 2019; Zank, 2020). Indeed, as noticed in (Steinbach and Zank, 2019; Zank, 2020), the stability of a conforming (w.r.t. classic anisotropic Sobolev spaces) tensor-product space-time discretization with piecewise linear, continuous solution and test functions of (1.1), requires a Courant – Friedrichs – Lewy (CFL) condition, i.e.,

$$h_t \leq Ch_x, \tag{4.1}$$

with a constant $C > 0$, depending on the constant of a spatial inverse inequality, where h_t and h_x are the uniform mesh-sizes in time and space. In particular, constraint (4.1) follows from the conditioned stability of the piecewise continuous linear FEM applied to (3.1) with uniform mesh-size.

In this Section we briefly recall O. Steinbach and M. Zank’s main results for the conditioned stability of FEM discretization of the ODE (3.1) and we show some numerical results that we obtain by testing their theoretical considerations.

Let us define the discrete spaces

$$S_{h;0,*}^1 := \{v_h \in S_h^1(0, T) \mid v_h(0) = 0\} = S_h^1(0, T) \cap H_{0,*}^1(0, T), \quad (4.2)$$

$$S_{h,*;0}^1 := \{v_h \in S_h^1(0, T) \mid v_h(T) = 0\} = S_h^1(0, T) \cap H_{*,0}^1(0, T), \quad (4.3)$$

where $S_h^1(0, T)$ is the classic space of piecewise continuous linear functions on $[0, T]$ with maximal mesh-size h .

In Theorem 4.7 of (Steinbach and Zank, 2020), which we extend to the isogeometric case with Theorem 3.2.8, the authors prove that if the mesh-size h satisfies

$$h \leq \frac{2\sqrt{3}}{(2 + \sqrt{\mu T})\mu T}, \quad (4.4)$$

then the discrete Galerkin-Bubnov formulation of (3.1) is well-posed with a uniform (w.r.t h) lower bound on the discrete inf-sup, i.e.,

$$\frac{8}{(2 + \sqrt{\mu T})^2(4 + \mu T^2)} |u_h|_{H^1(0, T)} \leq \sup_{0 \neq v_h \in S_{h,0,*}^1} \frac{a(u_h, \overline{\mathcal{H}}_T v_h)}{|v_h|_{H^1(0, T)}}, \quad (4.5)$$

for all $u_h \in S_{h,0,*}^1$, where $a(\cdot, \cdot)$ is the bilinear form defined in (3.3) and $\overline{\mathcal{H}}_T(\cdot)$ is the isometric isomorphism defined in (3.5), and where we corrected a missing second power of $\frac{T}{2}$.

Remark 4.1.1. As a consequence of the sharp Poincaré's inequalities (2.1), the estimate (4.4) can be slightly improved with the more accurate bound

$$h \leq \frac{\sqrt{3}\pi}{\sqrt{2}(2 + \sqrt{\mu T})\mu T}, \quad (4.6)$$

as observed in (Zank, 2020). Therefore, we consider this bound in our numerical experiments.

Remark 4.1.2. The well-posedness of the Galerkin-Bubnov FEM discretization of (3.1) is equivalent to the well-posedness (with the same stability constants) of its Galerkin-Petrov FEM discretization. Indeed, as in the isogeometric setting, the restriction of operator $\overline{\mathcal{H}}_T(\cdot)$ to the discrete trial space $S_{h,0,*}^1$ is actually an isometric isomorphism between $S_{h,0,*}^1$ and the test space $S_{h,*;0}^1$.

With classic arguments, in (Steinbach and Zank, 2020) the authors prove that the discrete solution of the piecewise continuous linear FEM discretization of (3.1) converges linearly in $|\cdot|_{H^1(0, T)}$ to the solution u of (3.2) if $u \in H^2(0, T)$ (Theorem 4.8, Steinbach and Zank, 2020). Moreover, using Aubin-Nitsche's trick, it is also possible to prove quadratic convergence in $\|\cdot\|_{L^2(0, T)}$ norm, if the exact solution satisfies $u \in H^2(0, T)$.

Under the assumption of a uniform mesh-size, the linear system obtained from the Galerkin-Petrov FEM discretization of (3.1) can be seen as a finite

difference scheme; see Remark 4.2.8 of (Zank, 2020). In these condition, the stability of the corresponding finite difference scheme holds if and only if

$$h < \sqrt{\frac{12}{\mu}}, \quad (4.7)$$

as a consequence of Chapter III.3 of (Hairer, Nørsett, and Wanner, 1993). Let us note that the stability considered in (4.7) is a uniform (w.r.t. h) boundness condition for the discrete solution in $\|\cdot\|_{L^\infty(0,T)}$ norm, which is necessary for stability of the discrete solution in classic Sobolev seminorms, due to the fact that the norm $\|\cdot\|_{L^\infty(0,T)}$ is controlled in $H^1(0,T)$, as a consequence of Morrey's Theorem.

Remark 4.1.3. Constraint (4.7) is related to the CFL condition for the tensor-product space-time discretization with piecewise continuous linear solution and test functions of the wave propagatin problem (1.1). The details are explained in (Steinbach and Zank, 2019; Zank, 2020).

As in (Steinbach and Zank, 2019; Zank, 2020), as a numerical example for the Galerkin-Petrov finite element methods we consider a uniform discretization of the time interval $(0, T)$ with $T = 10$ and a mesh-size $h = T/N$. For $\mu = 1000$ we consider the strong solution $u(t) = \sin^2\left(\frac{5}{4}\pi t\right)$ and we compute the integrals appearing at the right-hand side using high-order integration rules.

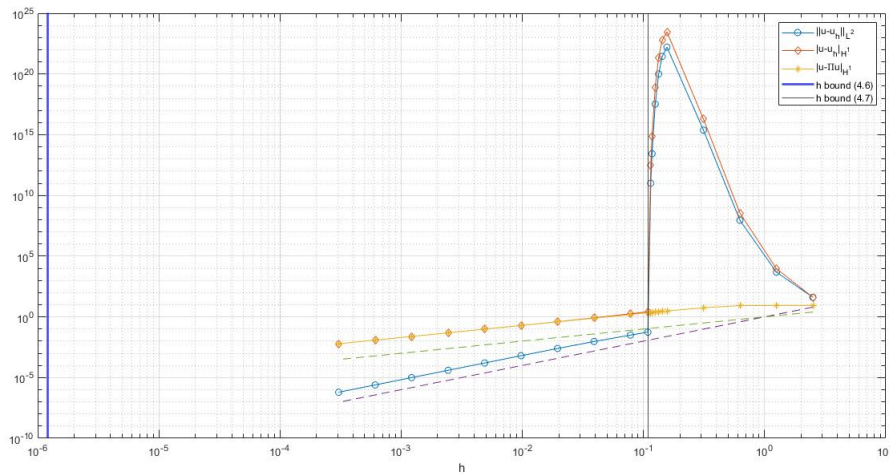


FIGURE 4.1: A log-log plot of errors committed by piecewise continuous linear FEM in $|\cdot|_{H^1(0,T)}$ seminorm and in $\|\cdot\|_{L^2(0,T)}$ norm, with respect to a uniform mesh-size h . Also, the best approximation error in $|\cdot|_{H^1(0,T)}$ seminorm and bounds (4.6), (4.7) are represented. The square of the wave number is $\mu = 1000$ and the final time is $T = 10$.

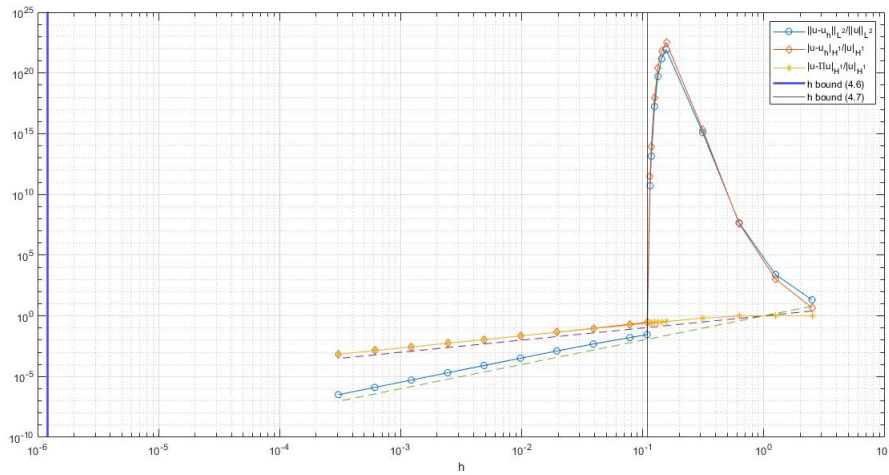


FIGURE 4.2: A log-log plot of relative errors committed by piecewise continuous linear FEM in $|\cdot|_{H^1(0,T)}$ seminorm and in $\|\cdot\|_{L^2(0,T)}$ norm, with respect to a uniform mesh-size h . Also, the best approximation error in $|\cdot|_{H^1(0,T)}$ seminorm and bounds (4.6), (4.7) are represented. The square of the wave number is $\mu = 1000$ and the final time is $T = 10$.

We consider approximation errors since they are a reflection of instability.

The minimum number of elements chosen is $N = 4$, the maximum number is $N = 32768$, as in (Steinbach and Zank, 2019).

From Figure 4.1, we can see that the maximal error occurs at $N = 64$: it is of order of 10^{23} in seminorm $|\cdot|_{H^1(0,T)}$ and 10^{22} in norm $\|\cdot\|_{L^2(0,T)}$, as we expect from (Steinbach and Zank, 2019).

As we can note in Figure 4.1, there is convergence only for sufficiently small mesh-size h . In particular, convergence is linear in $|\cdot|_{H^1(0,T)}$ seminorm and is quadratic in $\|\cdot\|_{L^2(0,T)}$ norm, as we expect. Clearly, the bound (4.6) is suboptimal, since convergence starts for h much larger than this threshold. Instead, the bound (4.7) seems to be sharp with respect to the error committed by the finite elements: this suggests that there is a uniform (w.r.t. h) inf-sup value already for $h < \sqrt{\frac{12}{\mu}}$. Thus, it remains open to improve assumption (4.6) to ensure a uniform inf-sup condition of (4.5) type.

Remark 4.1.4. Let us define $k := \sqrt{\mu}$ to follow the notation used in the literature we refer to in this comment. It is well known that the numerical solution of the Helmholtz equation

$$-\Delta_x u(x) - k^2 u(x) = f(x)$$

with boundary conditions, obtained by classic Galerkin FEM, differs significantly from the best approximation with increasing wave number k . This phenomena is the so-called pollution effect. The Galerkin FEM leads to quasi-optimal error estimates in which the constant factor by which the accuracy of the Galerkin solution differs from the best approximation error increases with increasing wave number (Harari and Hughes, 1991; Babuška and Ihlenburg, 1995; Babuška et al., 1995; Babuška and Sauter, 2000). On the other hand, it was shown in (Aziz, Kellogg, and Stephens,

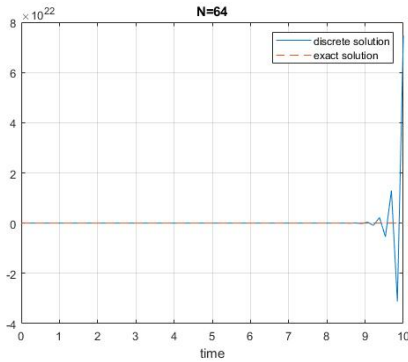


FIGURE 4.3: Exact and discrete solutions by piecewise linear FEM for $\mu = 1000$ and $N = 64$ elements (i.e., $h = 0.1563$).

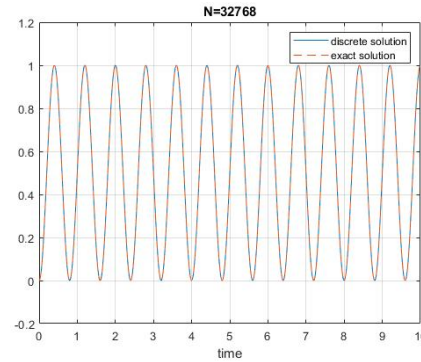


FIGURE 4.4: Exact and discrete solutions by piecewise linear FEM for $\mu = 1000$ and $N = 32768$ elements (i.e., $h = 0.0003$).

1988) that the condition “ k^2h is small” would be sufficient to guarantee that the error of the Galerkin solution is of the same magnitude as the error of the best approximation. However, this condition involves considerable computational complexity in three dimensions (Babuška and Sauter, 2000). Therefore, many attempts have been made in the mathematical and engineering literature to overcome this lack of robustness of the classic Galerkin FEM with respect to k (Harari and Hughes, 1991; Babuška et al., 1995).

Our model problem (3.1) is a wave propagation problem of Helmholtz type with initial conditions, instead of boundary conditions. Therefore, morally, we could expect “a certain pollution effect”. Hence, we decide to plot the best approximation error in order to estimate some kind of pollution error, which could be related to the conditioned stability of the classic Galerkin FEM.

Note that, unlike Helmholtz, in our model problem (3.1) we have two types of error-source frequencies. The first one is the frequency of the equation operator, i.e., $\sqrt{\mu} = \sqrt{1000}$ in our example, which dictates the number of oscillations in the unit time of typical solutions (e.g. homogeneous) of the problem. The second one is the specific frequency of the solution we consider, i.e., $f := \frac{\omega}{2\pi} = \frac{10\pi}{4} \frac{1}{2\pi} = \frac{5}{4}$ in our example, which dictates the number of oscillations in the unit time of this specific solution. Only the former is the source of a certain pollution error for this problem, whereas the latter is related to the best approximation error. However, both are related to the choice of the mesh-size in order to get a discrete space whose Galerkin error is “small”.

4.1.2 Inf-sup tests for piecewise continuous linear finite element method

As noticed in Section 4.1.1, the bound (4.7) seems to be sharp with respect to the error committed by the finite elements: this suggests that there is a uniform (w.r.t. h) inf-sup value already for $h < \sqrt{\frac{12}{\mu}}$. Therefore, we make inf-sup tests for the discrete bilinear form of the piecewise continuous linear

FEM discretization. The idea is to numerically estimate the discrete inf-sup and visualize its behaviour with respect to (μ, h) : we expect that in the region satisfying $h \geq \sqrt{\frac{12}{\mu}}$ there are infinitesimal inf-sup values, whereas we expect a uniformly (w.r.t. h) limited behaviour in the complementary region.

Numerical estimate of the discrete inf-sup. Let us define:

$$\beta(\mu, h, T) := \inf_{u_h \in S_{h;0,*}^1} \sup_{v_h \in S_{h;*,0}^1} \frac{a(u_h, v_h)}{|u_h|_{H^1(0,T)} |v_h|_{H^1(0,T)}}, \quad (4.8)$$

where $a(\cdot, \cdot)$ is the bilinear form defined in (3.3). Let us also define the matrices $\mathbf{A}, \mathbf{H}_1, \mathbf{H}_2$ such that

$$[\mathbf{A}]_{i,j} := -\langle \partial_t b_{1,j}, \partial_t b_{1,i} \rangle_{L^2(0,T)} + \mu \langle b_{1,j}, b_{1,i} \rangle_{L^2(0,T)} \quad (4.9)$$

for $i = 1, \dots, M-1, j = 2, \dots, M$

$$[\mathbf{H}_1]_{i,j} := \langle \partial_t b_{1,i}, \partial_t b_{1,j} \rangle_{L^2(0,T)} \quad \text{for } i, j = 2, \dots, M, \quad (4.10)$$

$$[\mathbf{H}_2]_{i,j} := \langle \partial_t b_{1,i}, \partial_t b_{1,j} \rangle_{L^2(0,T)} \quad \text{for } i, j = 1, \dots, M-1, \quad (4.11)$$

where $b_{1,k}$ for $k = 1, \dots, M$ are the classic *hat functions* such that $S_h^1(0, T) = \text{span}\{b_{1,k}\}_{k=1}^M$. Through this matrices we can estimate the discrete inf-sup value (4.8).

Proposition 4.1.5. *The discrete inf-sup value (4.8) satisfies*

$$\beta(\mu, h, T) = \sqrt{\lambda_{\min}},$$

where $\lambda_{\min} \geq 0$ is the minimum eigenvalue of the generalised eigenvalue problem:

$$\mathbf{A}^T \mathbf{H}_2^{-1} \mathbf{A} \vec{x} = \lambda \mathbf{H}_1 \vec{x}, \quad \text{for some } \vec{x} \in \mathbb{R}^{M-1}.$$

Proof. Let $u_h \in S_{h;0,*}^1$ and $v_h \in S_{h;*,0}^1$. They can be represented as

$$u_h = \sum_{j=2}^M u_j b_{1,j},$$

$$v_h = \sum_{i=1}^{M-1} v_i b_{1,i}.$$

Let us define $\vec{u} := (u_2, \dots, u_M)^T \in \mathbb{R}^{M-1}$, $\vec{v} := (v_1, \dots, v_{M-1})^T \in \mathbb{R}^{M-1}$. Therefore,

$$\begin{cases} a(u_h, v_h) = \vec{u}^T \mathbf{A}^T \vec{v}, \\ |u_h|_{H^1(0,T)}^2 = \vec{u}^T \mathbf{H}_1 \vec{u}, \\ |v_h|_{H^1(0,T)}^2 = \vec{v}^T \mathbf{H}_2 \vec{v}. \end{cases} \quad (4.12)$$

In order to lighten the notation we will denote \vec{u} with u and \vec{v} with v . By (4.12) the following equality holds

$$\inf_{u_h \in S_{h,0}^1, v_h \in S_{h,*}^1} \sup \frac{a(u_h, v_h)}{|u_h|_{H^1(0,T)} |v_h|_{H^1(0,T)}} = \inf_{u \in \mathbb{R}^{M-1}} \sup_{v \in \mathbb{R}^{M-1}} \frac{u^T \mathbf{A}^T v}{\sqrt{u^T \mathbf{H}_1 u} \sqrt{v^T \mathbf{H}_2 v}}.$$

\mathbf{H}_2 is a symmetric real positive-definite matrix, thus $\mathbf{H}_2 = \mathbf{H}_2^{\frac{1}{2}} \mathbf{H}_2^{\frac{1}{2}}$. With the change of variable $\tilde{v} := \mathbf{H}_2^{\frac{1}{2}} v$, the following equalities hold:

$$\sup_{v \in \mathbb{R}^{M-1}} \frac{u^T \mathbf{A}^T v}{\sqrt{v^T \mathbf{H}_2 v}} = \sup_{\tilde{v} \in \mathbb{R}^{M-1}} \frac{u^T \mathbf{A}^T \mathbf{H}_2^{-\frac{1}{2}} \tilde{v}}{\sqrt{\tilde{v}^T \tilde{v}}} = \left\| \mathbf{H}_2^{-\frac{1}{2}} \mathbf{A} u \right\|_2,$$

where $\| \cdot \|_2$ denote the euclidean norm of a vector.

\mathbf{H}_1 is a symmetric real positive-definite matrix, thus $\mathbf{H}_1 = \mathbf{H}_1^{\frac{1}{2}} \mathbf{H}_1^{\frac{1}{2}}$. With the change of variable $\tilde{u} := \mathbf{H}_1^{\frac{1}{2}} u$, the following equalities hold:

$$\begin{aligned} \left\| \mathbf{H}_2^{-\frac{1}{2}} \mathbf{A} u \right\|_2^2 &= u^T \mathbf{A}^T \mathbf{H}_2^{-\frac{1}{2}} \mathbf{H}_2^{-\frac{1}{2}} \mathbf{A} u = u^T \mathbf{A}^T \mathbf{H}_2^{-1} \mathbf{A} u \\ &= \tilde{u}^T \mathbf{H}_1^{-\frac{1}{2}} \mathbf{A}^T \mathbf{H}_2^{-1} \mathbf{A} \mathbf{H}_1^{-\frac{1}{2}} \tilde{u}. \end{aligned}$$

Therefore,

$$\begin{aligned} \beta(\mu, h, T) &= \inf_{\tilde{u} \in \mathbb{R}^{M-1}} \sqrt{\frac{\tilde{u}^T \mathbf{H}_1^{-\frac{1}{2}} \mathbf{A}^T \mathbf{H}_2^{-1} \mathbf{A} \mathbf{H}_1^{-\frac{1}{2}} \tilde{u}}{\tilde{u}^T \tilde{u}}} \\ &= \sqrt{\inf_{\tilde{u} \in \mathbb{R}^{M-1}} \frac{\tilde{u}^T \mathbf{H}_1^{-\frac{1}{2}} \mathbf{A}^T \mathbf{H}_2^{-1} \mathbf{A} \mathbf{H}_1^{-\frac{1}{2}} \tilde{u}}{\tilde{u}^T \tilde{u}}} \\ &= \sqrt{\lambda_{\min}}, \end{aligned}$$

where λ_{\min} is the minimum eigenvalue of the symmetric real positive-semidefinite matrix $\mathbf{H}_1^{-\frac{1}{2}} \mathbf{A}^T \mathbf{H}_2^{-1} \mathbf{A} \mathbf{H}_1^{-\frac{1}{2}}$. This means that λ_{\min} is the smallest number that satisfies

$$\mathbf{H}_1^{-\frac{1}{2}} \mathbf{A}^T \mathbf{H}_2^{-1} \mathbf{A} \mathbf{H}_1^{-\frac{1}{2}} \vec{x} = \lambda \vec{x}, \quad \text{for some } \vec{x} \in \mathbb{R}^{M-1},$$

i.e.,

$$\mathbf{A}^T \mathbf{H}_2^{-1} \mathbf{A} \mathbf{H}_1^{-\frac{1}{2}} \vec{x} = \lambda \mathbf{H}_1^{\frac{1}{2}} \vec{x}, \quad \text{for some } \vec{x} \in \mathbb{R}^{M-1}.$$

In order to lighten the notation we will denote \vec{x} with x . With the change of variable $\tilde{x} := \mathbf{H}_1^{-\frac{1}{2}} x$, λ_{\min} is the minimum of

$$\mathbf{A}^T \mathbf{H}_2^{-1} \mathbf{A} \tilde{x} = \lambda \mathbf{H}_1 \tilde{x}, \quad \text{for some } \tilde{x} \in \mathbb{R}^{M-1}.$$

The thesis is therefore proven. \square

We fix the final time $T = 10$ and a uniform mesh. We numerically study the behaviour of $\beta(\mu, h)$ of (4.8) with respect to (μ, h) by means of a p-colour plot of $\log(\beta)$ depending on $(\log(\mu), \log(h))$, so as to visualize the development of $\beta(\mu, h)$ more effectively.

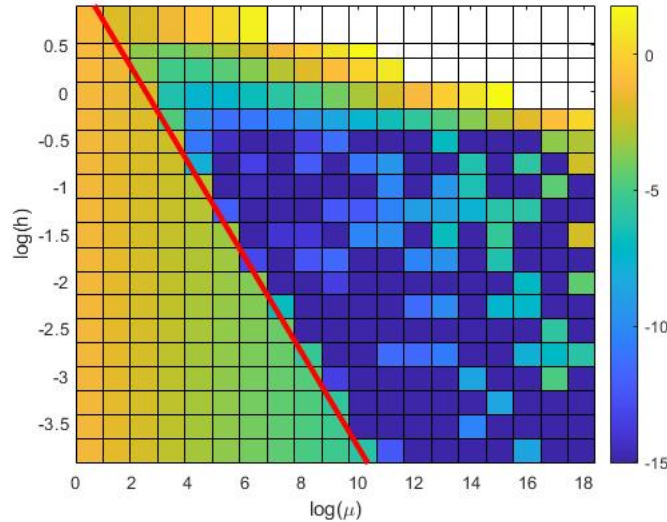


FIGURE 4.5: A p-color plot of $\log(\beta)$ of piecewise continuous linear FEM with respect to $(\log(\mu), \log(h))$. The red line is the natural logarithm of the upper bound in (4.7).

Firstly, let us note that the MATLAB function *p-color* sets by default the MATLAB values *-Inf* (i.e., numbers whose absolute value is too large to be represented as conventional floating-point values) to dark blue: we have checked this numerically and it is also clarified by Figure 4.6, where the empty regions correspond to $\log(\beta) = -\text{Inf}$.

The red line of Figure 4.5 is the natural logarithm of the upper bound in (4.7). We can clearly see in Figure 4.5 that it is the separation margin of two regions in which we observe a significantly different behaviour of $\beta(\mu, h)$. In the region below the red line, i.e., for $h < \sqrt{\frac{12}{\mu}}$, we observe a uniformly (w.r.t. h) bounded $\beta(\mu, h)$, whereas in the region above the red line, i.e., for $h > \sqrt{\frac{12}{\mu}}$, we observe a predominantly infinitesimal $\beta(\mu, h)$. This behaviour of the discrete inf-sup is indeed what we expect from Figure 4.1, in which the bound (4.7) on h seemed to be sharp, suggesting to us a uniformly (w.r.t. h) bounded discrete inf-sup already for $h < \sqrt{\frac{12}{\mu}}$. In the stability region, we can see a dependency of the discrete inf-sup on μ of order $\mu^{-\frac{1}{2}}$, as noticed in (Zank, 2020).

Note that in Figure 4.5 we do not consider the values of discrete inf-sup in the upper-right white region. In this region, the values of $\log(\beta)$ are greater than 10^2 . Actually, as a consequence of h “coarse” and “high” wave-number,

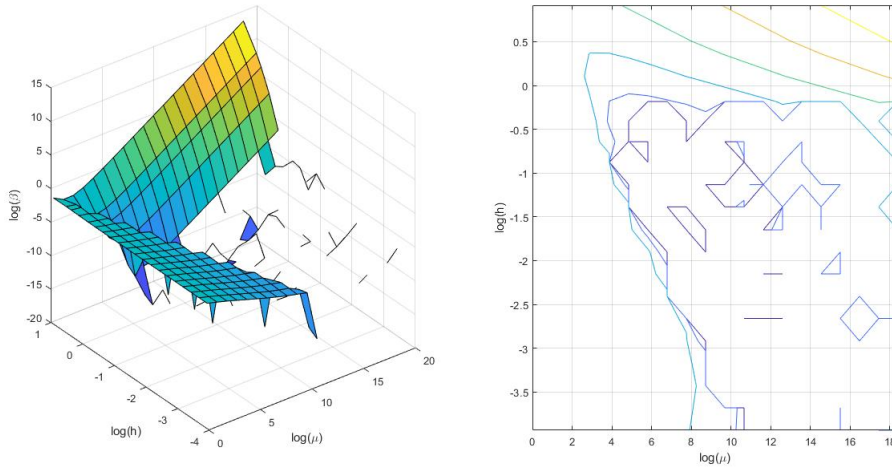


FIGURE 4.6: On the left, a three-dimensional plot of $\log(\beta)$ of piecewise continuous linear FEM with respect to $(\log(\mu), \log(h))$. On the right, the contour lines of $\log(\beta)$ with respect to $(\log(\mu), \log(h))$.

such large values for the discrete inf-sup are natural results, since value (4.8) is directly proportional to μ for wave-number and mesh-size that are “very large”. This is due to inverse inequalities which allow the term L^2 to dominate the derivatives. We are not interested in working under these conditions, since, for those wave numbers, h is too coarse compared to the resolution we expect to need in order to obtain satisfactory numerical results. Therefore, we do not visualize the corresponding inf-sup values.

4.1.3 Errors committed by quadratic isogeometric discretization with maximal regularity

In this Section we show some numerical results that we obtain by testing our theoretical considerations of Section 3.2.

As in Section 4.1.1 and in (Steinbach and Zank, 2019; Zank, 2020), as a numerical example for the Galerkin-Petrov quadratic isogeometric discretization with maximal regularity, we consider a uniform discretization of the time interval $(0, T)$ with $T = 10$ and a mesh-size $h = T/N$. For $\mu = 1000$ we consider the strong solution $u(t) = \sin^2\left(\frac{5}{4}\pi t\right)$ and we compute the integrals appearing at the right-hand side using high-order integration rules.

As in Section 4.1.1 we consider approximation errors since they are a reflection of instability.

The minimum number of elements chosen is $N = 4$, the maximum number is $N = 4096$ (it is not $N = 32768$ due to the memory limits of the laptop used).

From Figure 4.7, you can see that the maximal error occurs at $N = 64$: it is of order of 10^{16} in seminorm $|\cdot|_{H^1(0,T)}$ and 10^{15} in norm $\|\cdot\|_{L^2(0,T)}$. Note that the maximal error, and more generally for all values of h , is strictly smaller

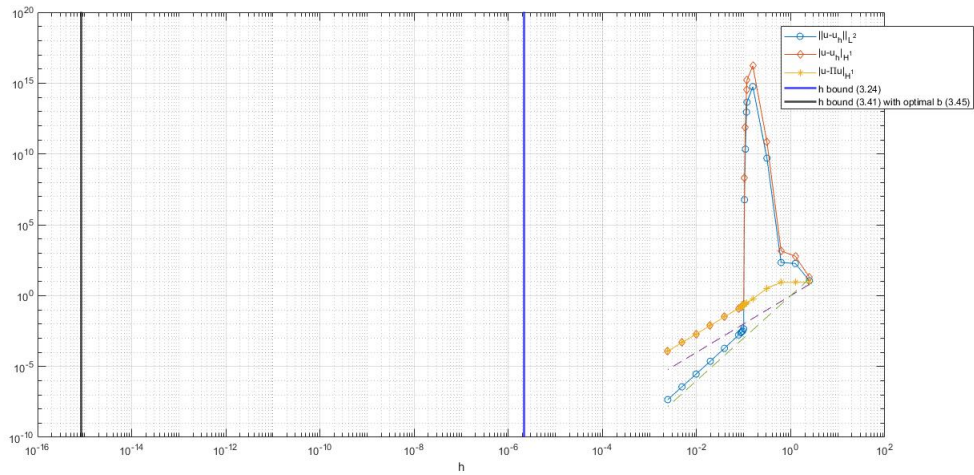


FIGURE 4.7: A log-log plot of errors committed by quadratic IGA, with maximal regularity, in $|\cdot|_{H^1(0,T)}$ seminorm and in $\|\cdot\|_{L^2(0,T)}$ norm, with respect to a uniform mesh-size h . Also, the best approximation error in $|\cdot|_{H^1(0,T)}$ seminorm and bounds (3.24), (3.41) (with the optimal choice (3.45)) are represented. The square of the wave number is $\mu = 1000$ and the final time is $T = 10$.

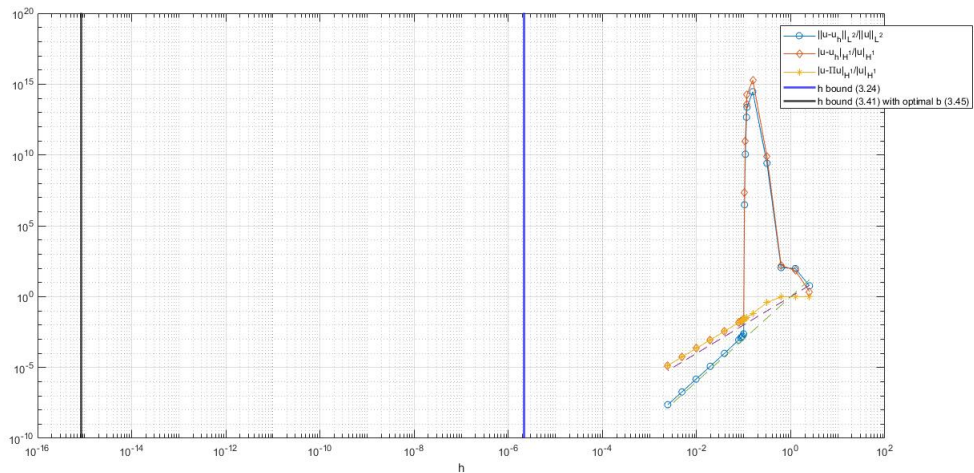


FIGURE 4.8: A log-log plot of relative errors committed by quadratic IGA, with maximal regularity, in $|\cdot|_{H^1(0,T)}$ seminorm and in $\|\cdot\|_{L^2(0,T)}$ norm, with respect to a uniform mesh-size h . Also, the best approximation error in $|\cdot|_{H^1(0,T)}$ seminorm and bounds (3.24), (3.41) (with the optimal choice (3.45)) are represented. The square of the wave number is $\mu = 1000$ and the final time is $T = 10$.

than the error committed by piecewise continuous linear FEM discretization, see Section 4.1.1. This result can be interpreted as a consequence of the good

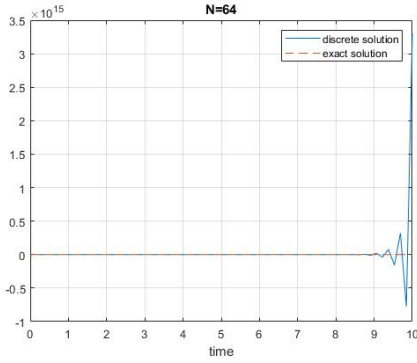


FIGURE 4.9: Exact and discrete solutions by quadratic IGA for $\mu = 1000$ and $N = 64$ elements (i.e., $h = 0.1563$).

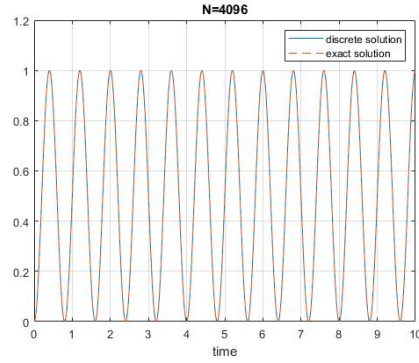


FIGURE 4.10: Exact and discrete solutions by quadratic IGA for $\mu = 1000$ and $N = 4096$ elements (i.e., $h = 0.0024$).

approximation properties of B-spline technology (Hughes, Reali, and Sangalli, 2008; Sande, Manni, and Speleers, 2019).

As you can see in Figure 4.7, there is convergence only for sufficiently small mesh-size h . In particular, convergence is quadratic in $|\cdot|_{H^1(0,T)}$ semi-norm, as we expect from Section 3.2, and it is cubic in $\|\cdot\|_{L^2(0,T)}$ norm. Note that in our theoretical discussion of Section 3.2 we did not estimate the order of convergence in $\|\cdot\|_{L^2(0,T)}$ norm, since it was beyond our interest. However, using Aubin-Nitsche's trick, one can verify that the L^2 -error converges cubically if the exact solution u satisfies $u \in H^3(0, T)$.

Clearly, both bounds (3.24), (3.41) (with the optimal choice (3.45)) are sub-optimal, since a beginning of convergence is observed for h much larger than these thresholds, see Figure 4.7. Moreover, the constraint (3.41) is more stringent than (3.24), as we expect to happen asymptotically (i.e., $\mu \rightarrow \infty$) from Remark 3.2.17. Thus, it remains open to improve assumptions (3.24), (3.41) to ensure stability conditions of (3.37), (3.42) type, respectively. That is, we are interested in an upper bound on the mesh-size that provides us with stability and is sharp.

4.1.4 Inf-sup tests for quadratic isogeometric discretization with maximal regularity

In this Section we numerically estimate the discrete inf-sup value and visualize its behaviour with respect to (μ, h) , with a uniform mesh-size h and final instant $T = 10$. Since the development of the error committed by the quadratic IGA is similar to that of the linear FEM, we expect the behaviour of the discrete inf-sup to be similar as well. In particular, if we numerically study $\beta(\mu, h)$ of (4.8) with respect to (μ, h) by means of a p-colour plot of $\log(\beta)$ depending on $(\log(\mu), \log(h))$, we expect to visualize a line that is the separation margin of stability and instability regions. This line corresponds to the sharp bound on h that, if satisfied, ensures the desired stability.

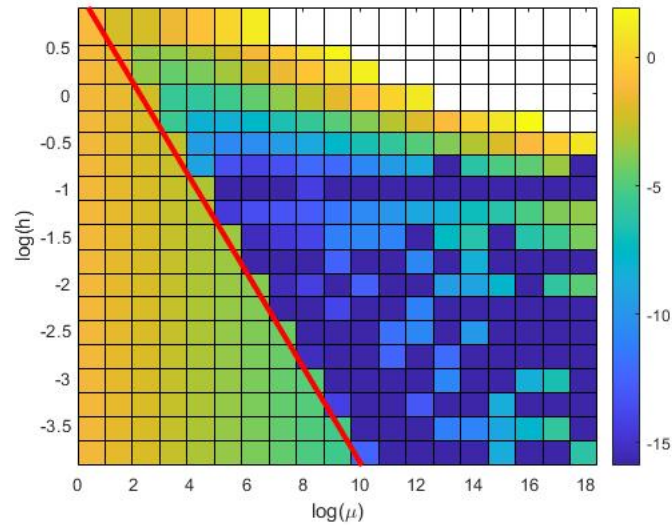


FIGURE 4.11: A p-color plot of $\log(\beta)$ of quadratic IGA with maximal regularity with respect to $(\log(\mu), \log(h))$. The red line represents $\log(h) = \frac{1}{2} \log(9) - \frac{1}{2} \log(\mu)$.

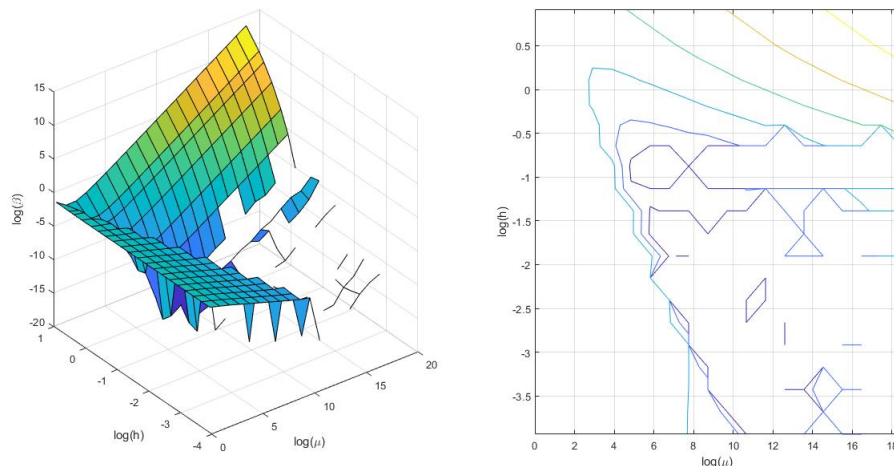


FIGURE 4.12: On the left, a three-dimensional plot of $\log(\beta)$ of quadratic IGA with maximal regularity with respect to $(\log(\mu), \log(h))$. On the right, the contour lines of $\log(\beta)$ with respect to $(\log(\mu), \log(h))$.

We estimate the isogeometric discrete inf-sup using Proposition 4.1.5 with the discrete solution and test spaces defined in (3.10), (3.11), respectively.

The numerical results in Figure 4.11 and Figure 4.12 confirm what we expect. The red line of Figure 4.11 corresponds to the constraint

$$h < \sqrt{\frac{9}{\mu}}. \quad (4.13)$$

Indeed, in the region below the red line, i.e., for $h < \sqrt{\frac{9}{\mu}}$, we observe a uniformly (w.r.t. h) bounded $\beta(\mu, h)$, whereas in the region above the red line, i.e., for $h > \sqrt{\frac{9}{\mu}}$, we observe a predominantly infinitesimal $\beta(\mu, h)$. In the stability region, we can see a dependency of the discrete inf-sup on μ of order $\mu^{-1/2}$, as in the continuous linear FEM case of Section 4.1.2.

In Figure 4.11 we do not consider the values of discrete inf-sup that are greater than 10^2 . Indeed these values are not a physical phenomenon, but simply the result of an unsuitable discretization of the problem, as observed in Section 4.1.2.

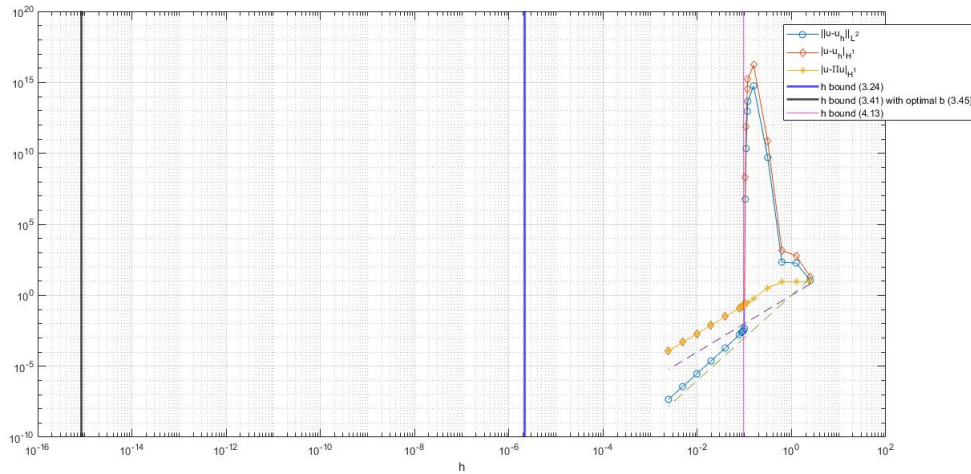


FIGURE 4.13: A log-log plot of errors committed by quadratic IGA, with maximal regularity, in $|\cdot|_{H^1(0,T)}$ seminorm and in $\|\cdot\|_{L^2(0,T)}$ norm, with respect to a uniform mesh-size h . Also, the best approximation error in $|\cdot|_{H^1(0,T)}$ seminorm and bounds (3.24), (3.41) (with the optimal choice (3.45)), (4.13) are represented. The square of the wave number is $\mu = 1000$ and the final time is $T = 10$.

In Figure 4.13 one can note the sharpness of the constraint (4.13) with respect to the error committed by the quadratic IGA with maximal regularity. This result is what we actually expect, as a consequence of the inf-sup stability for $h < \sqrt{\frac{9}{\mu}}$.

Another interesting numerical test displays, in the stability region given by (4.13), the numerically estimated isogeometric inf-sup with respect to the mesh-size h at a fixed μ , see Figure 4.14. This is useful to further see that the discrete inf-sup is actually uniformly limited in the region given by the constraint (4.13).

Comparing the theoretical inf-sup estimates (3.25), (3.42) of Section 3.2 with the numerical inf-sup could be useful in order to understand how accurate the theoretical bounds are. Therefore, in Figure 4.15 we visualize the three stability bounds (4.13), (3.24), (3.41) and the relative inf-sup estimates

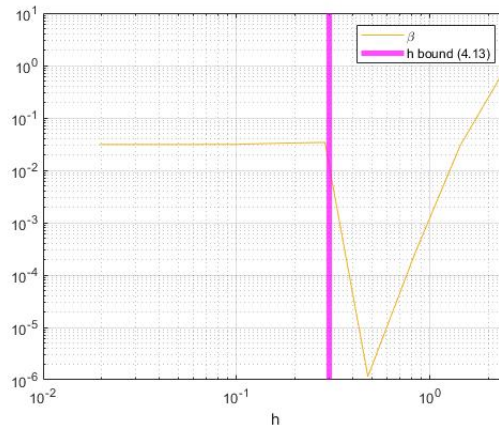


FIGURE 4.14: A log-log plot of the isogeometric inf-sup value with respect to a uniform mesh-size h , for a fixed $\mu = 100$.

at fixed h . It is sufficient to fix h and compare them as functions of the single variable μ , since in the stability region their mesh-size dependence disappears. In order to represent these three constraints on the mesh-size with respect to μ , we approximate (3.24), (3.41) as in Remark 3.2.17, i.e.,

$$\begin{aligned} h &< \mu^{-3/2}, \\ h &< \mu^{-7/2}, \end{aligned}$$

respectively, which result in

$$\begin{aligned} \mu &< h^{-2/3}, \\ \mu &< h^{-2/7}. \end{aligned}$$

Since the approximation of (3.41) with $h < \mu^{-7/2}$ corresponds to the slightly suboptimal value $b = \mu T^2$, plotting the inf-sup estimate of Theorem 3.2.13 with this choice is natural.

As one can note in Figure 4.15, the inf-sup estimate of Theorem 3.2.13 with the choice $b = \mu T^2$ decreases more slowly for $\mu \rightarrow \infty$ than the inf-sup (3.25), as we expect from Remark 3.2.17. Moreover, the former is more accurate than the latter, being larger at the same h and μ for which they are comparable.

4.2 Unconditional stability

4.2.1 Stabilization of piecewise continuous linear finite element method

In (Steinbach and Zank, 2019; Zank, 2020) the authors introduce a stabilized piecewise continuous linear finite element discretization of (3.1) in order to overcome the mesh constraints (4.6), (4.7). In this Section we briefly recall their main results about this stabilization and we show some numerical experiments that we make to test their theoretical considerations.

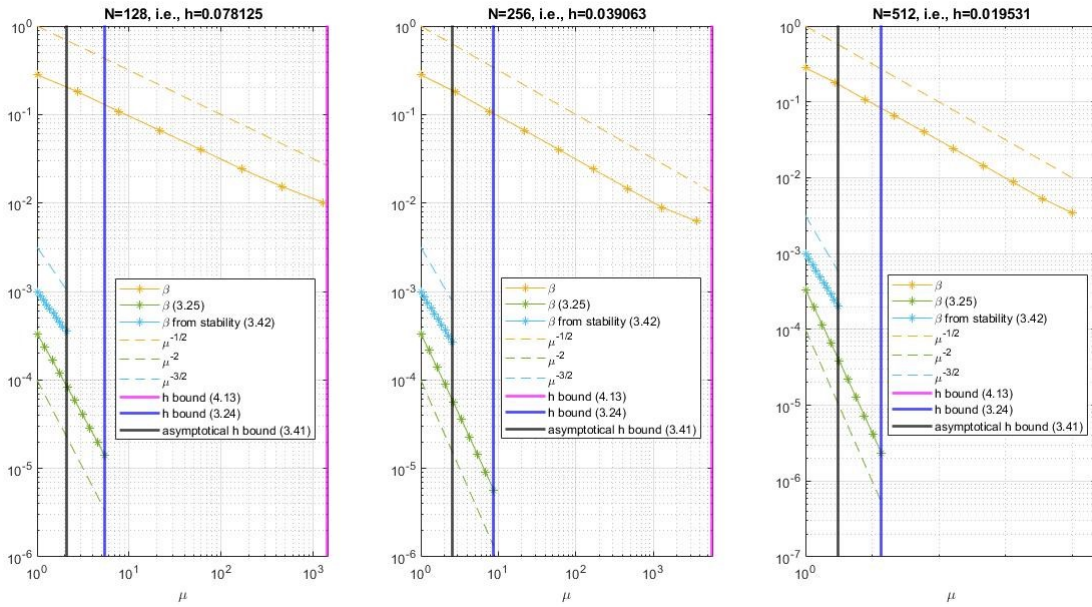


FIGURE 4.15: Three log-log plots of the isogeometric inf-sup value and of its lower-bounds with respect to μ for a fixed uniform mesh-sizes h .

O. Steinbach and M. Zank define a new discrete bilinear form $a_h : S_{h;0,*}^1 \times S_{h;*,0}^1 \rightarrow \mathbb{R}$ such that

$$a_h(u_h, v_h) := -\langle \partial_t u_h, \partial_t v_h \rangle_{L^2(0,T)} + \mu \langle u_h, Q_h^0 v_h \rangle_{L^2(0,T)}, \quad (4.14)$$

for all $u_h \in S_{h;0,*}^1$, $v_h \in S_{h;*,0}^1$, where $Q_h^0 : L^2(0, T) \rightarrow S_h^0(0, T)$ denotes the L^2 orthogonal projection on the piecewise constant finite element space $S_h^0(0, T)$. So basically, they do an under-integration in the $L^2(0, T)$ norm. That is, instead of integrating exactly the $L^2(0, T)$ scalar product $\langle u_h, v_h \rangle_{L^2(0,T)}$, they approximate it by projecting v_h on the piecewise constant finite element space $S_h^0(0, T)$.

As a consequence of the properties of the projection operator Q_h^0 and of the piecewise linear nodal interpolation operator $I_h : C[0, T] \rightarrow S_h^1(0, T)$ (Lemma 17.1, Lemma 17.2, Lemma 17.3, Lemma 17.4, Lemma 17.5 of Steinbach and Zank, 2019), the new bilinear form (4.14) satisfies the uniform (w.r.t. h) inf-sup condition

$$\frac{1}{1 + \sqrt{2}\mu T^2} |u_h|_{H^1(0,T)} \leq \sup_{0 \neq v_h \in S_{h;*,0}^1} \frac{a_h(u_h, v_h)}{|v_h|_{H^1(0,T)}}, \quad (4.15)$$

see Lemma 17.6 of (Steinbach and Zank, 2019).

Therefore, O. Steinbach and M. Zank consider the following perturbed problem

$$\begin{cases} \text{Find } u_h \in S_{h,0,*}^1 & \text{such that} \\ a_h(u_h, v_h) = \langle f, v_h \rangle_{(0,T)} & \forall v_h \in S_{h,*}^1, \end{cases} \quad (4.16)$$

where $T > 0$ and $f \in [H_{*,0}^1(0, T)]'$ are given, and the notation $\langle \cdot, \cdot \rangle_{(0,T)}$ denotes the duality pairing as extension of the inner product in $L^2(0, T)$. Thanks to (4.15) estimate, problem (4.16) is well-posed and the following stability condition holds

$$|\tilde{u}_h|_{H^1(0,T)} \leq (1 + \sqrt{2\mu T^2}) \|f\|_{[H_{*,0}^1(0,T)]'}$$

where $\tilde{u}_h \in S_{h,0,*}^1$ is the unique solution related to the fixed right-hand side $f \in [H_{*,0}^1(0, T)]'$.

Using an alternative representation (Corollary 17.1 of Steinbach and Zank, 2019) of the bilinear form $a(\cdot, \cdot)$ defined in (3.3) and some standard techniques, such as Galerkin orthogonality and interpolation error estimates, also linear convergence in $|\cdot|_{H^1(0,T)}$ of the discrete solution \tilde{u}_h of (4.16) to the solution $u \in H_{0,*}^1(0, T)$ of (3.2) are proven, if $u \in H^2(0, T)$; see Theorem 17.1 of (Steinbach and Zank, 2019) for more details. Furthermore, quadratic convergence in $\|\cdot\|_{L^2(0,T)}$ is shown, if the exact solution satisfies $u \in H^2(0, T)$; see Theorem 4.2.21 of (Zank, 2020).

We fix the final time $T = 10$, and we test their stabilization by numerically estimating the discrete inf-sup of the bilinear form (4.15) by means of Proposition 4.1.5 with uniform mesh.

As one can see from Figures 4.16, 4.17, the behaviour of the discrete inf-sup related to (4.14) is uniformly (w.r.t. h) bounded. In particular, the red line of Figure 4.16 corresponds to the upper-bound (4.7) and now, in the stabilized case, it no longer separates two different discrete inf-sup regimes.

As we expect from Remark 4.2.20 of (Zank, 2020), in Figure 4.16 one can note that the optimal discrete inf-sup constant shows a dependency of order $\mu^{-\frac{1}{2}}$, like the discrete inf-sup constant of (3.3) in the stability region given by (4.7), i.e., defined by

$$h < \sqrt{\frac{12}{\mu}}.$$

As before, in Figure 4.16 we do not consider the values of the discrete inf-sup that are greater than 10^2 . Indeed these values are not a physical phenomenon, but simply the result of an unsuitable discretization of the problem, as observed in Section 4.1.2.

We test O. Steinbach and M. Zank's stabilization also by studying the error committed in the approximation of an exact solution of (3.2). As in previous Sections and in (Steinbach and Zank, 2019; Zank, 2020), as a numerical

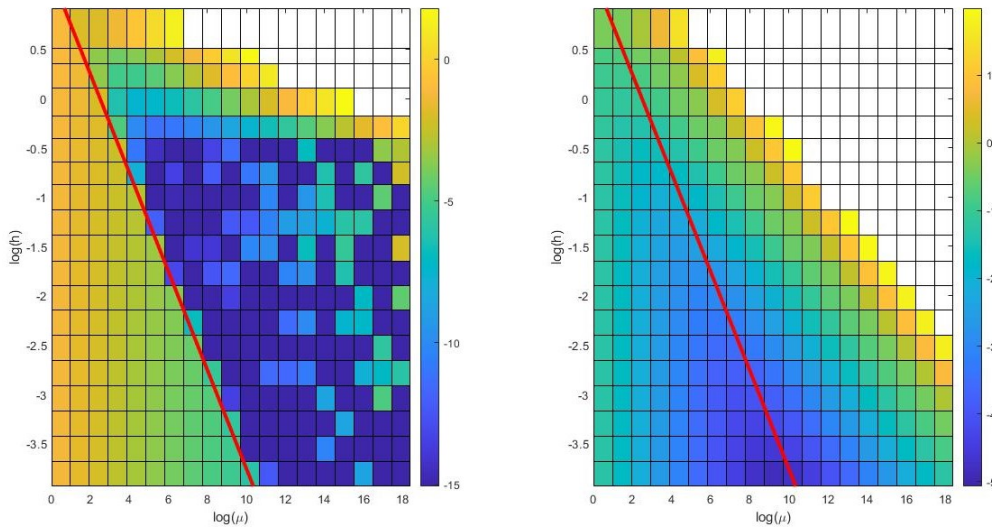


FIGURE 4.16: On the left a p-color plot of $\log(\beta)$ with respect to $(\log(\mu), \log(h))$, where β is the discrete inf-sup value of the bilinear form (3.3). On the right a p-color plot of $\log(\beta)$ with respect to $(\log(\mu), \log(h))$, where β is the inf-sup value of the bilinear form (4.14). In both Figures the red line is the natural logarithm of the upper bound (4.7).

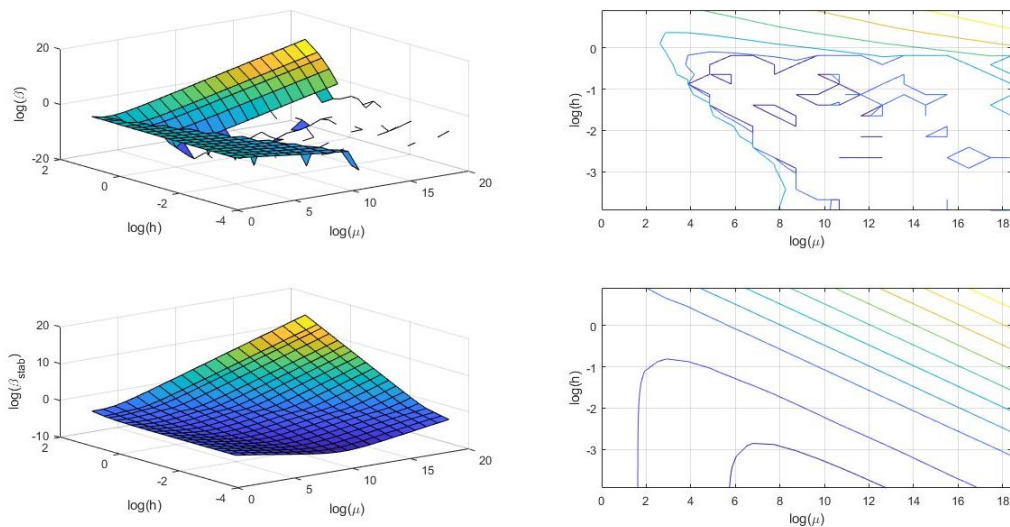


FIGURE 4.17: On the left, two three-dimensional plots of $\log(\beta)$ with respect to $(\log(\mu), \log(h))$. On the right, the contour lines of $\log(\beta)$ with respect to $(\log(\mu), \log(h))$. The top two figures correspond to the bilinear form defined in (3.3) restricted to the FEM discrete spaces (4.2), (4.3), and the bottom two to the stabilised bilinear form (4.14).

example for the perturbed Galerkin piecewise continuous linear FEM (4.16), we consider a uniform discretization of the time interval $(0, T)$ with $T = 10$

and a mesh-size $h = T/N$. For $\mu = 1000$ we consider the strong solution $u(t) = \sin^2\left(\frac{5}{4}\pi t\right)$ and we compute the integrals appearing at the right-hand side using high-order integration rules.

The minimum number of elements chosen is $N = 4$, the maximum number is $N = 32768$, as in Section 4.1.1.

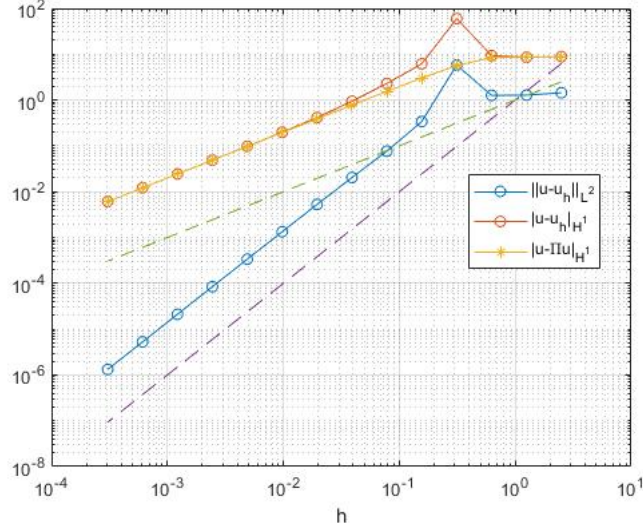


FIGURE 4.18: A log-log plot of errors committed by perturbed piecewise continuous linear FEM (4.16) in $|\cdot|_{H^1(0,T)}$ seminorm and in $\|\cdot\|_{L^2(0,T)}$ norm, with respect to a uniform mesh-size h . Also, the best approximation error in $|\cdot|_{H^1(0,T)}$ seminorm is represented. The square of the wave number is $\mu = 1000$.

As one can see in Figure 4.18, linear and quadratic convergence, respectively, in $|\cdot|_{H^1(0,T)}$ seminorm and in $\|\cdot\|_{L^2(0,T)}$ norm are confirmed.

Empirical reason for the unconditional stability of the perturbed FEM discretization

The following representation holds (Lemma 17.2 of Steinbach and Zank, 2019)

$$a_h(u_h, v_h) = -\langle \partial_t u_h, \partial_t v_h \rangle_{L^2(0,T)} - \frac{\mu}{12} \sum_{l=1}^N h_l^2 \langle \partial_t u_h, \partial_t v_h \rangle_{L^2(\tau_l)} + \mu \langle u_h, v_h \rangle_{L^2(0,T)}, \quad (4.17)$$

for all $u_h \in S_{h;0,*}^1$, $v_h \in S_{h;*;0}^1$, where τ_l , for $l = 1, \dots, N$, are the subintervals of $(0, T)$ given by the Galerkin discretization. Note that (4.17) results in

$$a_h(u_h, v_h) = -\left(1 + \frac{\mu h^2}{12}\right) \langle \partial_t u_h, \partial_t v_h \rangle_{L^2(0,T)} + \mu \langle u_h, v_h \rangle_{L^2(0,T)}, \quad (4.18)$$

for all $u_h \in S_{h;0,*}^1$, $v_h \in S_{h;*;0}^1$, in the case of a uniform mesh-size.

The representation (4.18) suggests another justification to the inf-sup stability of the perturbed bilinear form $a_h(\cdot, \cdot)$ in the case of a uniform mesh-size.

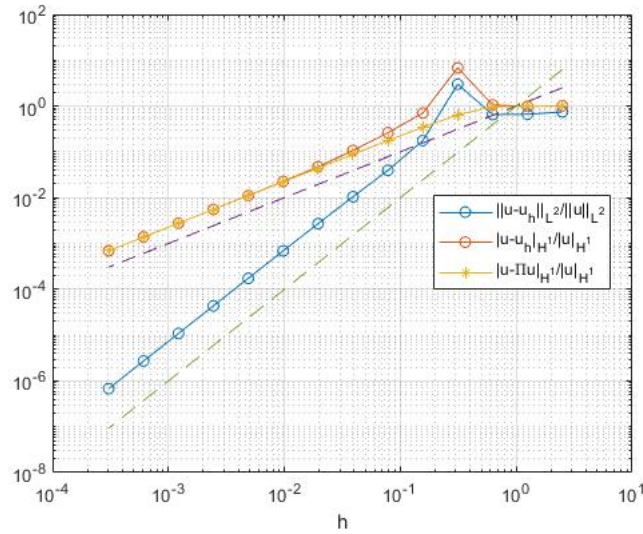


FIGURE 4.19: A log-log plot of relative errors committed by perturbed piecewise continuous linear FEM (4.16) in $|\cdot|_{H^1(0,T)}$ seminorm and in $\|\cdot\|_{L^2(0,T)}$ norm, with respect to a uniform mesh-size h . Also, the best approximation error in $|\cdot|_{H^1(0,T)}$ seminorm is represented. The square of the wave number is $\mu = 1000$.

Indeed, the bilinear form (4.18) corresponds to the perturbed problem

$$\partial_{tt}u(t) + \mu_h u(t) = f(t), \quad \text{for } t \in (0, T), \quad u(0) = \partial_t u(t)|_{t=0} = 0,$$

where

$$\mu_h := \frac{\mu}{1 + \frac{\mu h^2}{12}}.$$

Since the mesh-size h always satisfies

$$h < \sqrt{\frac{12}{\mu_h}} < \sqrt{\frac{12}{\mu} + h^2},$$

the perturbed bilinear form (4.14) with a uniform mesh-size is inf-sup stable with an inf-sup value that has a dependency on μ_h of order $\mu_h^{-\frac{1}{2}}$, as a consequence of the numerical results of Section 4.1.2. In particular,

$$\mu^{-\frac{1}{2}} \leq \mu_h^{-\frac{1}{2}} \simeq \inf_{0 \neq u_h \in S_{h,0,*}^1} \sup_{0 \neq v_h \in S_{h,*}^1} \frac{a_h(u_h, v_h)}{|v_h|_{H^1(0,T)}},$$

for all $u_h \in S_{h,0,*}^1$, $v_h \in S_{h,*}^1$. Note that these arguments are not intended to replace the analysis of (Steinbach and Zank, 2019; Zank, 2020), which is more complete. They are meant to give an empirical motivation that explains why the stabilization proposed by O. Steinbach and M. Zank actually works.

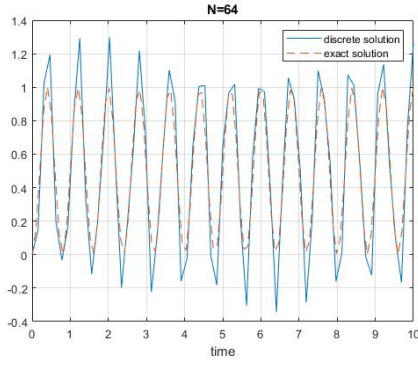


FIGURE 4.20: Exact and discrete solutions of the perturbed problem (4.16) for $\mu = 1000$ and $N = 64$ elements (i.e., $h = 0.1563$).

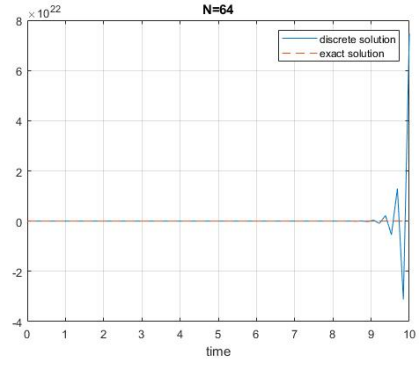


FIGURE 4.21: Exact and discrete solutions by unperturbed piecewise linear FEM for $\mu = 1000$ and $N = 64$ elements (i.e., $h = 0.1563$).

4.2.2 Stabilization for quadratic isogeometric discretization with maximal regularity

In this Section we consider three different stabilization techniques. The first two give poor results, whereas the performances of the last one are satisfactory.

Inspired by (4.14), we firstly try to perturb the quadratic isogeometric discretization with maximal regularity in the same way, i.e., defining

$$a_h(u_h, v_h) := -\langle \partial_t u_h, \partial_t v_h \rangle_{L^2(0,T)} + \mu \langle u_h, Q_h^0 v_h \rangle_{L^2(0,T)}, \quad (4.19)$$

for all $u_h \in V_{0,*}^h$ of (3.10) and $v_h \in V_{*,0}^h$ of (3.11), and considering the modified discrete problem

$$\begin{cases} \text{Find } u_h \in V_{0,*}^h & \text{such that} \\ a_h(u_h, v_h) = \langle f, v_h \rangle_{(0,T)} & \forall v_h \in V_{*,0}^h. \end{cases} \quad (4.20)$$

Remark 4.2.1. Another possible perturbation consists of defining

$$a_h(u_h, v_h) := -\langle \partial_t u_h, \partial_t v_h \rangle_{L^2(0,T)} + \mu \langle u_h, Q_h^1 v_h \rangle_{L^2(0,T)},$$

for all $u_h \in V_{0,*}^h$ and $v_h \in V_{*,0}^h$, where $Q_h^1 : L^2(0,T) \rightarrow S_h^1(0,T)$ denotes the $L^2(0,T)$ orthogonal projection on the piecewise continuous linear finite element space $S_h^1(0,T)$.

As in previous Sections, we test perturbation (4.19) by studying the error committed in the approximation of an exact solution of (3.2). In particular, as before, as a numerical example we consider a uniform discretization of the time interval $(0,T)$ with $T = 10$ and a mesh-size $h = T/N$. For $\mu = 1000$ we choose the strong solution $u(t) = \sin^2\left(\frac{5}{4}\pi t\right)$ and we compute the integrals appearing at the right-hand side using high-order integration rules.

The minimum number of elements chosen is $N = 4$, the maximum number is $N = 4096$, as in Section 4.1.3.

The results that we obtain are in Figure 4.22, which are far from promising, since the errors are even larger than those ones made by the conditionally stable method (3.12). A possible explanation is that we are exceeding in the under-integration if compared to the regularity of the test and trial functions we consider.

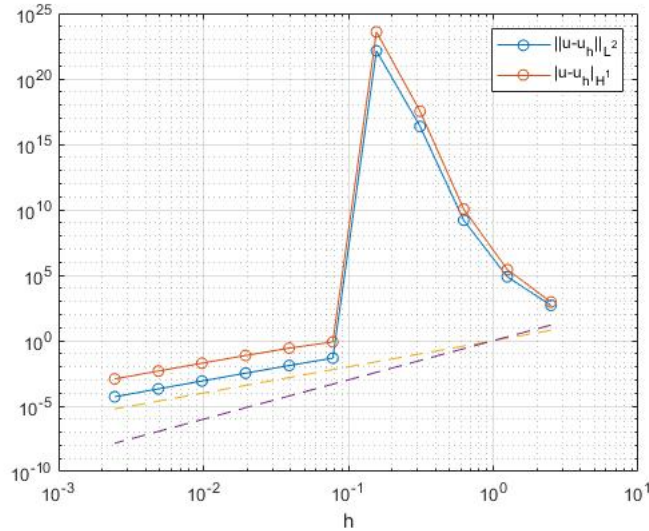


FIGURE 4.22: A log-log plot of errors committed by perturbed quadratic IGA with maximal regularity (4.19) in $|\cdot|_{H^1(0,T)}$ semi-norm and in $\|\cdot\|_{L^2(0,T)}$ norm, with respect to a uniform mesh-size h . The square of the wave number is $\mu = 1000$.

We then decide to change perspective by considering the perturbation (4.18), inspired by the observations at the end of Section 4.2.1. Since we numerically obtain the stability constraint (4.13), we define the following perturbation

$$a_h(u_h, v_h) = - \left(1 + \frac{\mu h^2}{9} \right) \langle \partial_t u_h, \partial_t v_h \rangle_{L^2(0,T)} + \mu \langle u_h, v_h \rangle_{L^2(0,T)}, \quad (4.21)$$

for all $u_h \in V_{0,*}^h$ and $v_h \in V_{*,0}^h$, if the mesh-size is uniform. We then test this perturbation by studying the error committed by the discrete solution of (4.20) considering the perturbed bilinear form (4.21). We choose the same exact solution and assumptions of Figure 4.22. The results that we achieve are in Figure 4.23 and are quite promising, as we could expect from the empirical analysis at the end of Section 4.2.1. Indeed, bounded errors are a consequence of stability. However, we do not obtain the orders of convergence that we expect for quadratic IGA of maximal regularity, since we only get quadratic convergence in $\|\cdot\|_{L^2(0,T)}$ norm.

In order to gain a method that is unconditionally stable whose orders of convergence in $|\cdot|_{H^1(0,T)}$ and $\|\cdot\|_{L^2(0,T)}$ are what we expect for quadratic

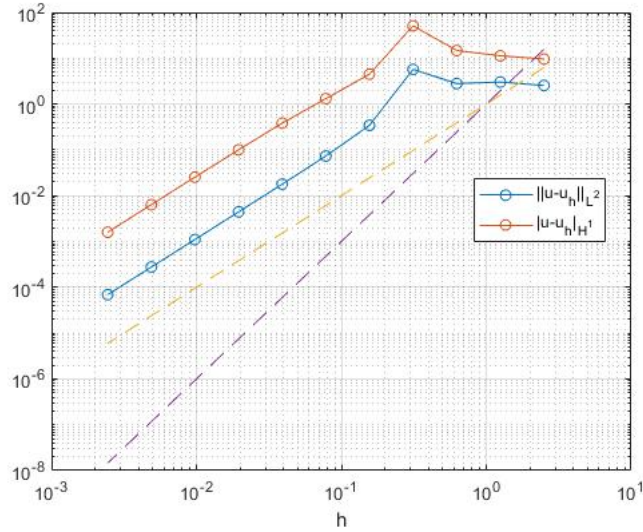


FIGURE 4.23: A log-log plot of errors committed by perturbed quadratic IGA with maximal regularity (4.21) in $|\cdot|_{H^1(0,T)}$ seminorm and in $\|\cdot\|_{L^2(0,T)}$ norm, with respect to a uniform mesh-size h . The square of the wave number is $\mu = 1000$.

splines with $C^1(0, T)$ global regularity, we decide to define the following perturbed bilinear form in the case of a uniform mesh-size

$$a_h(u_h, v_h) = -\langle \partial_t u_h, \partial_t v_h \rangle_{L^2(0,T)} + \mu \langle u_h, v_h \rangle_{L^2(0,T)} - \delta \mu h^4 \langle \partial_t^2 u_h, \partial_t^2 v_h \rangle_{L^2(0,T)}, \quad (4.22)$$

for all $u_h \in V_{0,*}^h$ and $v_h \in V_{*,0}^h$, where $\delta > 0$ is a fixed real value.

Let us note that both the bilinear forms (4.21), (4.22) are defined by a non consistent perturbation, since, in general, if $\tilde{u}_h \in V_{0,*}^h$ is a solution of their related perturbed problem (4.20), \tilde{u}_h is not a solution of the non perturbed problem (3.12).

The behaviour of (4.22) depends on the choice of the coefficient δ . Therefore, we test this perturbation by studying the error committed by the discrete solution of (4.20) considering the perturbed bilinear form (4.22) with different choice of δ . In particular, we consider $\delta \in \{\frac{1}{100}, \frac{1}{10}, 1, 10, 100\}$ in order to see how the errors behave for different orders of magnitude of the perturbation coefficient. We choose the same exact solution and assumptions of Figures 4.22, 4.23.

Figure 4.24 represents log-log plots of relative errors committed by perturbed quadratic IGA with maximal regularity (4.22) in $|\cdot|_{H^1(0,T)}$ seminorm and in $\|\cdot\|_{L^2(0,T)}$ norm, with respect to a uniform mesh-size h . The smallest global errors are obtained for $\delta = \frac{1}{100}$. In particular, they are satisfactory since the errors in $|\cdot|_{H^1(0,T)}$ and $\|\cdot\|_{L^2(0,T)}$ have a maximum that is smaller than 10^2 , but also because we achieve quadratic convergence in $|\cdot|_{H^1(0,T)}$ and cubic convergence in $\|\cdot\|_{L^2(0,T)}$, as we expect from quadratic IGA discretization.

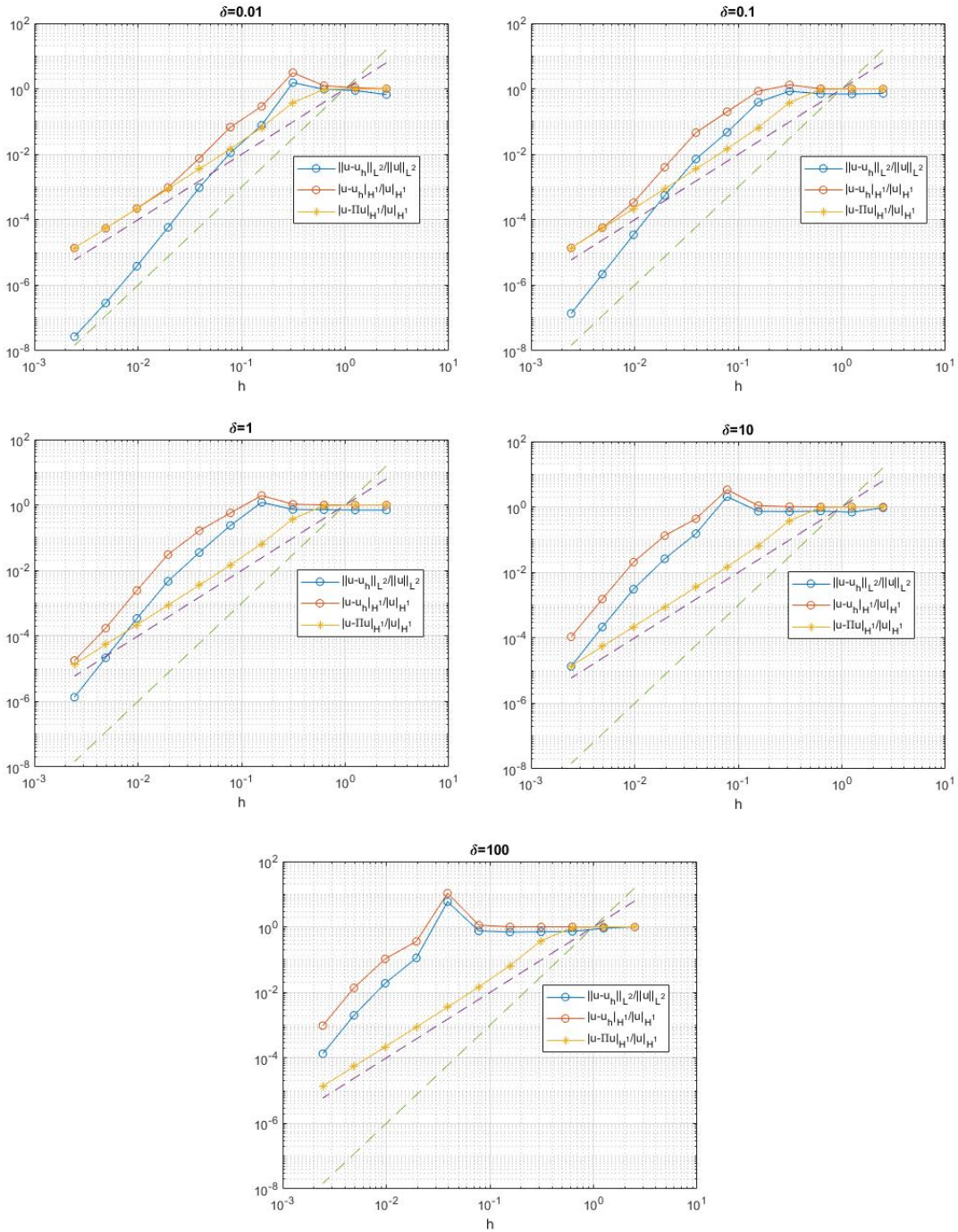


FIGURE 4.24: log-log plots of relative errors committed by perturbed quadratic IGA with maximal regularity (4.22) in $|\cdot|_{H^1(0,T)}$ seminorm and in $\|\cdot\|_{L^2(0,T)}$ norm, with respect to a uniform mesh-size h . Also, the best approximation error in $|\cdot|_{H^1(0,T)}$ seminorm is represented. The square of the wave number is $\mu = 1000$.

Since the new bilinear form (4.22) with $\delta = \frac{1}{100}$ returns significantly small errors that converge with “the right orders” of convergence, we are now interested in numerically studying how its inf-sup value behaves with respect

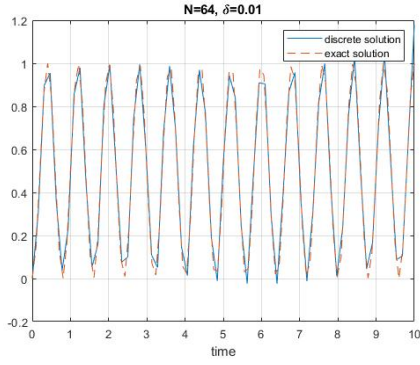


FIGURE 4.25: Exact and discrete solutions of the perturbed problem (4.20) with (4.22) and $\delta = \frac{1}{100}$, for $\mu = 1000$ and $N = 64$ elements (i.e., $h = 0.1563$).

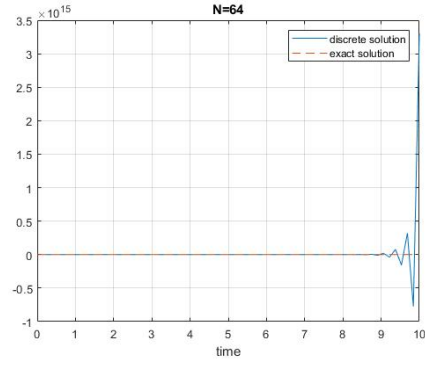


FIGURE 4.26: Exact and discrete solutions by unperturbed quadratic IGA for $\mu = 1000$ and $N = 64$ elements (i.e., $h = 0.1563$).

to (μ, h) . As before, we fix the final time $T=10$ and a uniform mesh and we numerically estimate the discrete inf-sup of the bilinear form (4.22) by means of Proposition 4.1.5.

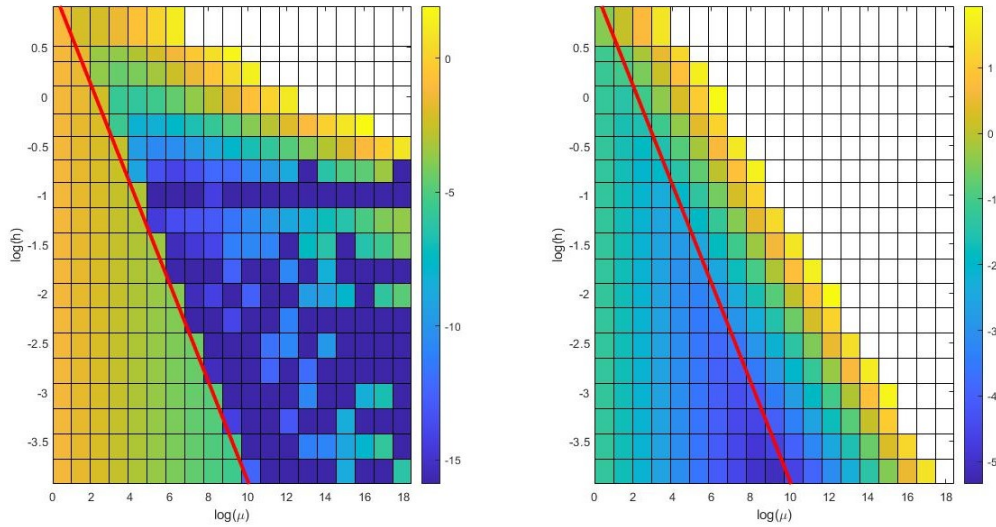


FIGURE 4.27: On the left a p-color plot of $\log(\beta)$ with respect to $(\log(\mu), \log(h))$, where β is the discrete inf-sup value of the bilinear form (3.3). On the right a p-color plot of $\log(\beta)$ with respect to $(\log(\mu), \log(h))$, where β is the inf-sup value of the bilinear form (4.22) with $\delta = \frac{1}{100}$. In both Figures the red line is the natural logarithm of the upper bound (4.13) and the square of the wave number is $\mu = 1000$.

As one can see from Figures 4.27, 4.28, the behaviour of the discrete inf-sup of (4.22) is uniformly (w.r.t. h) bounded. In particular, the red line of Figure 4.27 corresponds to the upper-bound (4.13) and now, in the stabilized case, it no longer separates two different discrete inf-sup regimes.

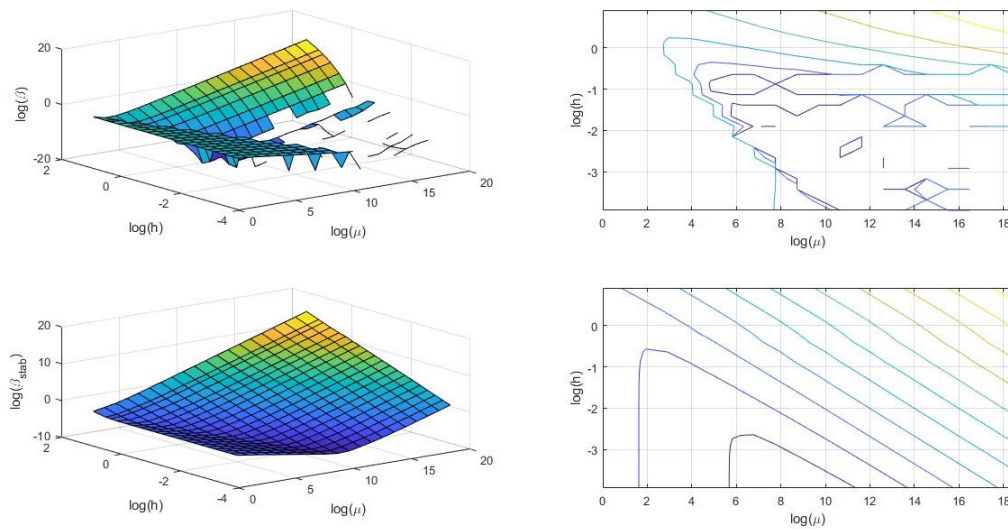


FIGURE 4.28: On the left, two three-dimensional plots of $\log(\beta)$ with respect to $(\log(\mu), \log(h))$. On the right, the contour lines of $\log(\beta)$ with respect to $(\log(\mu), \log(h))$. The top two figures correspond to the bilinear form defined in (3.3) restricted to the discrete IGA spaces (3.10), (3.11), and the bottom two to the stabilised bilinear form (4.22) with $\delta = \frac{1}{100}$. The square of the wave number is $\mu = 1000$.

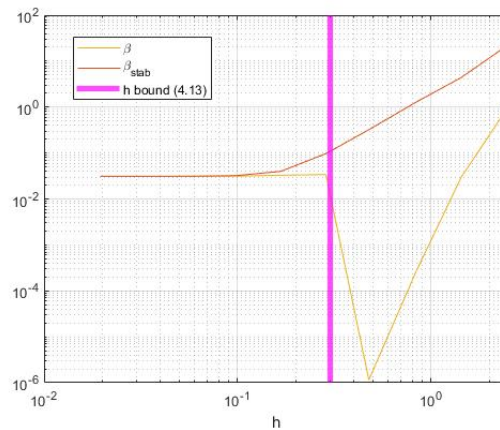


FIGURE 4.29: A log-log plot of the isogeometric inf-sup values of (3.3), (4.22) with respect to a uniform mesh-size h , for $\delta = \frac{1}{100}$ and a fixed $\mu = 100$.

Figure 4.29 clearly shows the uniformly bounded behaviour (w.r.t. h) of the numerically estimated inf-sup of the perturbed bilinear form (4.22).

In Figure 4.27 one can note that the optimal discrete inf-sup constant shows a dependency on μ of order $\mu^{-\frac{1}{2}}$, as the discrete inf-sup constant of

(3.3) in the stability region given by (4.13), i.e., defined by

$$h < \sqrt{\frac{9}{\mu}}.$$

As before, in Figure 4.27 we do not consider the values of discrete inf-sup that are greater than 10^2 , since they are not a physical phenomenon, but simply the result of an unsuitable discretization of the problem, as observed in Section 4.1.2.

It might be interesting to further improve the stabilization by choosing the optimal δ in relation to the empirical stability constraint (4.13), but the perturbation of order four that we are operating does not allow us to apply the reasoning explained at the end of Section 4.2.1. However, an improvement of δ could be obtained by writing it as an appropriate function of μ .

Chapter 5

Conclusions

The goal of this thesis is to investigate the first steps towards an unconditionally stable space-time isogeometric method with maximal regularity, using a tensor-product approach, for the wave problem (1.1).

Inspired by the work (Steinbach and Zank, 2019), our starting point is studying the conditioned stability of the conforming quadratic IGA discretization with global $C^1(0, T)$ regularity of the related ordinary differential problem (3.1). In Chapter 3 we hence obtain two explicit upper bounds on the mesh-size, which, if respected, guarantee stability. The first one (3.24), i.e.,

$$h \leq \frac{\pi^2}{\sqrt{2}(2 + \sqrt{\mu}T)\mu T},$$

is an extension to quadratic IGA with maximal regularity of Theorem 4.7 of (Steinbach and Zank, 2020), which is a result for the piecewise continuous linear FEM discretization. In particular, our upper bound is about twice as large as the FEM one, and the discrete stability constant of (3.25), i.e.,

$$\beta_1(\mu, T) := \frac{2\pi^2}{(2 + \sqrt{\mu}T)^2(\pi^2 + 4\mu T^2)},$$

depends on the coefficient $\mu > 0$ and on the final time $T > 0$ of the ODE (3.1) with the same order as the FEM one. The second upper bound (3.41), i.e.,

$$h \leq \frac{\pi^5}{(\pi^2 + 4\mu T^2)[\pi^2 + 2\mu T^2(2 + \sqrt{\mu}T)]} \sqrt{\frac{2b - \mu T^2}{2b(2 + b)\mu}}$$

where $b > \frac{\mu T^2}{2}$ is an arbitrary fixed real value, is obtained by the theory of *Galerkin method applied to Gårding-type problems*.

The asymptotic case, i.e., μ that is significantly large, seems to us the most interesting situation for the problem of instability (Remark 4.1.4) and for the wave equation. Thus, in Remark 3.2.17 we compare the obtained bounds and the corresponding stability constants for $\mu \rightarrow \infty$. It follows that, for “a very large” μ , the first bound (3.24) is a weaker constraint than the second bound (3.41). Moreover, some numerical results of Chapter 4 show that the latter, with the optimal choice for b (3.45), can be a stronger constraint than the former even if μ is not extremely large.

Let us define

$$C_1(\mu, T) := \frac{1}{\beta_1(\mu, T)},$$

where $\beta_1(\mu, T)$ is the discrete inf-sup constant of (3.25) that we recall above. In Remark 3.2.17 we note that the stability constant of (3.42), i.e.,

$$C_2(\mu, T) := \left[\frac{3b + \mu T^2 \left(\frac{8b}{\pi^2} - \frac{1}{2} \right)}{2b - \mu T^2} \right] \left(\text{for a fixed } b > \frac{\mu T^2}{2} \right),$$

that arises from the second upper bound (3.41) has a slower growth than $C_1(\mu, T)$ for $\mu \rightarrow \infty$. Thus, the theory of *Galerkin method applied to Gårding-type problems* is useful for our problem leading to a lower bound of the discrete inf-sup that, asymptotically, is sharper than that obtained by extending the analysis of O. Steinbach and M. Zank (Steinbach and Zank, 2020). In Chapter 4 there are also some numerical results showing that the inf-sup $\beta_2(\mu, T) := \frac{1}{C_2(\mu, T)}$ can be sharper than $\beta_1(\mu, T)$ even if μ is not significantly large.

In Chapter 4 we observe that the two upper bounds (3.24), (3.41) are not optimal. However, if the mesh-size is uniform, we manage to numerically find a stability constraint (4.13), i.e.,

$$h < \sqrt{\frac{9}{\mu}},$$

which, from the numerical results that we obtain, seems to be sharp. The upper bound (4.13) is of the same order (w.r.t μ) of the sharp upper bound (4.7) for the stability of FEM discretization, i.e.,

$$h < \sqrt{\frac{12}{\mu}}.$$

Quadratic IGA discretization of maximal regularity appears to be advantageous over piecewise continuous linear FEM. Indeed, the stability upper bounds on the mesh size of the former are very similar to the FEM ones, and the orders of convergence of the IGA method are of one order more than the FEM ones. Moreover, from the numerical tests we see that the error committed by the IGA is, for each mesh-size h , strictly smaller than the FEM one.

As observed in Remark 3.2.16, if we raise the degree of the splines to $p > 2$ while keeping maximal regularity, the constraint on the mesh-size (3.41) and the resulting stability constant do not change. On the other hand, how the upper bound (3.24) behaves in h is not immediately clear from the proof of Theorem 3.2.8. However, we are sure that the orders of convergence of the discrete solution to the exact solution will be p in $\|\cdot\|_{H^1(0,T)}$ and $p+1$ in $\|\cdot\|_{L^2(0,T)}$, if the exact solution is sufficiently regular. Also, we could expect that the maximal error, and more generally for all values of h , is strictly

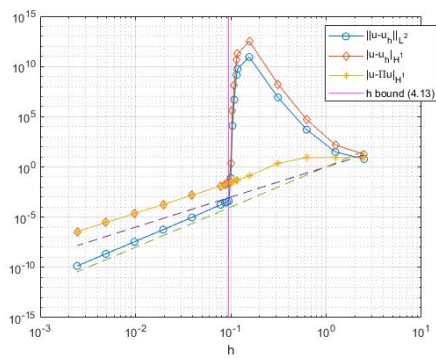


FIGURE 5.1: A log-log plot of errors committed by cubic IGA, with maximal regularity, in $|\cdot|_{H^1(0,T)}$ seminorm and in $\|\cdot\|_{L^2(0,T)}$ norm, with respect to a uniform mesh-size h . Also, the best approximation error in $|\cdot|_{H^1(0,T)}$ seminorm and the bound (4.13) are represented. The square of the wave number is $\mu = 1000$

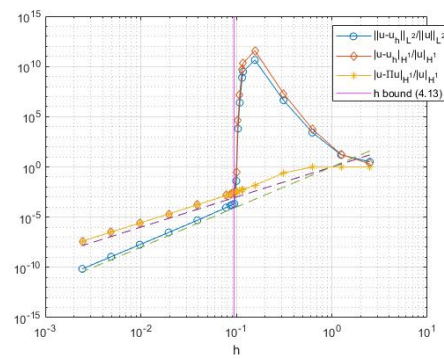


FIGURE 5.2: A log-log plot of relative errors committed by cubic IGA, with maximal regularity, in $|\cdot|_{H^1(0,T)}$ seminorm and in $\|\cdot\|_{L^2(0,T)}$ norm, with respect to a uniform mesh-size h . Also, the best approximation error in $|\cdot|_{H^1(0,T)}$ seminorm and the bound (4.13) are represented. The square of the wave number is $\mu = 1000$

smaller than the error committed by continuous, linear FEM and quadratic $C^1(0, T)$ IGA discretizations. This behaviour of the error would be a consequence of high degree of approximation of B-spline technology (Hughes, Reali, and Sangalli, 2008; Sande, Manni, and Speleers, 2019) and of the “good behaviour” of high-order methods with respect to wave propagation problems (Babuška and Sauter, 2000). These error considerations are indeed confirmed by our numerical tests in Figures 5.1, 5.2, 5.3, 5.4.

As in Chapter 4, as a numerical example for the Galerkin-Petrov finite element methods we consider a uniform discretization of the time interval $(0, T)$ with $T = 10$ and a mesh-size $h = T/N$. For $\mu = 1000$ we consider the strong solution $u(t) = \sin^2\left(\frac{5}{4}\pi t\right)$ and we compute the integrals appearing at the right-hand side using high-order integration rules.

As one can note in Figures 5.1, 5.2, 5.3, 5.4 the constraint (4.13) seems to remain optimal with respect to the error by raising the degree and regularity of the splines.

Although the errors diminish by raising the degree and regularity of the splines, it is of significant importance to find a method that is stable for every degree and regularity, so that we are not forced to work with dense matrices, which cause a high computational cost.

Finally, let us note that we expect the IGA discretization of degree $p \geq 2$ and regularity $C^{p-1}(0, T)$ to perform better than the piecewise continuous FEM of degree p . Indeed, although the IGA matrices have more non-zero entries, the FEM discretization uses more basis functions. Furthermore, we expect that, while approximating solutions of wave propagation problems, the error committed by the IGA method is smaller than the FEM one (Babuška

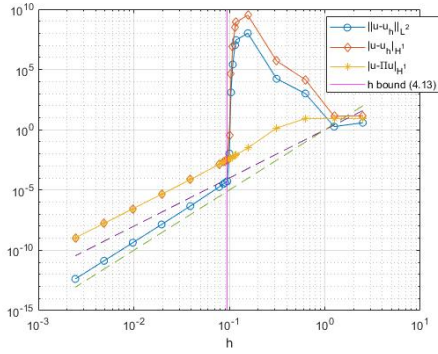


FIGURE 5.3: A log-log plot of errors committed by IGA of fourth degree, with maximal regularity, in $|\cdot|_{H^1(0,T)}$ seminorm and in $\|\cdot\|_{L^2(0,T)}$ norm, with respect to a uniform mesh-size h . Also, the best approximation error in $|\cdot|_{H^1(0,T)}$ seminorm and the bound (4.13) are represented. The square of the wave number is $\mu = 1000$

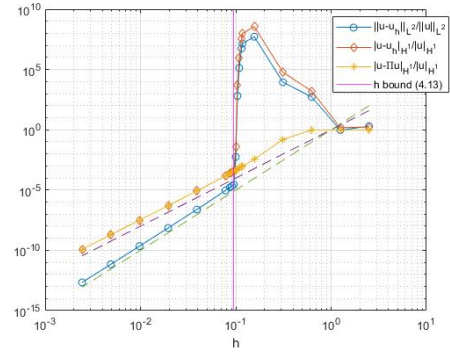


FIGURE 5.4: A log-log plot of relative errors committed by IGA of fourth degree, with maximal regularity, in $|\cdot|_{H^1(0,T)}$ seminorm and in $\|\cdot\|_{L^2(0,T)}$ norm, with respect to a uniform mesh-size h . Also, the best approximation error in $|\cdot|_{H^1(0,T)}$ seminorm and the bound (4.13) are represented. The square of the wave number is $\mu = 1000$

and Sauter, 2000).

Our proposals of stabilizations are all based on non-consistent perturbations.

In order to stabilize the quadratic IGA with maximal regularity, if the mesh-size is uniform, we propose to consider the perturbed bilinear form (4.22), i.e.,

$$a_h(u_h, v_h) = -\langle \partial_t u_h, \partial_t v_h \rangle_{L^2(0,T)} + \mu \langle u_h, v_h \rangle_{L^2(0,T)} - \delta \mu h^4 \langle \partial_t^2 u_h, \partial_t^2 v_h \rangle_{L^2(0,T)},$$

for all $u_h \in V_{0,*}^h$ and $v_h \in V_{*,0}^h$, where $\delta > 0$ is a fixed real value. Our numerical results are very promising in the case of $\delta = \frac{1}{100}$. It would therefore be interesting to study the theory that could explain why this stabilization works and then propose an optimal δ .

For IGA method with generic polynomial degree p and maximal regularity, we propose to consider the following perturbed bilinear form

$$a_h(u_h, v_h) = -\langle \partial_t u_h, \partial_t v_h \rangle_{L^2(0,T)} + \mu \langle u_h, v_h \rangle_{L^2(0,T)} - \delta \mu h^{2p} \langle \partial_t^p u_h, \partial_t^p v_h \rangle_{L^2(0,T)}, \quad (5.1)$$

for all u_h and v_h , respectively, in the discrete trial and test spaces, where $\delta > 0$ is a fixed real value.

If the mesh-size is non-uniform, we suggest considering

$$a_h(u_h, v_h) = -\langle \partial_t u_h, \partial_t v_h \rangle_{L^2(0,T)} + \mu \langle u_h, v_h \rangle_{L^2(0,T)} - \delta \mu \sum_{l=1}^N h_l^{2p} \langle \partial_t^p u_h, \partial_t^p v_h \rangle_{L^2(\tau_l)}, \quad (5.2)$$

for all u_h and v_h , respectively, in the discrete trial and test spaces, where τ_l , for $l = 1, \dots, N$, are the subintervals of $(0, T)$ given by the Galerkin discretization and $\delta > 0$ is a fixed real value. Actually, (5.1) is a subcase of (5.2).

Finally, let us briefly consider the homogeneous Dirichlet problem for the second-order wave equation (1.1), i.e.,

$$\begin{cases} \partial_{tt}u(x, t) - \Delta_x u(x, t) = g(x, t) & (x, t) \in Q := \Omega \times (0, T) \\ u(x, t) = 0 & (x, t) \in \partial\Omega \times [0, T] \\ u(x, 0) = \partial_t u(x, t)|_{t=0} = 0 & x \in \Omega, \end{cases} \quad (5.3)$$

where $\Omega \subset \mathbb{R}^d$, with $d = 1, 2, 3$, is an open bounded Lipschitz domain and, for a real value $T > 0$, $(0, T)$ is a time interval. In (Steinbach and Zank, 2020) the authors introduce a space-time variational formulation of (1.1), where integration by parts is also applied with respect to the time variable, and the classic anisotropic Sobolev spaces with homogeneous initial and boundary conditions are employed. Inspired by (Steinbach and Zank, 2019; Zank, 2020), a possible unconditionally stable space-time IGA method with maximal regularity based on a tensor-product approach could be obtained by considering the perturbed bilinear form

$$a_h(u_h, v_h) = -\langle \partial_t u_h, \partial_t v_h \rangle_{L^2(Q)} + \langle \nabla_x u_h, \nabla_x v_h \rangle_{L^2(Q)} - \delta \sum_{m=1}^d \sum_{l=1}^{N_t} h_l^{2p} \langle \partial_t^p \partial_{x_m} u_h, \partial_t^p \partial_{x_m} v_h \rangle_{L^2(\Omega \times \tau_l)}, \quad (5.4)$$

for all u_h and v_h , respectively, in the discrete trial and test spaces, where τ_l , for $l = 1, \dots, N_t$, are the subintervals of $(0, T)$ given by the Galerkin discretization and $\delta > 0$ is a fixed real value. We expect this stabilization to perform well, given the appreciable numerical results of the perturbation (4.22). However, we have not tested (5.4) yet, since we prefer to give priority to a full analysis of the IGA discretization of our model problem (3.2), which, given its link to the wave equation, we expect to be significantly useful.

Bibliography

- Aubin, J.P. (2000). *Applied Functional Analysis*. Pure and Applied Mathematics: A Wiley Series of Texts, Monographs and Tracts. Wiley.
- Aziz, A., R. Kellogg, and A. B. Stephens (1988). "A two point boundary value problem with a rapidly oscillating solution". In: *Numerische Mathematik* 53, pp. 107–121.
- Babuška, I. and F. Ihlenburg (1995). "Finite element solution of the Helmholtz equation with high wave number Part I: The h-version of the FEM". In: *Computers & Mathematics with Applications* 30.9, pp. 9–37.
- Babuška, I. and S. Sauter (2000). "Is the Pollution Effect of the FEM Avoidable for the Helmholtz Equation Considering High Wave Numbers?" In: *SIAM Rev.* 42, pp. 451–484.
- Babuška, I. et al. (1995). "A Generalized Finite Element Method for solving the Helmholtz equation in two dimensions with minimal pollution". In: *Computer Methods in Applied Mechanics and Engineering* 128.3, pp. 325–359.
- Brezis, H. (1973). *Opérateurs maximaux monotones et semi-groupes de contractions dans les espaces de Hilbert*. ISSN. Elsevier Science.
- (2011). *Functional Analysis, Sobolev Spaces and Partial Differential Equations*. New York, NY: Springer New York.
- Courant, R., K. Friedrichs, and H. Lewy (1928). "Über die partiellen Differenzgleichungen der mathematischen Physik". In: *Mathematische Annalen* 100, pp. 32–74.
- De Boor, C. (1978). *A Practical Guide to Splines*. Applied Mathematical Sciences. Springer New York.
- Ern, A. and J-L. Guermond (2004). *Theory and Practice of Finite Elements*. New York, NY: Springer New York.
- Evans, L.C. and American Mathematical Society (1998). *Partial Differential Equations*. Graduate studies in mathematics. American Mathematical Society.
- Fessler, J. (2004). *Linear operators and adjoints*. Classnotes.
- Gander, M. J. (2015). "50 Years of Time Parallel Time Integration". In: *Multiple Shooting and Time Domain Decomposition Methods*. Ed. by T. Carraro et al. Cham: Springer International Publishing, pp. 69–113.
- Gasinski, L. and N.S. Papageorgiou (2005). *Nonlinear Analysis*. Mathematical Analysis and Applications. CRC Press.
- Hackbusch, W. (2013). *Multi-Grid Methods and Applications*. Springer Series in Computational Mathematics. Springer Berlin Heidelberg.
- Hairer, E., S.P. Nørsett, and G. Wanner (1993). *Solving Ordinary Differential Equations I Nonstiff problems*. Second. Berlin: Springer.

- Harari, I. and T.J.R. Hughes (1991). "Finite element methods for the helmholtz equation in an exterior domain: Model problems". In: *Computer Methods in Applied Mechanics and Engineering* 87.1, pp. 59–96.
- Höllig, K. and J. Hörner (2013). *Approximation and Modeling with B-Splines*.
- Hughes, T.J.R., J.A. Cottrell, and Y. Bazilevs (2005). *Isogeometric analysis: CAD, finite elements, NURBS, exact geometry and mesh refinement*. Vol. 194. 39-41. Elsevier, pp. 4135–4195.
- Hughes, T.J.R., A. Reali, and G. Sangalli (2008). "Duality and unified analysis of discrete approximations in structural dynamics and wave propagation: Comparison of p-method finite elements with k-method NURBS". In: *Computer Methods in Applied Mechanics and Engineering* 197.49, pp. 4104–4124.
- Loli, G. et al. (2020). "An efficient solver for space–time isogeometric Galerkin methods for parabolic problems". In: *Computers & Mathematics with Applications* 80.11. High-Order Finite Element and Isogeometric Methods 2019, pp. 2586–2603.
- Löscher, R., O. Steinbach, and M. Zank (2021). *Numerical results for an unconditionally stable space-time finite element method for the wave equation*. arXiv: 2103.04324 [math.NA].
- Lyche, T., C. Manni, and H. Speleers (2018). "Foundations of Spline Theory: B-Splines, Spline Approximation, and Hierarchical Refinement". In: *Splines and PDEs: From Approximation Theory to Numerical Linear Algebra: Cetraro, Italy 2017*. Ed. by Tom Lyche, Carla Manni, and Hendrik Speleers. Cham: Springer International Publishing, pp. 1–76.
- Moiola, A. (2021). *Scattering of time-harmonic acoustic waves: Helmholtz equation, boundary integral equations and BEM*. Classnotes.
- Norikazu, S. (2018). *Notes on the Banach-Necas-Babuska theorem and Kato's minimum modulus of operators*. arXiv: 1711.01533 [math.NA].
- Quarteroni, A. (2009). *Modellistica Numerica per Problemi Differenziali*. UNITEXT. Springer Milan.
- Sande, E., C. Manni, and H. Speleers (2019). *Sharp error estimates for spline approximation: Explicit constants, n-widths, and eigenfunction convergence*. Vol. 29. 06. World Scientific Pub Co Pte Lt.
- Sayas, F.-J. (2006). *Introduction to the boundary element method. A case study: the Helmholtz equation*. Classnotes.
- Sayas, F.J., T.S. Brown, and M.E. Hassell (2019). *Variational Techniques for Elliptic Partial Differential Equations: Theoretical Tools and Advanced Applications*. CRC Press.
- Schumaker, L. (2007). *Spline Functions: Basic Theory*. Cambridge Mathematical Library. Cambridge University Press.
- Spence, E.A. (2014). "When all else fails, integrate by parts – an overview of new and old variational formulations for linear elliptic PDEs". In: *Unified Transform for Boundary Value Problems: Applications and Advances*. Ed. by A.S. Fokas and B. Pelloni. Other Titles in Applied Mathematics. Society for Industrial and Applied Mathematics, pp. 93–159.
- Steinbach, O. and M. Zank (2019). "A Stabilized Space–Time Finite Element Method for the Wave Equation". In: *Advanced Finite Element Methods with*

- Applications: Selected Papers from the 30th Chemnitz Finite Element Symposium 2017*. Ed. by Thomas Apel et al. Cham: Springer International Publishing, pp. 341–370.
- (2020). “Coercive space-time finite element methods for initial boundary value problems”. In: *ETNA - Electronic Transactions on Numerical Analysis* 52, pp. 154–194.
 - (2021a). *A generalized inf-sup stable variational formulation for the wave equation*. arXiv: [2101.06293](https://arxiv.org/abs/2101.06293) [math.NA].
 - (2021b). “A note on the efficient evaluation of a modified Hilbert transformation”. In: vol. 29. 1, pp. 47–61.
- Vázquez, R. (2016). “A new design for the implementation of isogeometric analysis in Octave and Matlab: GeoPDEs 3.0”. In: *Computers & Mathematics with Applications* 72.3, pp. 523–554.
- Wloka, J., C.B. Thomas, and M.J. Thomas (1987). *Partial Differential Equations*. Cambridge University Press.
- Zank, M. (2020). *Inf-Sup Stable Space-Time Methods for Time-Dependent Partial Differential Equations*. Verlag d. Technischen Universität Graz.
- (2021a). “An Exact Realization of a Modified Hilbert Transformation for Space-Time Methods for Parabolic Evolution Equations”. In: *Computational Methods in Applied Mathematics* 21.2, pp. 479–496.
 - (Feb. 2021b). “Higher-Order Space-Time Continuous Galerkin Methods for the Wave Equation”. In: *arXiv e-prints*. arXiv: [2102.07562](https://arxiv.org/abs/2102.07562) [math.NA].
- Zlotnik, A.A. (2017). “Convergence rate estimates of finite-element methods for second-order hyperbolic equations”. In: *Numerical Methods and Applications (1994)*. Ed. by G.I. Marchuk. CRC Press Revivals. CRC Press, pp. 155–220.